Final Report

MM5 METEOROLOGICAL MODELING OF TEXAS FOR JUNE 2006

Work Order No. 582-07-83986-FY08-02

Prepared for

Texas Commission on Environmental Quality
12118 Park 35 Circle
Austin, Texas 78753

Prepared by

Christopher Emery
Jeremiah Johnson
Piti Piyachaturawat
Greg Yarwood

ENVIRON International Corporation
773 San Marin Drive, Suite 2115
Novato, CA 94998

July 31, 2009

TABLE OF CONTENTS

Page

EXECUTIVE SUMMARY ES-1

ES.1. Introduction ES-1
ES.2. Approach ES-1
ES.3. Results ES-2
ES.4. Recommendations ES-3

1. INTRODUCTION 1-1

1.1. Background 1-1
1.2. Objectives 1-2
1.3. Overview of MM5 1-2
1.4. Overview of Approach 1-5

2. ALTERNATIVE PBL TREATMENT 2-1

2.1. San Antonio 2-1
2.2. Austin 2-5
2.3. Dallas 2-9
2.4. Northeast Texas 2-13
2.5. Evaluation of PBL and Precipitation 2-17

3. ALTERNATIVE SOIL MODEL 3-1

3.1. San Antonio 3-1
3.2. Austin 3-5
3.3. Dallas 3-9
3.4. Northeast Texas 3-13
3.5. Evaluation of PBL and Precipitation 3-17

4. SURFACE ANALYSIS NUDGING 4-1

4.1. San Antonio 4-1
4.2. Austin 4-5
4.3. Dallas 4-9
4.4. Northeast Texas 4-13
4.5. Evaluation of PBL and Precipitation 4-17

5. CONCLUSION 5-1

REFERENCES R-1

TABLES

Table 1-1. MM5 vertical layer structure. 1-4
Table 1-2. Physics options used for the AACOG/CAPCOG June 2006 MM5 "Run 8" simulation by grid (Emery et al., 2009a). 1-6
Table 1-3. Analysis nudging coefficients used in the AACOG/CAPCOG "Run 8" June 2006 MM5 simulation. 1-7
Table 1-4. Observation nudging coefficients used in the AACOG/CAPCOG "Run 8" June 2006 MM5 simulation. 1-7

FIGURES

Figure 1-1. Four MM5 nested modeling domains showing the location of tropospheric profiler sites (blue triangles). The model projection is Lambert Conformal, with origin at 100°W/40°N, and true latitudes at 30°N and 60°N. Note that the 4-km grid shown here represents the original size defined by TCEQ; the current study employed a slightly enlarged 4-km grid to support the AACOG/CAPCOG photochemical modeling grid. 1-3
Figure 1-2. Locations of wind profiler sites throughout Texas at which PBL depths were derived by STI (2007). PBL depths were compared to MM5 simulated values at New Braunfels (NBF), Moody (MDY), Cleburne (CLE), Huntsville (HVE), and Longview (LVW). 1-10
Figure 1-3. Locations of surface meteorological measurement sites available in the DS472 dataset in the vicinity of San Antonio. 1-10
Figure 1-4. Locations of surface meteorological measurement sites available in the DS472 dataset in the vicinity of Austin. 1-11
Figure 1-5. Locations of surface meteorological measurement sites available in the DS472 dataset in the vicinity of Dallas. 1-11
Figure 1-6. Locations of surface meteorological measurement sites available in the DS472 dataset in the vicinity of Northeast Texas. 1-12

Figure 2-1. Scatter plots of hourly wind speed (m/s; top) and hourly wind direction (degrees, bottom) at DS472 sites in San Antonio for AACOG/CAPCOG Run 4 (left) and for Run 9 (right). Blue points are nighttime hours, red point are daytime hours. The green dash line is the best fit line to all data; the black dotted lines are the ±2 m/s error envelope (top) and the ±30 degree error envelope (bottom). Fractions of data points within different bias ranges are shown at the top right of each plot. 2-2
Figure 2-2. Scatter plots of hourly temperature (K; top) and hourly humidity (g/kg, bottom) at DS472 sites in San Antonio for AACOG/CAPCOG Run 4 (left) and for Run 9 (right). Blue points are nighttime hours, red point are daytime hours. The green dash line is the best fit line to all data; the black dotted lines are the ±2 K error envelope (top) and the ±2 g/kg error envelope (bottom). Fractions of data points within different bias ranges are shown at the top right of each plot. 2-3

Figure 2-3. Scatter plots of daily statistical performance against DS472 data in San Antonio for wind speed (top left), wind direction (top right), temperature (bottom left) and humidity (bottom right). Each plot shows daily performance from AACOG/CAPCOG Run 4 (red dots) and Run 9 (blue dots). The blue boxes represent the bias/error space bounded by the statistical performance benchmarks described in Section 1. 2-4

Figure 2-4. Scatter plots of hourly wind speed (m/s; top) and hourly wind direction (degrees, bottom) at DS472 sites in Austin for AACOG/CAPCOG Run 4 (left) and for Run 9 (right). Blue points are nighttime hours, red point are daytime hours. The green dash line is the best fit line to all data; the black dotted lines are the ±2 m/s error envelope (top) and the ±30 degree error envelope (bottom). Fractions of data points within different bias ranges are shown at the top right of each plot. 2-6

Figure 2-5. Scatter plots of hourly temperature (K; top) and hourly humidity (g/kg, bottom) at DS472 sites in Austin for AACOG/CAPCOG Run 4 (left) and for Run 9 (right). Blue points are nighttime hours, red point are daytime hours. The green dash line is the best fit line to all data; the black dotted lines are the ±2 K error envelope (top) and the ±2 g/kg error envelope (bottom). Fractions of data points within different bias ranges are shown at the top right of each plot. 2-7

Figure 2-6. Scatter plots of daily statistical performance against DS472 data in Austin for wind speed (top left), wind direction (top right), temperature (bottom left) and humidity (bottom right). Each plot shows daily performance from AACOG/CAPCOG Run 4 (red dots) and Run 9 (blue dots). The blue boxes represent the bias/error space bounded by the statistical performance benchmarks described in Section 1. 2-8

Figure 2-7. Scatter plots of hourly wind speed (m/s; top) and hourly wind direction (degrees, bottom) at DS472 sites in Dallas for AACOG/CAPCOG Run 4 (left) and for Run 9 (right). Blue points are nighttime hours, red point are daytime hours. The green dash line is the best fit line to all data; the black dotted lines are the ±2 m/s error envelope (top) and the ±30 degree error envelope (bottom). Fractions of data points within different bias ranges are shown at the top right of each plot. 2-10

Figure 2-8. Scatter plots of hourly temperature (K; top) and hourly humidity (g/kg, bottom) at DS472 sites in Dallas for AACOG/CAPCOG Run 4 (left) and for Run 9 (right). Blue points are nighttime hours, red point are daytime hours. The green dash line is the best fit line to all data; the black dotted lines are the ±2 K error envelope (top) and the ±2 g/kg error envelope (bottom). Fractions of data points within different bias ranges are shown at the top right of each plot. 2-11

Figure 2-9. Scatter plots of daily statistical performance against DS472 data in Dallas for wind speed (top left), wind direction (top right), temperature (bottom left) and humidity (bottom right). Each plot shows daily performance from AACOG/CAPCOG Run 4 (red dots) and Run 9 (blue dots). The blue boxes represent the bias/error space bounded by the statistical performance benchmarks described in Section 1. 2-12

Figure 2-10. Scatter plots of hourly wind speed (m/s; top) and hourly wind direction (degrees, bottom) at DS472 sites in Northeast Texas for AACOG/CAPCOG Run 4 (left) and for Run 9 (right). Blue points are nighttime hours, red point are daytime hours. The green dash line is the best fit line to all data; the black dotted lines are the ±2 m/s error envelope (top) and the ±30 degree error envelope (bottom). Fractions of data points within different bias ranges are shown at the top right of each plot. 2-14

Figure 2-11. Scatter plots of hourly temperature (K; top) and hourly humidity (g/kg, bottom) at DS472 sites in Northeast Texas for AACOG/CAPCOG Run 4 (left) and for Run 9 (right). Blue points are nighttime hours, red point are daytime hours. The green dash line is the best fit line to all data; the black dotted lines are the ±2 K error envelope (top) and the ±2 g/kg error envelope (bottom). Fractions of data points within different bias ranges are shown at the top right of each plot. 2-15

Figure 2-12. Scatter plots of daily statistical performance against DS472 data in Northeast Texas for wind speed (top left), wind direction (top right), temperature (bottom left) and humidity (bottom right). Each plot shows daily performance from AACOG/CAPCOG Run 4 (red dots) and Run 9 (blue dots). The blue boxes represent the bias/error space bounded by the statistical performance benchmarks described in Section 1. 2-16

Figure 2-13. Hourly time series of predicted (MM5 Runs 8 and 9) and diagnosed PBL depths from the New Braunfels wind profiler. 2-18

Figure 2-14. Hourly time series of predicted (MM5 Runs 8 and 9) and diagnosed PBL depths from the Moody wind profiler. 2-18

Figure 2-15. Hourly time series of predicted (MM5 Runs 8 and 9) and diagnosed PBL depths from the Huntsville wind profiler. 2-18

Figure 2-16. Hourly time series of predicted (MM5 Runs 8 and 9) and diagnosed PBL depths from the Cleburne wind profiler. 2-19

Figure 2-17. Hourly time series of predicted (MM5 Runs 8 and 9) and diagnosed PBL depths from the Longview wind profiler. 2-19

Figure 2-18. Observed (AHPS; top left) and MM5 simulated 24-hour accumulated precipitation (mm) for Runs 8 (top right) and 9 (bottom right), 7 AM June 14 to 7 AM June 15, 2006. 2-20

Figure 2-19. Simulated wind fields (left), CAMx cloud cover (middle), and rainfall (right) from MM5 Run 8 at 4 PM, June 13, 2006. 2-21

Figure 2-20. Simulated wind fields (left), CAMx cloud cover (middle), and rainfall (right) from MM5 Run 9 at 4 PM, June 13, 2006. 2-22

Figure 3-1. Scatter plots of hourly wind speed (m/s; top) and hourly wind direction (degrees, bottom) at DS472 sites in San Antonio for Run 9 (left) and for Run 10 (right). Blue points are nighttime hours, red point are daytime hours. The green dash line is the best fit line to all data; the black dotted lines are the ±2 m/s error envelope (top) and the ±30 degree error envelope (bottom). Fractions of data points within different bias ranges are shown at the top right of each plot. 3-2

Figure 3-2. Scatter plots of hourly temperature (K; top) and hourly humidity (g/kg, bottom) at DS472 sites in San Antonio for Run 9 (left) and for Run 10 (right). Blue points are nighttime hours, red point are daytime hours. The green dash line is the best fit line to all data; the black dotted lines are the ±2 K error envelope (top) and the ±2 g/kg error envelope (bottom). Fractions of data points within different bias ranges are shown at the top right of each plot. 3-3

Figure 3-3. Scatter plots of daily statistical performance against DS472 data in San Antonio for wind speed (top left), wind direction (top right), temperature (bottom left) and humidity (bottom right). Each plot shows daily performance from AACOG/CAPCOG Run 4 (red dots) and Run 10 (blue dots). The blue boxes represent the bias/error space bounded by the statistical performance benchmarks described in Section 1. 3-4

Figure 3-4. Scatter plots of hourly wind speed (m/s; top) and hourly wind direction (degrees, bottom) at DS472 sites in Austin for Run 9 (left) and for Run 10 (right). Blue points are nighttime hours, red point are daytime hours. The green dash line is the best fit line to all data; the black dotted lines are the ±2 m/s error envelope (top) and the ±30 degree error envelope (bottom). Fractions of data points within different bias ranges are shown at the top right of each plot. 3-6

Figure 3-5. Scatter plots of hourly temperature (K; top) and hourly humidity (g/kg, bottom) at DS472 sites in Austin for Run 9 (left) and for Run 10 (right). Blue points are nighttime hours, red point are daytime hours. The green dash line is the best fit line to all data; the black dotted lines are the ±2 K error envelope (top) and the ±2 g/kg error envelope (bottom). Fractions of data points within different bias ranges are shown at the top right of each plot. 3-7

Figure 3-6. Scatter plots of daily statistical performance against DS472 data in Austin for wind speed (top left), wind direction (top right), temperature (bottom left) and humidity (bottom right). Each plot shows daily performance from AACOG/CAPCOG Run 4 (red dots) and Run 10 (blue dots). The blue boxes represent the bias/error space bounded by the statistical performance benchmarks described in Section 1. 3-8

Figure 3-7. Scatter plots of hourly wind speed (m/s; top) and hourly wind direction (degrees, bottom) at DS472 sites in Dallas for Run 9 (left) and for Run 10 (right). Blue points are nighttime hours, red point are daytime hours. The green dash line is the best fit line to all data; the black dotted lines are the ±2 m/s error envelope (top) and the ±30 degree error envelope (bottom). Fractions of data points within different bias ranges are shown at the top right of each plot. 3-10

Figure 3-8. Scatter plots of hourly temperature (K; top) and hourly humidity (g/kg, bottom) at DS472 sites in Dallas for Run 9 (left) and for Run 10 (right). Blue points are nighttime hours, red point are daytime hours. The green dash line is the best fit line to all data; the black dotted lines are the ±2 K error envelope (top) and the ±2 g/kg error envelope (bottom). Fractions of data points within different bias ranges are shown at the top right of each plot. 3-11

Figure 3-9. Scatter plots of daily statistical performance against DS472 data in Dallas for wind speed (top left), wind direction (top right), temperature (bottom left) and humidity (bottom right). Each plot shows daily performance from AACOG/CAPCOG Run 4 (red dots) and Run 10 (blue dots). The blue boxes represent the bias/error space bounded by the statistical performance benchmarks described in Section 1. 3-12

Figure 3-10. Scatter plots of hourly wind speed (m/s; top) and hourly wind direction (degrees, bottom) at DS472 sites in Northeast Texas for Run 9 (left) and for Run 10 (right). Blue points are nighttime hours, red point are daytime hours. The green dash line is the best fit line to all data; the black dotted lines are the ±2 m/s error envelope (top) and the ±30 degree error envelope (bottom). Fractions of data points within different bias ranges are shown at the top right of each plot. 3-14

Figure 3-11. Scatter plots of hourly temperature (K; top) and hourly humidity (g/kg, bottom) at DS472 sites in Northeast Texas for Run 9 (left) and for Run 10 (right). Blue points are nighttime hours, red point are daytime hours. The green dash line is the best fit line to all data; the black dotted lines are the ±2 K error envelope (top) and the ±2 g/kg error envelope (bottom). Fractions of data points within different bias ranges are shown at the top right of each plot. 3-15

Figure 3-12. Scatter plots of daily statistical performance against DS472 data in Northeast Texas for wind speed (top left), wind direction (top right), temperature (bottom left) and humidity (bottom right). Each plot shows daily performance from AACOG/CAPCOG Run 4 (red dots) and Run 10 (blue dots). The blue boxes represent the bias/error space bounded by the statistical performance benchmarks described in Section 1. 3-16

Figure 3-13. Hourly time series of predicted (MM5 Runs 9 and 10) and diagnosed PBL depths from the New Braunfels wind profiler. 3-18

Figure 3-14. Hourly time series of predicted (MM5 Runs 9 and 10) and diagnosed PBL depths from the Moody wind profiler. 3-18

Figure 3-15. Hourly time series of predicted (MM5 Runs 9 and 10) and diagnosed PBL depths from the Huntsville wind profiler. 3-18

Figure 3-16. Hourly time series of predicted (MM5 Runs 9 and 10) and diagnosed PBL depths from the Cleburne wind profiler. 3-19

Figure 3-17. Hourly time series of predicted (MM5 Runs 9 and 10) and diagnosed PBL depths from the Longview wind profiler. 3-19

Figure 3-18. Observed (AHPS; top left) and MM5 simulated 24-hour accumulated precipitation (mm) for Runs 9 (top right) and 10 (bottom right), 7 AM June 14 to 7 AM June 15, 2006. 3-20

Figure 3-19. Simulated wind fields (left), CAMx cloud cover (middle), and rainfall (right) from MM5 Run 9 at 4 PM, June 13, 2006. 3-21

Figure 3-20. Simulated wind fields (left), CAMx cloud cover (middle), and rainfall (right) from MM5 Run 10 at 4 PM, June 13, 2006. 3-22

Figure 4-1. Scatter plots of hourly wind speed (m/s; top) and hourly wind direction (degrees, bottom) at DS472 sites in San Antonio for Run 10 (left) and for Run 11 (right). Blue points are nighttime hours, red point are daytime hours. The green dash line is the best fit line to all data; the black dotted lines are the ±2 m/s error envelope (top) and the ±30 degree error envelope (bottom). Fractions of data points within different bias ranges are shown at the top right of each plot. 4-2

Figure 4-2. Scatter plots of hourly temperature (K; top) and hourly humidity (g/kg, bottom) at DS472 sites in San Antonio for Run 10 (left) and for Run 11 (right). Blue points are nighttime hours, red point are daytime hours. The green dash line is the best fit line to all data; the black dotted lines are the ±2 K error envelope (top) and the ±2 g/kg error envelope (bottom). Fractions of data points within different bias ranges are shown at the top right of each plot. 4-3

Figure 4-3. Scatter plots of daily statistical performance against DS472 data in San Antonio for wind speed (top left), wind direction (top right), temperature (bottom left) and humidity (bottom right). Each plot shows daily performance from AACOG/CAPCOG Run 4 (red dots) and Run 11 (blue dots). The blue boxes represent the bias/error space bounded by the statistical performance benchmarks described in Section 1. 4-4

Figure 4-4. Scatter plots of hourly wind speed (m/s; top) and hourly wind direction (degrees, bottom) at DS472 sites in Austin for Run 10 (left) and for Run 11 (right). Blue points are nighttime hours, red point are daytime hours. The green dash line is the best fit line to all data; the black dotted lines are the ±2 m/s error envelope (top) and the ±30 degree error envelope (bottom). Fractions of data points within different bias ranges are shown at the top right of each plot. 4-6

Figure 4-5. Scatter plots of hourly temperature (K; top) and hourly humidity (g/kg, bottom) at DS472 sites in Austin for Run 10 (left) and for Run 11 (right). Blue points are nighttime hours, red point are daytime hours. The green dash line is the best fit line to all data; the black dotted lines are the ±2 K error envelope (top) and the ±2 g/kg error envelope (bottom). Fractions of data points within different bias ranges are shown at the top right of each plot. 4-7

Figure 4-6. Scatter plots of daily statistical performance against DS472 data in Austin for wind speed (top left), wind direction (top right), temperature (bottom left) and humidity (bottom right). Each plot shows daily performance from AACOG/CAPCOG Run 4 (red dots) and Run 11 (blue dots). The blue boxes represent the bias/error space bounded by the statistical performance benchmarks described in Section 1. 4-8

Figure 4-7. Scatter plots of hourly wind speed (m/s; top) and hourly wind direction (degrees, bottom) at DS472 sites in Dallas for Run 10 (left) and for Run 11 (right). Blue points are nighttime hours, red point are daytime hours. The green dash line is the best fit line to all data; the black dotted lines are the ±2 m/s error envelope (top) and the ±30 degree error envelope (bottom). Fractions of data points within different bias ranges are shown at the top right of each plot. 4-10

Figure 4-8. Scatter plots of hourly temperature (K; top) and hourly humidity (g/kg, bottom) at DS472 sites in Dallas for Run 10 (left) and for Run 11 (right). Blue points are nighttime hours, red point are daytime hours. The green dash line is the best fit line to all data; the black dotted lines are the ±2 K error envelope (top) and the ±2 g/kg error envelope (bottom). Fractions of data points within different bias ranges are shown at the top right of each plot. 4-11

Figure 4-9. Scatter plots of daily statistical performance against DS472 data in Dallas for wind speed (top left), wind direction (top right), temperature (bottom left) and humidity (bottom right). Each plot shows daily performance from AACOG/CAPCOG Run 4 (red dots) and Run 11 (blue dots). The blue boxes represent the bias/error space bounded by the statistical performance benchmarks described in Section 1. 4-12

Figure 4-10. Scatter plots of hourly wind speed (m/s; top) and hourly wind direction (degrees, bottom) at DS472 sites in Northeast Texas for Run 10 (left) and for Run 11 (right). Blue points are nighttime hours, red point are daytime hours. The green dash line is the best fit line to all data; the black dotted lines are the ±2 m/s error envelope (top) and the ±30 degree error envelope (bottom). Fractions of data points within different bias ranges are shown at the top right of each plot. 4-14

Figure 4-11. Scatter plots of hourly temperature (K; top) and hourly humidity (g/kg, bottom) at DS472 sites in Northeast Texas for Run 10 (left) and for Run 11 (right). Blue points are nighttime hours, red point are daytime hours. The green dash line is the best fit line to all data; the black dotted lines are the ±2 K error envelope (top) and the ±2 g/kg error envelope (bottom). Fractions of data points within different bias ranges are shown at the top right of each plot. 4-15

Figure 4-12. Scatter plots of daily statistical performance against DS472 data in Northeast Texas for wind speed (top left), wind direction (top right), temperature (bottom left) and humidity (bottom right). Each plot shows daily performance from AACOG/CAPCOG Run 4 (red dots) and Run 11 (blue dots). The blue boxes represent the bias/error space bounded by the statistical performance benchmarks described in Section 1. 4-16

Figure 4-13. Hourly time series of predicted (MM5 Runs 10 and 11) and diagnosed PBL depths from the New Braunfels wind profiler. 4-18

Figure 4-14. Hourly time series of predicted (MM5 Runs 10 and 11) and diagnosed PBL depths from the Moody wind profiler. 4-18

Figure 4-15. Hourly time series of predicted (MM5 Runs 10 and 11) and diagnosed PBL depths from the Huntsville wind profiler. 4-18

Figure 4-16. Hourly time series of predicted (MM5 Runs 10 and 11) and diagnosed PBL depths from the Cleburne wind profiler. 4-19

Figure 4-17. Hourly time series of predicted (MM5 Runs 10 and 11) and diagnosed PBL depths from the Longview wind profiler. 4-19

Figure 4-18. Observed (AHPS; top left) and MM5 simulated 24-hour accumulated precipitation (mm) for Runs 10 (top right) and 11 (bottom right), 7 AM June 14 to 7 AM June 15, 2006. 4-20

Figure 4-19. Simulated wind fields (left), CAMx cloud cover (middle), and rainfall (right) from MM5 Run 10 at 4 PM, June 13, 2006. 4-21
Figure 4-20. Simulated wind fields (left), CAMx cloud cover (middle), and rainfall (right) from MM5 Run 11 at 4 PM, June 13, 2006. 4-22

EXECUTIVE SUMMARY

ES.1 INTRODUCTION

This report documents the continuation of a meteorological modeling project for the State of Texas to support photochemical modeling of ozone episodes that occurred in the central and eastern Texas during June 2006. Ambient ozone concentrations during this period exceeded both the 1997 and 2008 8-hour ozone standards (85 ppb and 75 ppb, respectively) for many days throughout the state. In 2007, the Texas Commission on Environmental Quality (TCEQ) and ENVIRON International Corporation conducted preliminary meteorological modeling of central/eastern Texas for the June 2006 period. In late 2008, the Alamo Area Council of Governments (AACOG) and the Capitol Area Council of Governments (CAPCOG) jointly sponsored a project to improve upon the preliminary modeling with a focus on maximizing model performance in the San Antonio and Austin areas to support immediate photochemical modeling. The purpose of the current project is to continue to improve upon the AACOG/CAPCOG meteorological modeling and to expand the performance evaluation to Dallas and Northeast Texas. The meteorological model employed in all of these projects is the Fifth Generation Mesoscale Model (MM5; Dudhia, 1993; Grell et al., 1994).

ES.2 APPROACH

Three new MM5 simulations of the May 29 – June 16, 2006 period were conducted in an attempt to improve upon some of the performance issues identified in the previous study, namely: (1) reducing spurious convection and removing associated ground-level outflow patterns that degraded wind performance; (2) increasing boundary layer depths to levels observed in radar profiler data; and (3) improving the diurnal patterns of surface temperatures and reducing daytime temperature bias. The best of these MM5 simulations are to be used this summer in AACOG's photochemical modeling.

The simulations were conducted on a 108/36/12/4 nested grid system, with a large 4 km nest covering all of east Texas. The domain definition and much of the model configuration was based on the TCEQ Houston modeling and the subsequent ENVIRON work reported previously. Note that the definition of the 4-km modeling grid used in this study was consistent with the enlarged domain develop under the AACOG/CAPCOG work so that it would cover the San Antonio/Austin photochemical modeling domain.

The analyses of MM5 performance described in this report focused on qualitative and statistical comparisons to observed conditions. Qualitative evaluations consisted of graphical comparisons of surface wind fields among different runs, simulated PBL heights against diagnostic calculations from profiler data, and graphical comparisons to observed precipitation patterns. The diagnosed PBL depths from several profilers operating in the State of Texas were developed by Sonoma Technology, Inc. (STI, 2007) and provided by TCEQ. Measured 24-hourly precipitation data were obtained from the Advanced Hydrologic Prediction Service (AHPS) dataset (http://water.weather.gov/about.php). Daily AHPS precipitation rates ending at 1200 UTC are comprised of a blend of rain gauge measurements and radar data and are gridded to roughly 4-km resolution. These data were then mapped to the MM5 4-km grid for direct comparison against simulated fields.

The statistical analysis was split into four performance "zones" covering San Antonio, Austin, Dallas, and Northeast Texas. The observation data used for the quantitative assessment in each performance zone were extracted from the hourly DS472 airport observations used in the observation nudging (which include wind, temperature, and humidity). Whereas results from the DS472 statistics would conceivably exhibit minimal wind bias given that the same data are used to nudge MM5 during the simulation, TCEQ and ENVIRON mutually agreed to use DS472 data over other sources (e.g., CAMS observations) because of their strict instrumentation protocols specific to meteorological measurements and consistency with values reported by MM5.

ES.2 RESULTS

The configuration and results of each of the three specific runs conducted in this study are briefly described below. In general, impacts from each of the MM5 configuration changes were similar in all four evaluation areas.

Run 9

Configuration: As in Run 8, run for the 4-km grid only, removing the shallow cumulus parameterization and replacing the ETA PBL scheme with the Medium Range Forecast (MRF) PBL scheme to investigate impacts on PBL evolution and cumulus convection.

Results: Wind speed/direction performance was moderately improved, the nighttime temperature under prediction bias was mostly eliminated (large daytime over prediction bias was not impacted), and humidity performance was improved. PBL depths were much better simulated (deeper, with more rapid morning growth rates). Spurious convective rainfall was reduced substantially, reducing impacts on surface wind patterns.

Run 10

Configuration: As in Run 9, replacing the NOAH LSM with the 5-layer soil model (soil parameters defined by internal look-up table) to investigate impacts on surface temperature, PBL evolution, and cumulus convection. The LSM change required that all grids be re-run (108/36/12-km grids run 2-way interactive, 4-km grid run separately using 1-way nesting).

Results: Wind speed/direction performance was not significantly impacted (as expected), but the large daytime over prediction bias was mostly eliminated (good nighttime temperature performance was maintained), and humidity performance was slightly degraded associated with a slight humidity increase with the alternative LSM. The PBL depths were not significantly impacted by this change, but there was some evidence of increased cloud cover. Rainfall was altered substantially, with less convective activity but a shift in patterns that did not agree with observed conditions. The reduction in convective rainfall further reduced impacts on surface wind patterns.

Run 11

Configuration: As in Run 10, but only for the 4-km grid replacing surface wind observation nudging with 1-hour surface wind analysis nudging using a 1-hour ADP observation dataset in conjunction with 3-hour EDAS analyses.

Results: Wind speed/direction performance was improved in each of the four analysis areas (especially wind direction), while temperature and humidity performance remained

similar to Run 10. PBL depths were also consistent with Run 10 with only minor differences day-to-day. Rainfall patterns agreed better with observations, but maintained low levels of convective activity with similar cloud cover and little impact on surface wind patterns.

Each of the three simulations described above exhibited incremental improvements in winds, temperature, humidity, PBL, and rainfall performance. Ultimately, Run 11 has resulted in a very good meteorological simulation of May 30 – June 16, 2006 for each of the four areas of Texas evaluated in this study. Statistical performance for Run 11 is superior in all respects to the last AACOG/CAPCOG simulation (Run 8), and based on our experience, Run 11 is in many ways consistent with or better than many other meteorological simulations recently developed in south-central U.S. (e.g., previous episodes for Dallas, Houston, and Baton Rouge).

ES.3 RECOMMENDATIONS

Early in this project, we realized that the results from Run 9 were significantly better than Run 8, and so ENVIRON immediately used the Run 9 MM5 output fields in CAMx simulations conducted for AACOG to evaluate impacts to photochemical model performance in San Antonio and Austin. With the additional significant improvements achieved in Runs 10 and 11, ENVIRON has sent these outputs to AACOG as well for follow-up CAMx sensitivity runs to be conducted by AACOG. ENVIRON recommends and endorses the use of MM5 Run 11 for future photochemical modeling of eastern Texas for early June 2006 ozone episodes. ENVIRON further recommends that Run 11 be extended through the remainder of June 2006 to support photochemical modeling of episodes that occurred in late June.

1. INTRODUCTION

This report documents the continuation of a meteorological modeling project for the State of Texas to support photochemical modeling of ozone episodes that occurred in the central and eastern Texas during June 2006. Ambient ozone concentrations during this period exceeded both the 1997 and 2008 8-hour ozone standards (85 ppb and 75 ppb, respectively) for many days throughout the state. In 2007, the Texas Commission on Environmental Quality (TCEQ) and ENVIRON International Corporation conducted preliminary meteorological modeling of central/eastern Texas for the June 2006 period. In late 2008, the Alamo Area Council of Governments (AACOG) and the Capitol Area Council of Governments (CAPCOG) jointly sponsored a project to improve upon the preliminary modeling with a focus on maximizing model performance in the San Antonio and Austin areas to support immediate photochemical modeling. The purpose of the current project is to continue to improve upon the AACOG/CAPCOG meteorological modeling and to expand the performance evaluation to Dallas and Northeast Texas.

1.1 BACKGROUND

In 2007 the TCEQ conducted meteorological modeling of the May 29 – June 17, 2006 period to support the next round of technical analyses for the Houston State Implementation Plan (SIP). The TCEQ achieved acceptable meteorological model performance in the Houston area for the first half of June 2006 using a specific configuration of the Fifth Generation Mesoscale Model (MM5; Dudhia, 1993; Grell et al., 1994). Since the entire June 2006 period includes several periods with high ozone in Dallas, Northeast Texas, Austin, and San Antonio, TCEQ recognized that further meteorological model development for this period will support ongoing ozone modeling throughout central and eastern Texas.

Later the same year, TCEQ contracted with ENVIRON to extend the Houston MM5 simulation to the entire May 29 – July 3, 2006 period and to evaluate its performance over broader areas of the state (Kemball-Cook et al., 2007). MM5 performance against standard hourly airport observations was found to be partially adequate for photochemical modeling, and the model was found to exhibit an over abundance of afternoon convective activity on some high ozone days. However, while considered a good starting point, limitations in funding prevented further development, improvements and performance evaluation of this episode. As noted in the original modeling documentation, ENVIRON recommended several improvements, including additional data assimilation, alternative convective parameterizations, and additional precipitation verification.

In 2008, AACOG and CAPCOG jointly sponsored a study to improve MM5 performance specifically in south-central Texas, and to support immediate photochemical modeling requirements in the San Antonio area (Emery et al., 2009a). The domain definition and model configuration were based on the TCEQ Houston modeling and the subsequent 2007 ENVIRON work, and by design followed many of the recommendations therein. Model performance evaluation focused on comparisons to ambient measurements in the San Antonio and Austin areas. The MM5 configuration evolved over seven different MM5 simulations. A final best-performing configuration was run for the entire June 2006 period on a slightly enlarged 4-km modeling grid that could support the San Antonio/Austin photochemical modeling domain. The

final MM5 meteorological dataset was used in subsequent photochemical modeling for the AACOG (Emery et al., 2009b).

1.2 OBJECTIVES

This report describes a continuation of the AACOG/CAPCOG MM5 meteorological modeling reported by Emery et al. (2009a). The model performance evaluation was expanded to include comparisons to ambient measurements in the Dallas and Northeast Texas areas. Three new MM5 simulations of the May 29 – June 16, 2006 period were conducted in an attempt to improve upon some of the performance issues identified in the previous study, namely: (1) reducing spurious convection and removing associated ground-level outflow patterns that degraded wind performance; (2) increasing boundary layer depths to levels observed in radar profiler data; and (3) improving the diurnal patterns of surface temperatures and reducing daytime temperature bias. The best of these MM5 simulations are to be used this summer in AACOG's photochemical modeling.

Figure 1-1 and Table 1-1 present the MM5 modeling grid definition. The simulations were conducted on a 108/36/12/4 nested grid system, with a large 4 km nest covering all of east Texas. The domain definition and much of the model configuration was based on the TCEQ Houston modeling and the subsequent ENVIRON work reported previously. Note that the definition of the 4-km modeling grid used in this study was consistent with the enlarged domain develop under the AACOG/CAPCOG work so that it would cover the San Antonio/Austin photochemical modeling domain.

1.3 OVERVIEW OF MM5

The MM5 (Dudhia, 1993; Grell et al., 1994) is a three-dimensional, limited-area, non-hydrostatic, primitive equation, prognostic meteorological model that has been used widely in regional air quality model applications (Seaman, 2000). Over the past decade, researchers at Pennsylvania State University (PSU), the National Center for Atmospheric Research (NCAR), and the U.S. Environmental Protection Agency (EPA) have collaborated in the refinement and extension of the current version of the MM5 system, version 3.7. Originally developed in the 1970s at PSU and first documented by Anthes and Warner (1978), the MM5 modeling system maintains its status as a state-of-the-science model through enhancements provided by a broad user community (e.g., Xiu and Pleim, 2000). The MM5 modeling system is routinely employed in forecasting projects as well as refined investigations of severe weather. Utilization of MM5 for historical air quality applications is also a common practice; in recent years, the MM5 modeling system has been successfully applied in continental scale annual simulations for the years 1996, and 2001 through 2006. The MM5 enjoys a far richer application history in regulatory modeling studies compared with other models. Furthermore, in comparisons with other models of similar complexity in over 60 regional scale air quality application studies since 1995, it has generally been found that MM5 tends to produce better photochemical model inputs than alternative models (Emery et al., 2001). Due to its ongoing scientific development worldwide, extensive historical applications, broad user community support, public availability, and established performance record compared with other applications-oriented prognostic models, the TCEQ has been utilizing the MM5 as its preferred meteorological model.

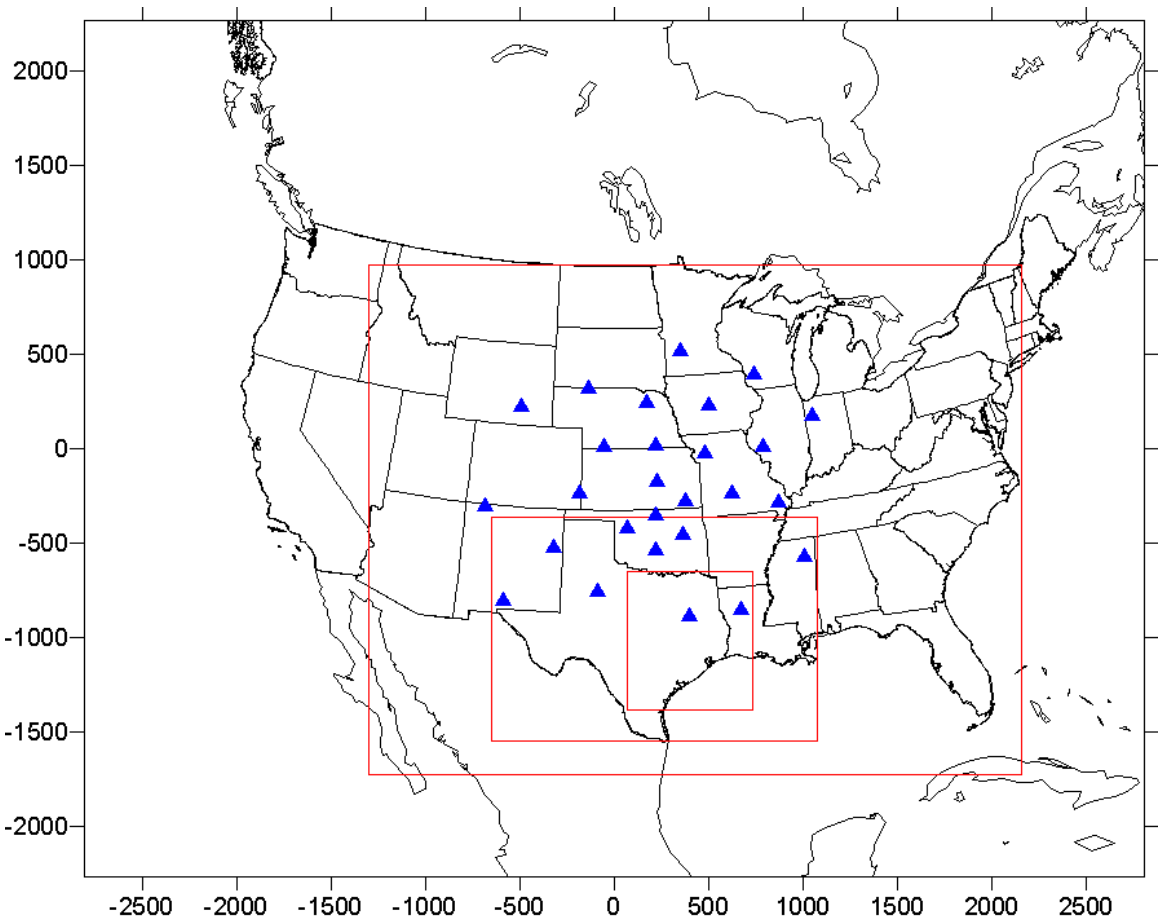

108 km Domain: 53 x 43
36 km Domain: 97 x 76
12 km Domain: 145 x 100
4 km Domain: 166 x 184

Figure 1-1. Four MM5 nested modeling domains showing the location of tropospheric profiler sites (blue triangles). The model projection is Lambert Conformal, with origin at 100°W/40°N, and true latitudes at 30°N and 60°N. Note that the 4-km grid shown here represents the original size defined by TCEQ; the current study employed a slightly enlarged 4-km grid to support the AACOG/CAPCOG photochemical modeling grid.

Table 1-1. MM5 vertical layer structure.

Layer	Sigma	Pressure (mb)	Height (m)	Thickness (m)
43	0.0000	50.00	20820.97	890.18
42	0.0100	59.63	19930.79	1152.48
41	0.0250	74.08	18778.31	1296.15
40	0.0450	93.34	17482.16	1103.86
39	0.0650	112.60	16378.30	1188.86
38	0.0900	136.67	15189.44	1033.53
37	0.1150	160.75	14155.91	1088.51
36	0.1450	189.64	13067.40	962.55
35	0.1750	218.53	12104.85	1000.66
34	0.2100	252.23	11104.19	1018.20
33	0.2500	290.75	10085.99	913.19
32	0.2900	329.27	9172.80	829.18
31	0.3300	367.79	8343.63	760.31
30	0.3700	406.31	7583.32	617.73
29	0.4050	440.02	6965.59	579.58
28	0.4400	473.72	6386.01	546.18
27	0.4750	507.43	5839.83	516.68
26	0.5100	541.13	5323.14	421.86
25	0.5400	570.02	4901.29	404.30
24	0.5700	598.91	4496.98	388.25
23	0.6000	627.80	4108.73	373.51
22	0.6300	656.69	3735.22	359.92
21	0.6600	685.58	3375.30	347.36
20	0.6900	714.47	3027.94	335.70
19	0.7200	743.36	2692.24	324.85
18	0.7500	772.25	2367.39	262.95
17	0.7750	796.33	2104.43	256.31
16	0.8000	820.40	1848.13	250.01
15	0.8250	844.48	1598.12	244.04
14	0.8500	868.55	1354.08	143.68
13	0.8650	883.00	1210.39	141.70
12	0.8800	897.44	1068.69	139.78
11	0.8950	911.89	928.92	137.91
10	0.9100	926.33	791.01	90.93
9	0.9200	935.96	700.08	90.13
8	0.9300	945.59	609.95	89.36
7	0.9400	955.22	520.59	88.59
6	0.9500	964.85	432.00	87.84
5	0.9600	974.48	344.15	87.11
4	0.9700	984.11	257.04	86.39
3	0.9800	993.74	170.66	85.68
2	0.9900	1003.37	84.98	51.07
1	0.9960	1009.15	33.91	33.91
0	1.0000	1013.00	0.00	

The databases required to set up, exercise, and evaluate MM5 for the June 2006 period consist of various fixed and variable inputs.

- High-resolution topographic (terrain elevation) fields available from NCAR;
- High-resolution vegetation type and land use fields available from NCAR;
- Large-scale observational analyses of winds, temperature, and humidity on standard pressure levels, and surface and soil temperature, available from NCAR and derived from the National Center for Environmental Prediction (NCEP) Eta Data Analysis System (EDAS) (40 km resolution);
- Surface and upper-air meteorological measurement data from the standard National Weather Service (NWS) reporting network available from NCAR, as well as special study data from the TexAQS II field campaign.

To give some historical context, one of the most important performance issues associated with MM5 is its sensitivity to the large number of options for coupling of the surface energy budget model (land surface model, or LSM) with the planetary boundary layer (PBL) model. First, the LSM-PBL couple frequently predicts spotty areas with very low mixing heights that can appear as "holes" in the PBL fields. These PBL holes are usually associated with convective activity and they often affect subsequent air quality modeling. Effects are often much worse in the more arid western U.S. Second, the land surface models, while representing the current state-of-the-science approach for surface heat budgets and momentum fluxes, are by necessity a broad-brush representation of soil and vegetation characteristics and are subject to the fidelity and resolution of current land cover and soil type databases. All of the land surface models employed in MM5 have a history of generating damped diurnal temperature waves (high temperatures at night, low temperatures during the day). Third, MM5 has been shown to generate too much convective warm-season precipitation, in both spatial coverage and intensity, which can have significant negative impacts on local wind, temperature, and PBL performance. Fourth, there is a stochastic component of real world meteorology that is not captured by MM5. For example, for some pollutant episodes stagnation is an important attribute that MM5 fails to simulate well as it tends to organize the flow fields. This often leads to an over prediction bias in wind speeds, and poor performance for wind direction under stagnant conditions. Finally, the MM5 model is showing its age, even though it represents approximately 20 years of development by various researchers. The many limitations in MM5 have spawned the development of a new meteorological model, the Weather Research Forecast (WRF) model, which is scheduled to ultimately replace MM5.

1.4 OVERVIEW OF APPROACH

ENVIRON ran three MM5 simulations in a stepwise manner to investigate impacts on performance in replicating local meteorological observation data in San Antonio, Austin, Dallas, and Northeast Texas. The approach followed the recommendations of Emery et al. (2009a) and TCEQ staff. The analysis of MM5 performance for each run was carried out in a manner similar to the previous modeling. To ensure consistency with ENVIRON's previous MM5 simulations, and to correctly diagnose the impact of observation nudging and various physics changes on the MM5 results, we carried the previous MM5 domain, physics, and nudging configuration from AACOG/CAPCOG "Run 8" forward into this project.

The three coarse domains (108/36/12 km) shown in Figure 1-1 were run following the exact methodology from the previous modeling, utilizing two-way nesting with 1-point feedback and

light smoothing. The 4 km domain was run with one-way nesting using 12 km MM5 model output to generate the 4 km domain boundary conditions through the MM5 NESTDOWN processor. The model physics options for AACOG/CAPCOG "Run 8" are summarized in Table 1-2.

Table 1-2. Physics options used for the AACOG/CAPCOG June 2006 MM5 "Run 8" simulation by grid (Emery et al., 2009a).

Treatment	108/36/12 km	4 km
Cumulus Parameterization	Grell	None
Shallow convection	No	Yes
Radiation (Long-wave/Short-wave)	RRTM/Dudhia	RRTM/Dudhia
Cloud Microphysics	Simple Ice	Simple Ice
PBL/LSM	ETA TKE/NOAH	ETA TKE/NOAH

RRTM = Rapid Radiative Transfer Model
ETA TKE = Turbulent kinetic energy (TKE) scheme used in the NCEP Eta model
NOAH = A variant of the Oregon State University LSM

Four Dimensional Data Assimilation (FDDA) is used to "nudge" model predictions toward observational analyses and/or discrete measurements to control model "drift" from conditions that actually occurred. This approach has consistently been shown to provide powerful advantages in running meteorological models for multi-day episodes, and has become the standard approach to support historical photochemical applications. MM5 may be nudged toward gridded observational analyses ("analysis nudging") or toward observational data recorded at discrete points ("observation nudging"). Analysis nudging is performed using three-dimensional (3D) and/or surface (2D) gridded fields from data sets such as EDAS, and is usually applied at 3 or 6 hour intervals. Usually, 3D analysis nudging is applied above the PBL depth to control the evolution of the free troposphere while letting the model evolve PBL features independently. Observational nudging is applied at the data reporting frequency, usually hourly.

Tables 1-3 and 1-4 display the nudging performed in the AACOG/CAPCOG "Run 8" simulation. 3D analysis nudging of all variables (winds, temperature, humidity) above the PBL were performed on all grids (108, 36, 12 and 4 km); surface analysis nudging was performed for all variables on the 108 and 36 km grids, and for winds on the 12 and 4 km grids. All analysis nudging files were developed from 3-hour EDAS fields. Observation nudging was performed using hourly winds from the National Oceanic and Atmospheric Administration (NOAA) Profiler Network (NPN), special TexAQS II profiler data, and hourly airport surface winds from datasets archived at NCAR (referred to as DS472). The DS472 surface data were used for surface observation nudging of wind only on all grids, while profiler data were used for observation nudging of upper air wind only on the 12 and 4 km grids. Note that nudging strengths for both surface and upper air observation nudging were set to the same value. Additional observation nudging parameters included:

Horizontal radius of influence = 60 km;
Vertical radius of influence = 0.001 sigma (roughly ±5 meters at sea level);
Half-period of time window = 40 min.

Table 1-3. Analysis nudging coefficients used in the AACOG/CAPCOG "Run 8" June 2006 MM5 simulation.

	3D Nudging Coefficients (s^{-1}) above PBL			
Nudged Field	**108 km**	**36 km**	**12 km**	**4km**
Winds	$2.5x10^{-4}$	$1.0x10^{-4}$	$1.0x10^{-4}$	$1.0x10^{-4}$
Temperature	$2.5x10^{-4}$	$1.0x10^{-4}$	$1.0x10^{-4}$	$1.0x10^{-4}$
Humidity	$1.0x10^{-5}$	$1.0x10^{-5}$	$1.0x10^{-5}$	$1.0x10^{-5}$
	Surface Nudging Coefficients (s^{-1})			
Winds	$2.5x10^{-4}$	$1.0x10^{-4}$	$1.0x10^{-4}$	n/a
Temperature	$2.5x10^{-4}$	$1.0x10^{-4}$	n/a	n/a
Humidity	$1.0x10^{-5}$	$1.0x10^{-5}$	n/a	n/a

Table 1-4. Observation nudging coefficients used in the AACOG/CAPCOG "Run 8" June 2006 MM5 simulation.

	Nudging Coefficients (s^{-1})			
Nudged Field	**108 km**	**36 km**	**12 km**	**4km**
Winds	$4.0x10^{-4}$ Surface Obs	$4.0x10^{-4}$ Surface Obs	$4.0x10^{-4}$ Profiler Obs + Surface Obs	$4.0x10^{-4}$ Profiler Obs + Surface Obs
Temperature	n/a	n/a	n/a	n/a
Humidity	n/a	n/a	n/a	n/a

The MM5 modeling period under study covers the period May 29 – June 16, 2006, requiring a 19-day simulation. The MM5 solution is subject to increasing error over the course of an extended simulation due to uncertainties in initial/boundary conditions, limits in spatial and temporal resolution, and simplification and discretization in the governing equations. To reduce error propagation through the simulation, MM5 was run in sequential 5-day segments, being re-initialized from EDAS fields at the beginning of each 5-day period. Each 5-day segment included an initial 24 hour spin-up period that overlapped the last 24 hours of the preceding segment. Previous MM5 modeling by many groups over the past decade has shown this practice produces reliable meteorological databases suitable for air quality modeling over extended time periods (Kemball-Cook et al. 2004). The May 29 – June 16, 2006 episode simulation consisted of five 5-day segments; each 5-day segment started at 12 UTC and was 7200 minutes in length.

ENVIRON ran three different MM5 sensitivity simulations and quantitatively compared model output fields on the 4 km grid against hourly surface wind, temperature, and humidity observations in the San Antonio, Austin, Dallas, and Northeast Texas areas. Qualitative assessments were also made for PBL depths, surface wind fields, rainfall patterns, and cloud distributions. Statistical and qualitative comparisons were also made against two previous AACOG/CAPCOG simulations, as described below:

> **Run 4**: As in Run 8, but with the original (smaller) 4-km modeling grid and without the shallow cumulus parameterization applied on the 4-km grid.
>
> **Run 8**: As described above, using the expanded 4 km grid and shallow cumulus parameterization applied on the 4-km grid.

The three specific runs conducted in this study are briefly described below:

Run 9: As in Run 8, run for the 4-km grid only, removing the shallow cumulus parameterization and replacing the ETA PBL scheme with the Medium Range Forecast (MRF) PBL scheme to investigate impacts on PBL evolution and cumulus convection.

Run 10: As in Run 9, replacing the NOAH LSM with the 5-layer soil model (soil parameters defined by internal look-up table) to investigate impacts on surface temperature, PBL evolution, and cumulus convection. The LSM change required that all grids be re-run (108/36/12-km grids run 2-way interactive, 4-km grid run separately using 1-way nesting).

Run 11: As in Run 10, but only for the 4-km grid replacing surface wind observation nudging with 1-hour surface wind analysis nudging using a 1-hour ADP observation dataset in conjunction with 3-hour EDAS analyses.

The following sections report on the results of each of these MM5 simulations, including both quantitative and qualitative assessments of performance. An overview of the performance evaluation approach is provided below.

1.4.1 Model Performance Evaluation

A detailed model evaluation over monthly time scales and regional spatial scales is very difficult to summarize in a single document; therefore we rely on statistics to characterize how well a model replicated conditions over the entire spatio-temporal scale. The model evaluation approach was based on a quantitative analysis of bias and error statistics for wind speed, direction, temperature, and humidity. Each statistical metric was compared to performance benchmarks to determine meteorological representativeness for the specific modeling period. The question then reduces to: "what represents acceptable vs. unacceptable statistical performance for this episode and location?"

Emery et al. (2001) derived and proposed a set of daily performance "benchmarks" for typical meteorological model performance. These standards were based upon the evaluation of about 30 meteorological simulations (using MM5, RAMS and other models) since 1993 in support of air quality applications as reported by Tesche et al. (2001) and other studies. The purpose of these benchmarks was not to give a passing or failing grade to any one particular meteorological model application, but rather to put its results into the proper context of other models and meteorological data sets. Since 2001, the benchmarks have been promoted by the EPA-sponsored National Ad Hoc Meteorological Modeling Group[1] and have been consistently relied upon to evaluate MM5 performance in many regulatory modeling projects throughout the U.S. The benchmarks for each variable are:

[1] The Ad Hoc Meteorological Modeling Group was assembled by EPA and the Lake Michigan Air Directors Consortium (LADCo) in 2000 as an annual forum to address meteorological modeling issues specifically in the context of supporting air quality modeling programs.

- Wind speed bias: ±0.5 m/s
- Wind speed RMSE[2]: 2.0 m/s
- Wind speed IoA[3]: 0.6
- Wind direction bias: ±10 degrees
- Wind direction gross error: 30 degrees
- Temperature bias: ±0.5 K
- Temperature gross error: 2.0 K
- Temperature IoA: 0.8
- Mixing ratio bias: ±1.0 g/kg
- Mixing ratio gross error: 2.0 g/kg
- Mixing ratio IoA: 0.6

Being outside one or more of these ranges does not mean the meteorological data fields for a particular parameter are unacceptable. However, such a result indicates that caution should be exercised in the use of such variables, and in interpreting subsequent air quality modeling based on those meteorological fields. Note that recently participants of the National Ad Hoc Meteorological Modeling Group have questioned the value of the Index of Agreement (IoA) metric as a reliable measure of model performance, and have suggested that it should be de-emphasized. Within the context of the modeling reported herein, if wind, temperature and humidity bias and error statistics are reasonably near their respective benchmarks, the meteorology was considered representative.

1.4.2 Data Used for Performance Evaluation

The analyses of MM5 performance described in this report focused on qualitative and statistical comparisons to observed conditions. Qualitative evaluations consisted of graphical comparisons of surface wind fields among different runs, simulated PBL heights against diagnostic calculations from profiler data, and graphical comparisons to observed precipitation patterns. The diagnosed PBL depths from several profilers operating in the State of Texas were developed by Sonoma Technology, Inc. (STI, 2007) and provided by TCEQ (Figure 1-2). Measured 24-hourly precipitation data were obtained from the Advanced Hydrologic Prediction Service (AHPS) dataset (http://water.weather.gov/about.php). Daily AHPS precipitation rates ending at 1200 UTC are comprised of a blend of rain gauge measurements and radar data and are gridded to roughly 4-km resolution. These data were then mapped to the MM5 4-km grid for direct comparison against simulated fields.

The statistical analysis was split into four performance "zones" covering San Antonio, Austin, Dallas, and Northeast Texas. The observation data used for the quantitative assessment in each performance zone were extracted from the hourly DS472 airport observations used in the observation nudging (which include wind, temperature, and humidity). The sites used in the statistical performance evaluation for each of the four areas are mapped in Figures 1-3 through 1-6. Whereas results from the DS472 statistics would conceivably exhibit minimal wind bias given that the same data are used to nudge MM5 during the simulation, TCEQ and ENVIRON mutually agreed to use DS472 data over other sources (e.g., CAMS observations) because of

[2] Root mean square error
[3] Index of agreement

their strict instrumentation protocols specific to meteorological measurements and consistency with values reported by MM5.

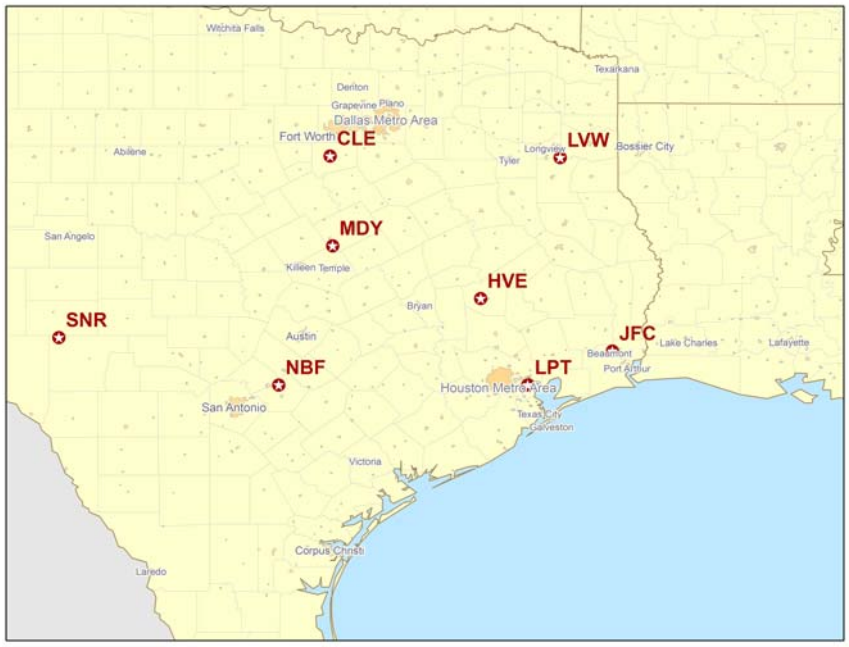

Figure 1-2. Locations of wind profiler sites throughout Texas at which PBL depths were derived by STI (2007). PBL depths were compared to MM5 simulated values at New Braunfels (NBF), Moody (MDY), Cleburne (CLE), Huntsville (HVE), and Longview (LVW).

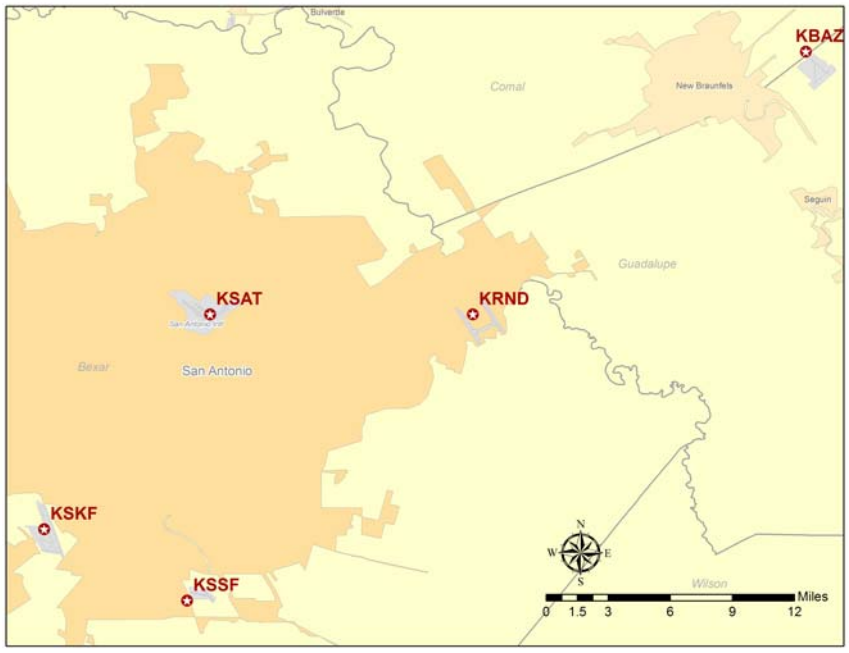

Figure 1-3. Locations of surface meteorological measurement sites available in the DS472 dataset in the vicinity of San Antonio.

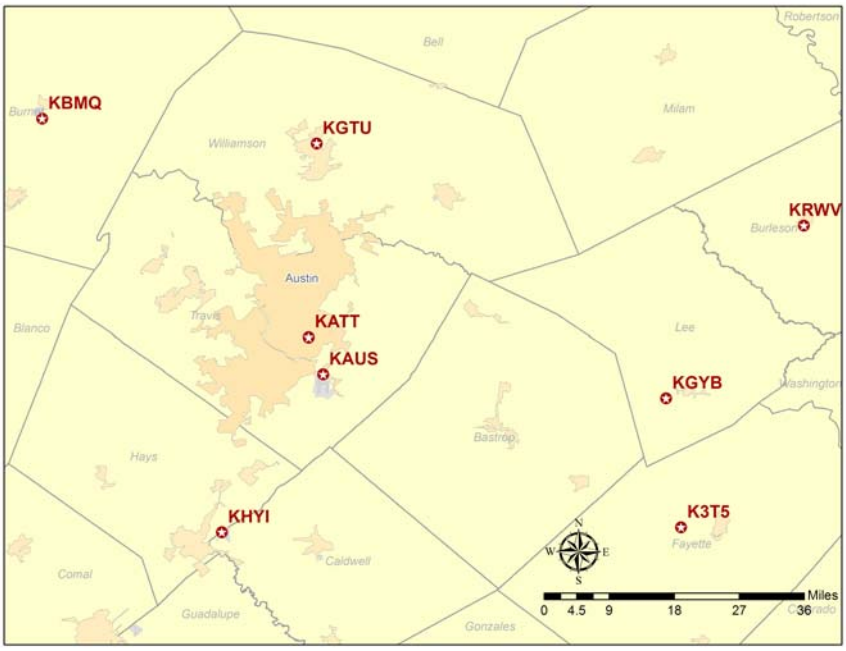

Figure 1-4. Locations of surface meteorological measurement sites available in the DS472 dataset in the vicinity of Austin.

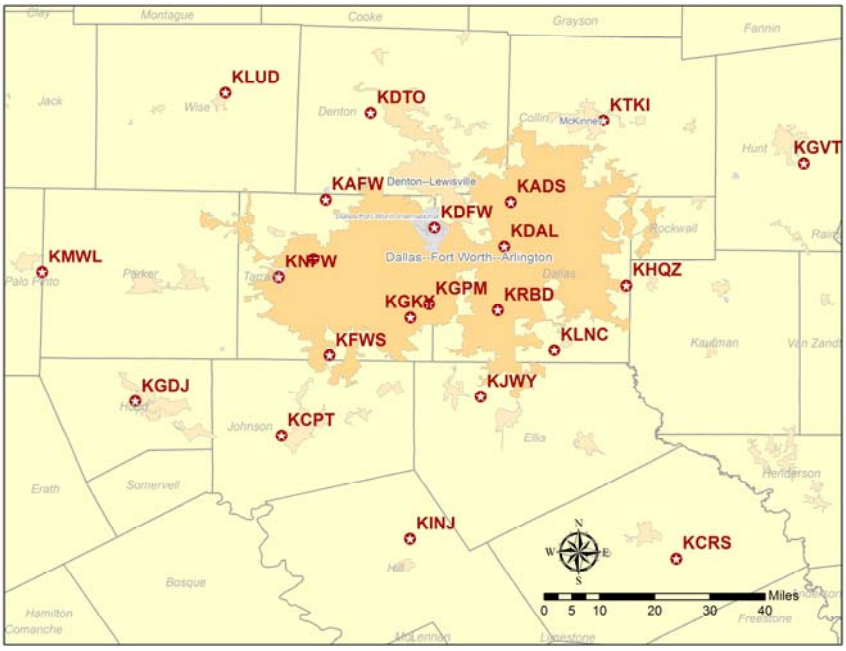

Figure 1-5. Locations of surface meteorological measurement sites available in the DS472 dataset in the vicinity of Dallas.

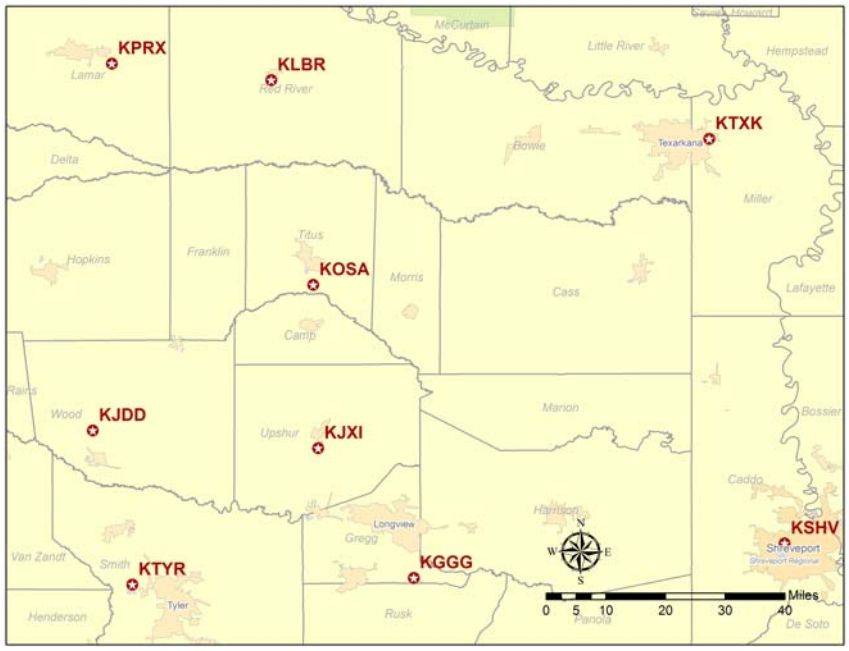

Figure 1-6. Locations of surface meteorological measurement sites available in the DS472 dataset in the vicinity of Northeast Texas.

2. ALTERNATIVE PBL TREATMENT

The first MM5 simulation conducted in this study (Run 9) was based on the final "Run 8" performed in the AACOG/CAPCOG modeling project. Run 9 was applied on the expanded 4-km grid only, removed the shallow cumulus parameterization, and replaced the ETA turbulent kinetic energy PBL scheme with the Medium Range Forecast (MRF) PBL scheme to investigate impacts on PBL evolution and cumulus convection. The MRF approach is not based on turbulent kinetic energy, but is instead a "K-theory" closure approach that derives a diffusivity profile according to surface layer stability during the daytime. Historically the MRF scheme has established a reputation for developing much deeper PBL mixing than any of the other options available in MM5, often too high. In contrast, the ETA scheme has historically developed much weaker and shallower mixing, often too low. This test was performed specifically to maximize boundary layer mixing to vent convective energy with the expectation that it would control spurious thunderstorm activity and improve daytime surface temperature.

Results of Run 9 were visually and statistically compared to a previous run reported by Emery et al. (2009a) to establish context for the performance of the first MM5 simulation undertaken in this project. The previous run selected for the comparison was Run 4, which from a physics configuration standpoint was the most consistent with Run 9 (no shallow convection) although Run 4 was not run on the expanded 4 km grid. Statistical bias and error metrics were generated on both hourly and daily time scales and compared to the benchmarks for meteorological model performance described in Section 1. The same types of performance figures are shown for all four analysis areas (San Antonio, Austin, Dallas, and Northeast Texas).

2.1 SAN ANTONIO

Figures 2-1 and 2-2 show scatter plots of hourly MM5 wind speed, wind direction, temperature, and humidity against DS472 observations in the San Antonio analysis region for MM5 Runs 4 and 9. Blue points are nighttime hours, red point are daytime hours. The green dash line is the best fit line to all data; the black dotted lines represent the benchmark error envelope. Fractions of data points within different bias ranges are shown at the top right of each plot.

Figure 2-3 shows scatter plots of daily statistical performance against DS472 observations for wind speed, wind direction, temperature, and humidity in the San Antonio analysis region. Each plot shows daily performance from Run 4 (red points) and Run 9 (blue points). The blue boxes represent the bias/error space bounded by the statistical performance benchmarks for described in Section 1.

These results show that Run 9 exhibits a better balance of hourly wind speed under and over predictions than Run 4 for both day and night hours, with a slightly larger fraction of points within all three bias ranges. The daily wind speed under prediction bias is somewhat improved throughout the modeling period. Hourly wind direction scatter points are also better aligned along the 1:1 line in Run 9 with a slightly larger fraction of points within all three bias ranges. Like Run 4, Run 9 shows more wind direction scatter in the daytime than during the night. Daily wind direction bias is slightly improved in Run 9.

Hourly temperature performance in Run 9 shows large gross error associated with over predictions of daytime temperature, but the under predictions of nighttime temperatures are

greatly improved relative to Run 4. The daily temperature bias shifts to large over predictions with minimal effect on daily gross error. Hourly humidity scatter diagrams do not look particularly better than Run 4, but the hourly statistics (regression, fraction of data within all bias envelopes, etc.) do show some improvements. The daily statistics show no significant improvement.

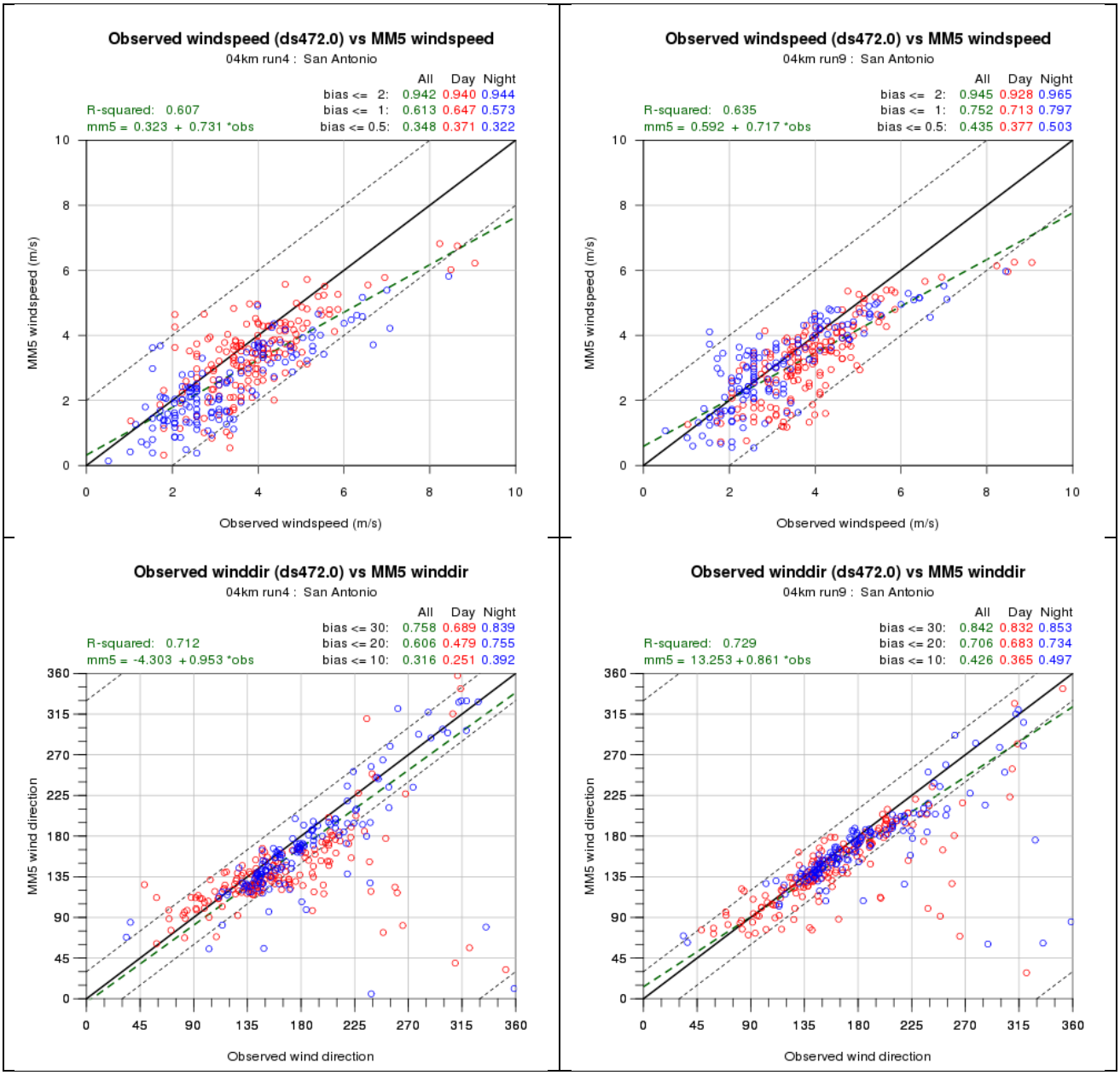

Figure 2-1. Scatter plots of hourly wind speed (m/s; top) and hourly wind direction (degrees, bottom) at DS472 sites in San Antonio for AACOG/CAPCOG Run 4 (left) and for Run 9 (right). Blue points are nighttime hours, red point are daytime hours. The green dash line is the best fit line to all data; the black dotted lines are the ±2 m/s error envelope (top) and the ±30 degree error envelope (bottom). Fractions of data points within different bias ranges are shown at the top right of each plot.

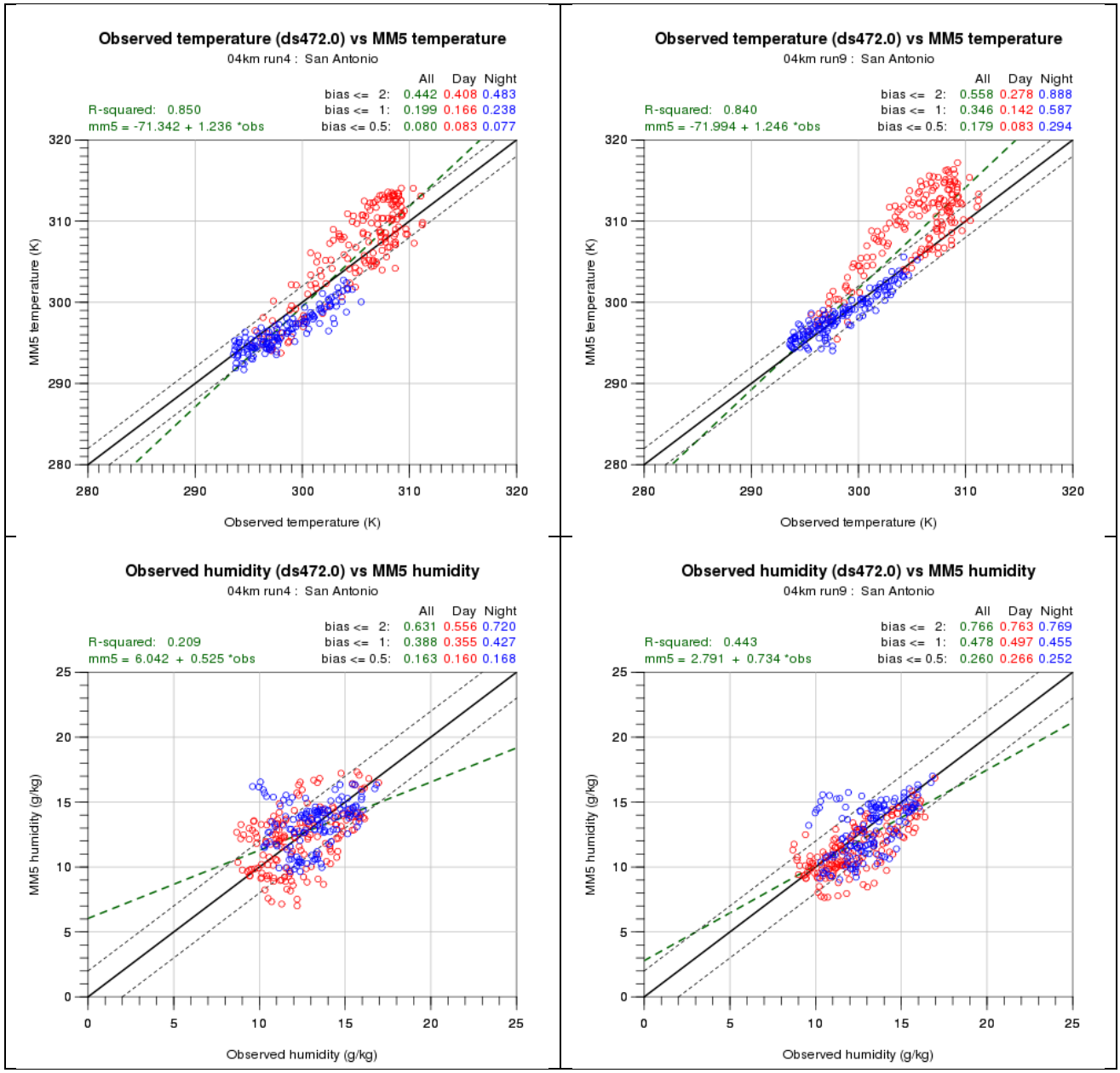

Figure 2-2. Scatter plots of hourly temperature (K; top) and hourly humidity (g/kg, bottom) at DS472 sites in San Antonio for AACOG/CAPCOG Run 4 (left) and for Run 9 (right). Blue points are nighttime hours, red point are daytime hours. The green dash line is the best fit line to all data; the black dotted lines are the ±2 K error envelope (top) and the ±2 g/kg error envelope (bottom). Fractions of data points within different bias ranges are shown at the top right of each plot.

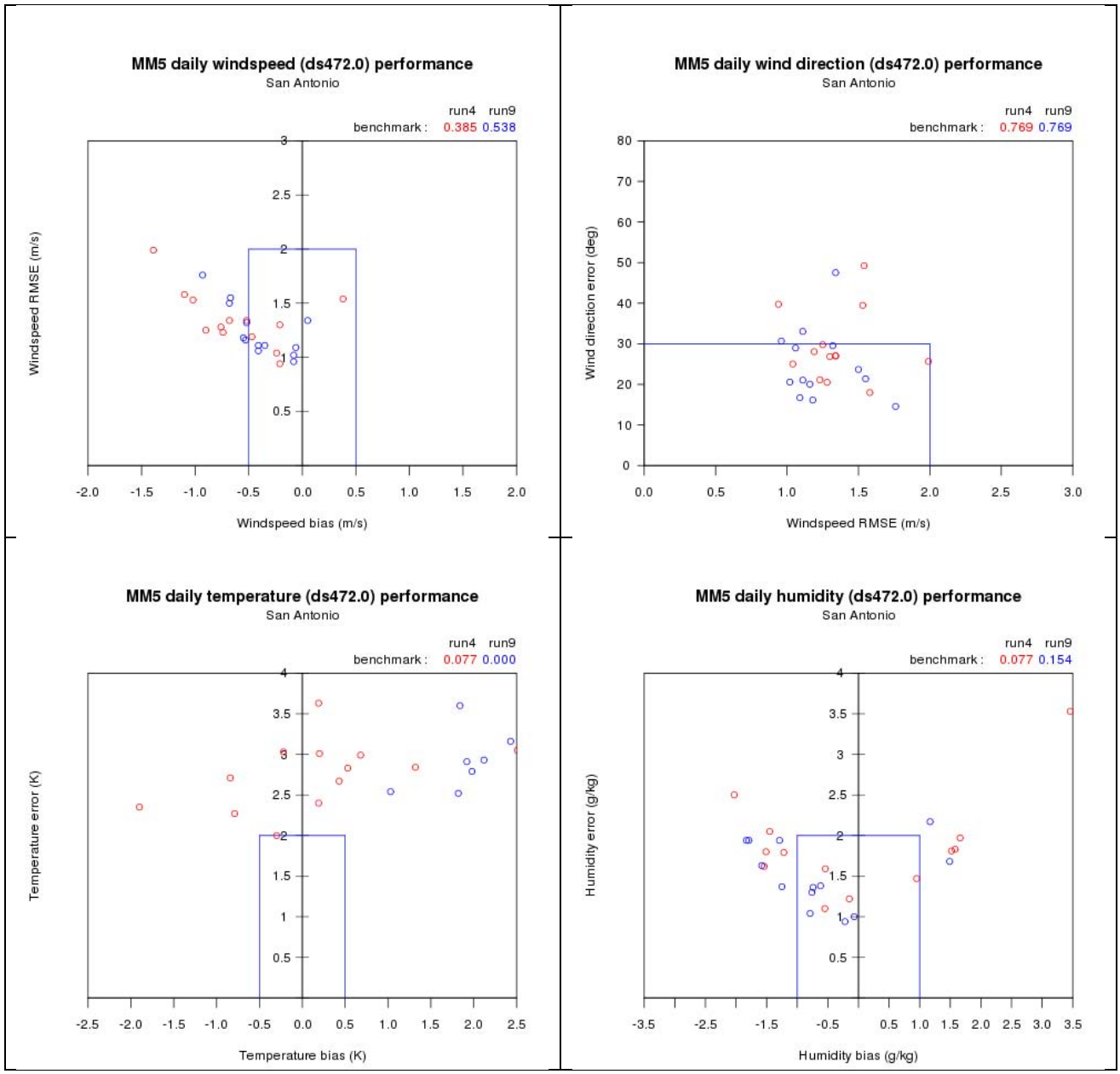

Figure 2-3. Scatter plots of daily statistical performance against DS472 data in San Antonio for wind speed (top left), wind direction (top right), temperature (bottom left) and humidity (bottom right). Each plot shows daily performance from AACOG/CAPCOG Run 4 (red dots) and Run 9 (blue dots). The blue boxes represent the bias/error space bounded by the statistical performance benchmarks described in Section 1.

2.2 AUSTIN

Figures 2-4 and 2-5 show scatter plots of hourly MM5 wind speed, wind direction, temperature, and humidity against DS472 observations in the Austin analysis region for MM5 Runs 4 and 9. Figure 2-6 shows scatter plots of daily statistical performance against DS472 observations for wind speed, wind direction, temperature, and humidity in the Austin analysis region.

Run 9 exhibits a shift from under to over predicted nighttime wind speed and a wider (but better balanced) spread of daytime wind speeds. This effect reduces the fraction of data within the three bias ranges, leading to slightly worse performance than Run 4. Daily average statistics show a similar shift from under to over prediction bias with little impact on RMSE. As seen in San Antonio, hourly wind direction scatter points are better aligned and contained along the 1:1 line in Run 9, but the various statistics are slightly (not significantly) worse. There are no obvious changes in daily wind direction performance. Overall, wind performance continues to be quite good in Austin.

As similarly seen in San Antonio, hourly temperature performance in Run 9 shows over predictions of daytime temperature, but the under predictions of nighttime temperatures are generally improved. The daily temperature bias shifts to large over predictions with some minor improvement to daily gross error. Hourly humidity scatter diagrams are similar to Run 4 with some improvements to hourly statistics. However, the daily statistics show a definite trend toward low bias and gross error.

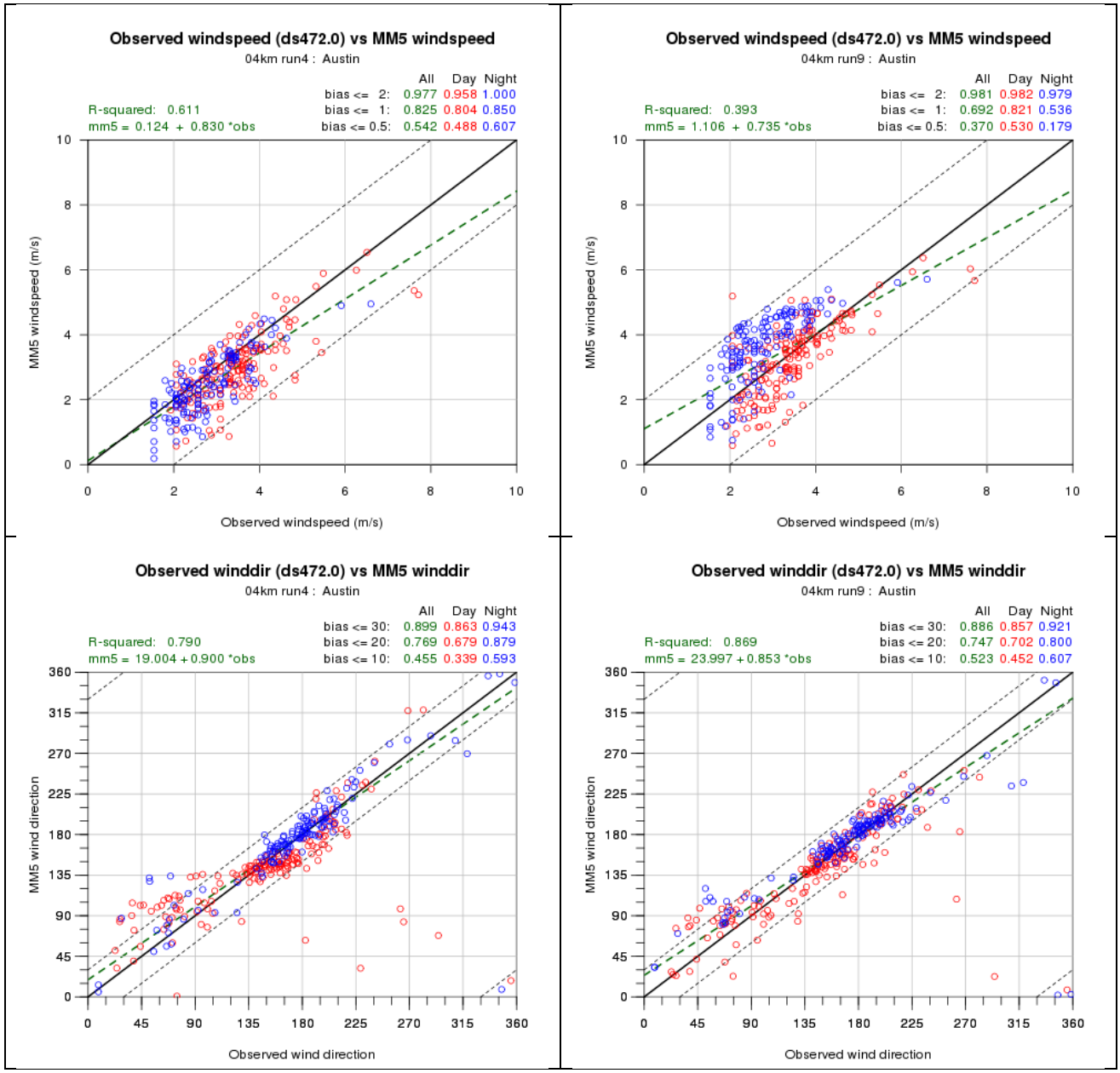

Figure 2-4. Scatter plots of hourly wind speed (m/s; top) and hourly wind direction (degrees, bottom) at DS472 sites in Austin for AACOG/CAPCOG Run 4 (left) and for Run 9 (right). Blue points are nighttime hours, red point are daytime hours. The green dash line is the best fit line to all data; the black dotted lines are the ±2 m/s error envelope (top) and the ±30 degree error envelope (bottom). Fractions of data points within different bias ranges are shown at the top right of each plot.

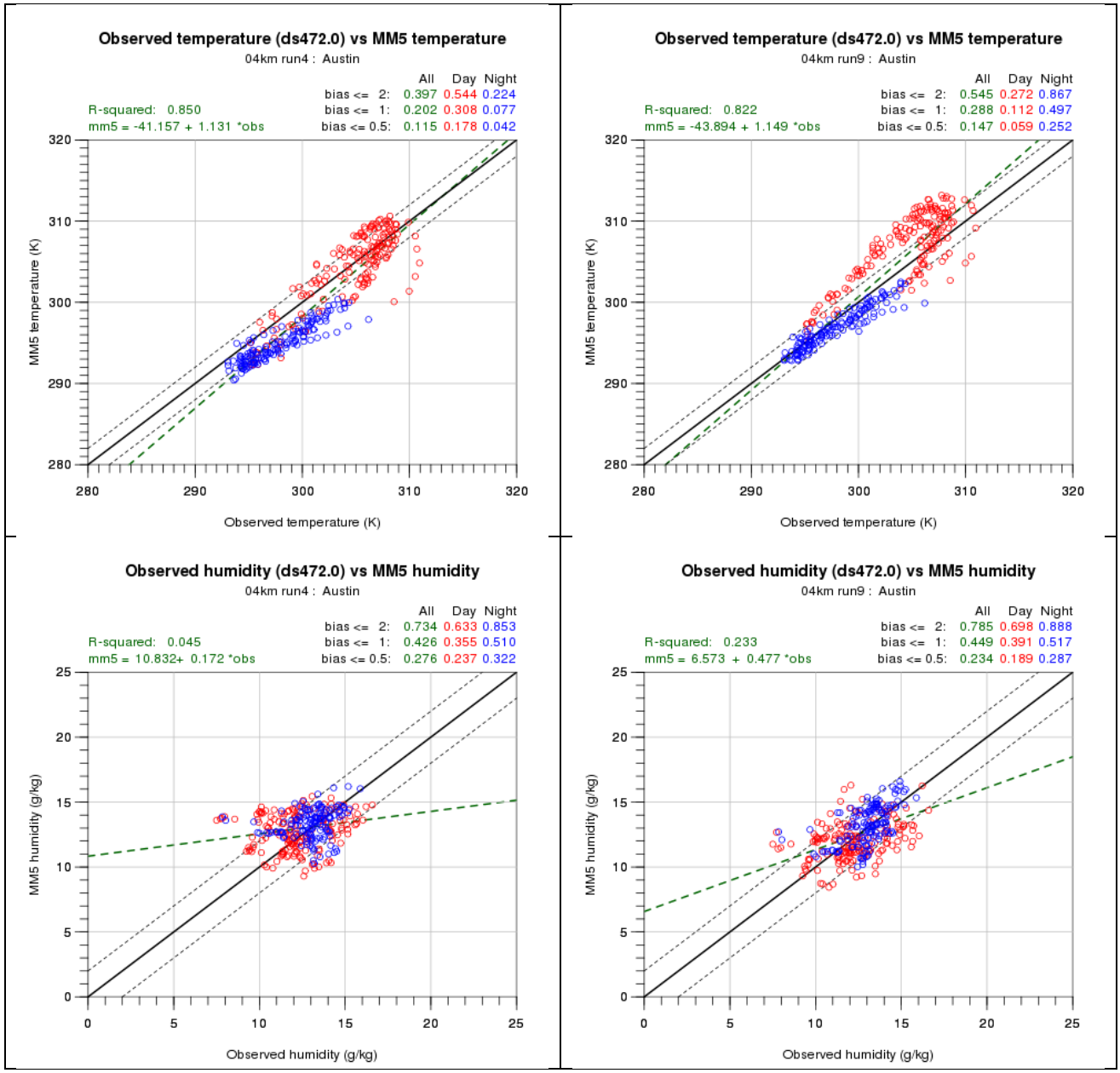

Figure 2-5. Scatter plots of hourly temperature (K; top) and hourly humidity (g/kg, bottom) at DS472 sites in Austin for AACOG/CAPCOG Run 4 (left) and for Run 9 (right). Blue points are nighttime hours, red point are daytime hours. The green dash line is the best fit line to all data; the black dotted lines are the ±2 K error envelope (top) and the ±2 g/kg error envelope (bottom). Fractions of data points within different bias ranges are shown at the top right of each plot.

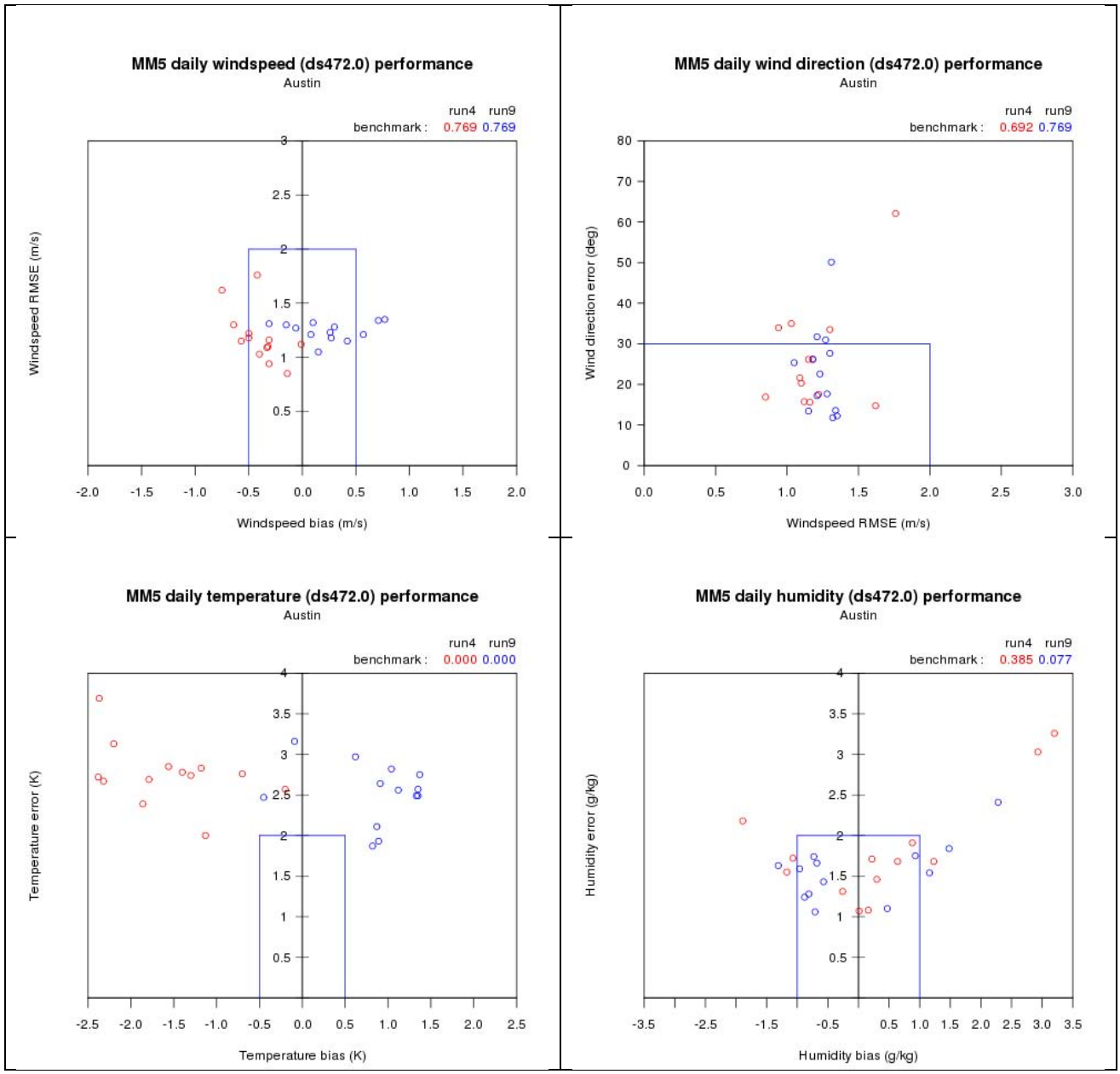

Figure 2-6. Scatter plots of daily statistical performance against DS472 data in Austin for wind speed (top left), wind direction (top right), temperature (bottom left) and humidity (bottom right). Each plot shows daily performance from AACOG/CAPCOG Run 4 (red dots) and Run 9 (blue dots). The blue boxes represent the bias/error space bounded by the statistical performance benchmarks described in Section 1.

2.3 DALLAS

Figures 2-7 and 2-8 show scatter plots of hourly MM5 wind speed, wind direction, temperature, and humidity against DS472 observations in the Dallas analysis region for MM5 Runs 4 and 9. Figure 2-9 shows scatter plots of daily statistical performance against DS472 observations for wind speed, wind direction, temperature, and humidity in the Dallas analysis region.

Hourly wind speed differences between Run 9 and Run 4 are mostly related to shifts from under to over predictions, with little change in overall spread of data points. Nighttime speeds in particular show an over prediction tendency. This impacts daily speed performance, with a shift to over predictions but little impact on RMSE. The daily average performance is slightly better, even with the apparent worse performance in hourly nighttime performance. Hourly wind direction scatter is much improved in Run 9, especially for daytime (and some nighttime) northeast winds. The daily average wind direction scatter plots are more tightly grouped, showing more consistent day-to-day performance than in Run 4; otherwise, wind performance was not significantly impacted in Run 9, and continues to be quite good.

As similarly seen in the southern cities, hourly temperature performance in Run 9 shows over predictions of daytime temperature, but the under predictions of nighttime temperatures are greatly improved. This shifts the daily temperature bias to large over predictions with no change to daily gross error. Hourly humidity scatter diagrams are also greatly improved relative to Run 4, which was not seen in the southern cities. Perhaps improved Run 9 precipitation patterns in north-central Texas have a positive impact on the humidity simulation. The daily statistics show much improved humidity performance and overall a very good simulation.

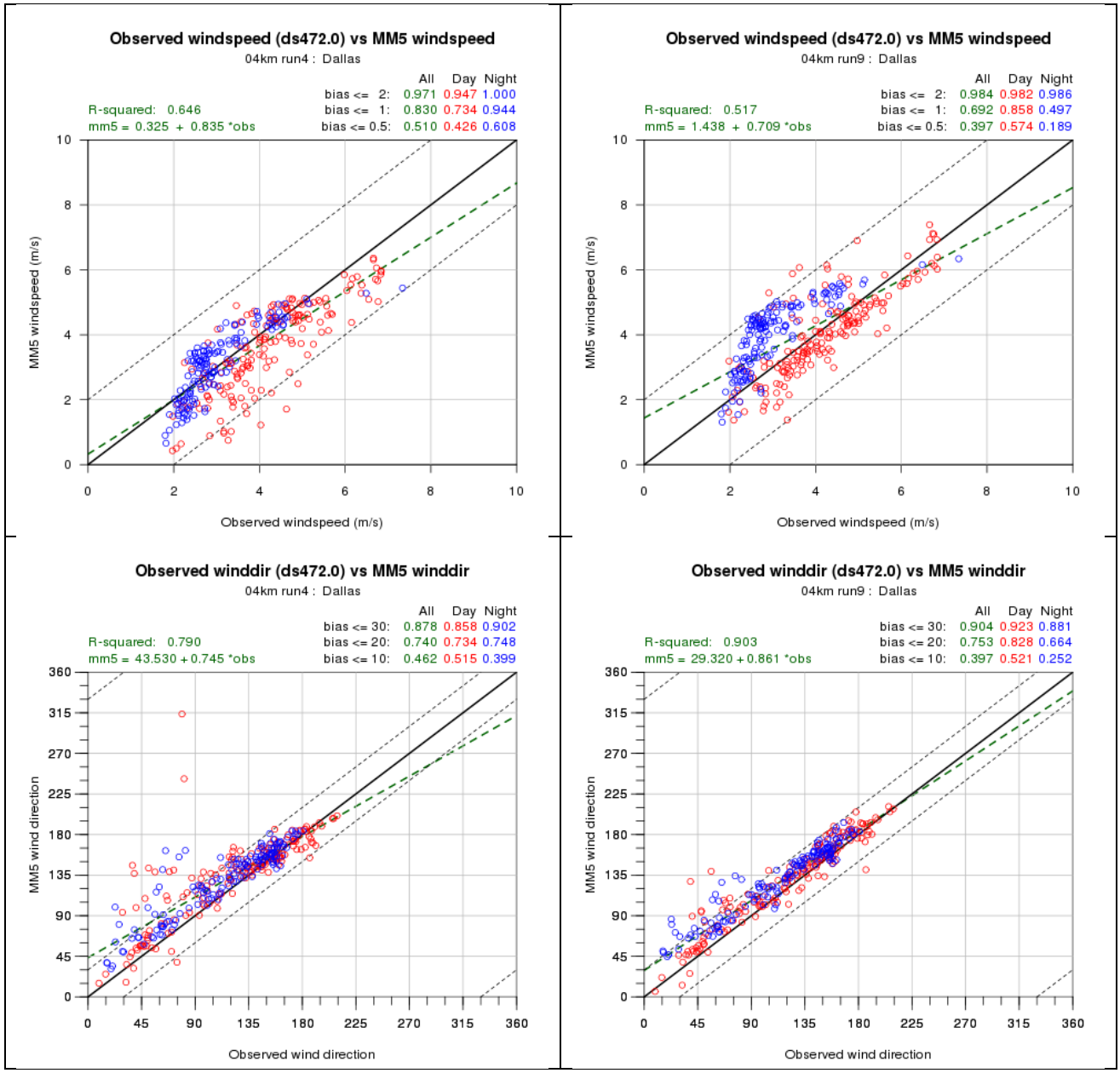

Figure 2-7. Scatter plots of hourly wind speed (m/s; top) and hourly wind direction (degrees, bottom) at DS472 sites in Dallas for AACOG/CAPCOG Run 4 (left) and for Run 9 (right). Blue points are nighttime hours, red point are daytime hours. The green dash line is the best fit line to all data; the black dotted lines are the ±2 m/s error envelope (top) and the ±30 degree error envelope (bottom). Fractions of data points within different bias ranges are shown at the top right of each plot.

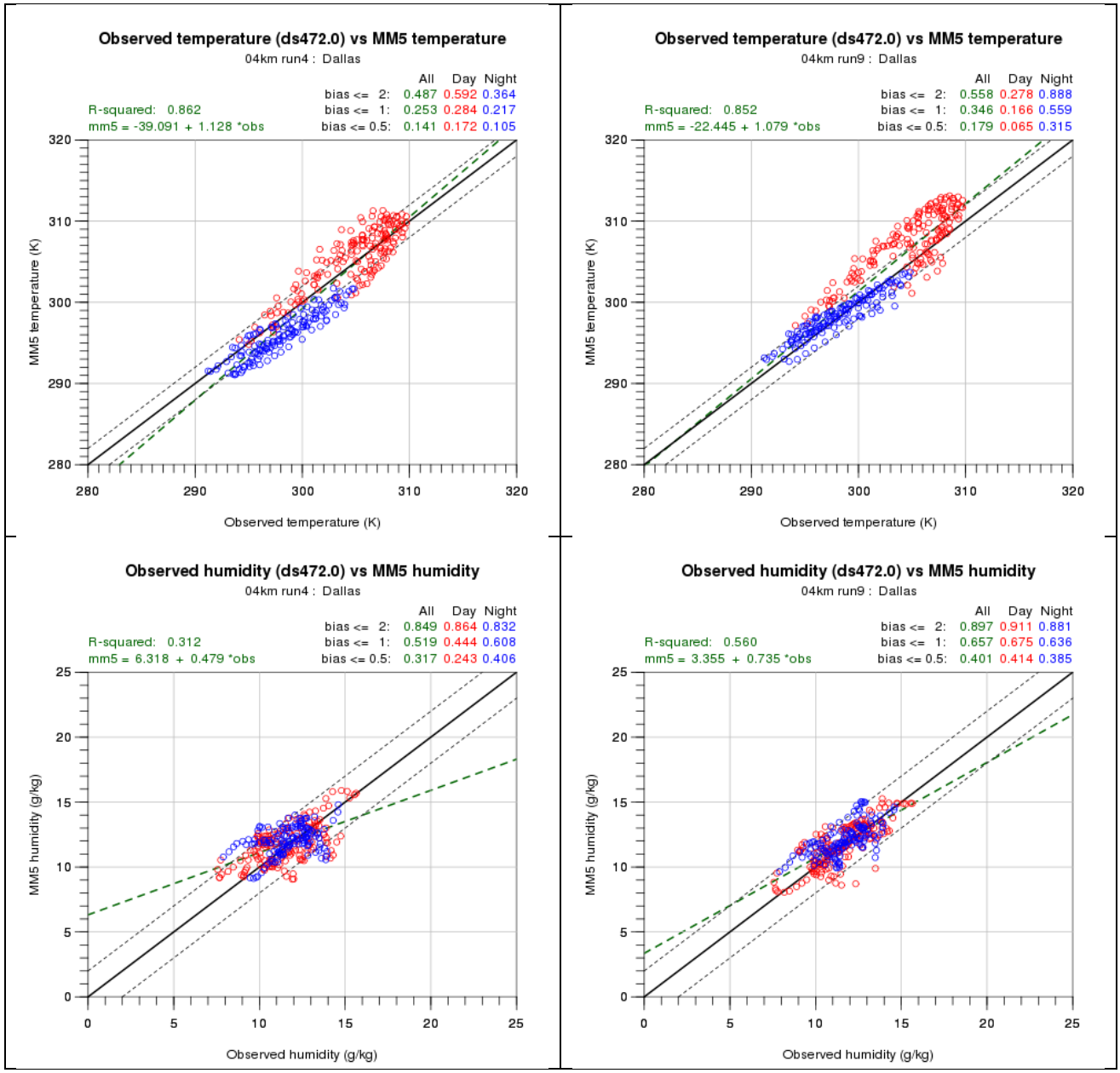

Figure 2-8. Scatter plots of hourly temperature (K; top) and hourly humidity (g/kg, bottom) at DS472 sites in Dallas for AACOG/CAPCOG Run 4 (left) and for Run 9 (right). Blue points are nighttime hours, red point are daytime hours. The green dash line is the best fit line to all data; the black dotted lines are the ±2 K error envelope (top) and the ±2 g/kg error envelope (bottom). Fractions of data points within different bias ranges are shown at the top right of each plot.

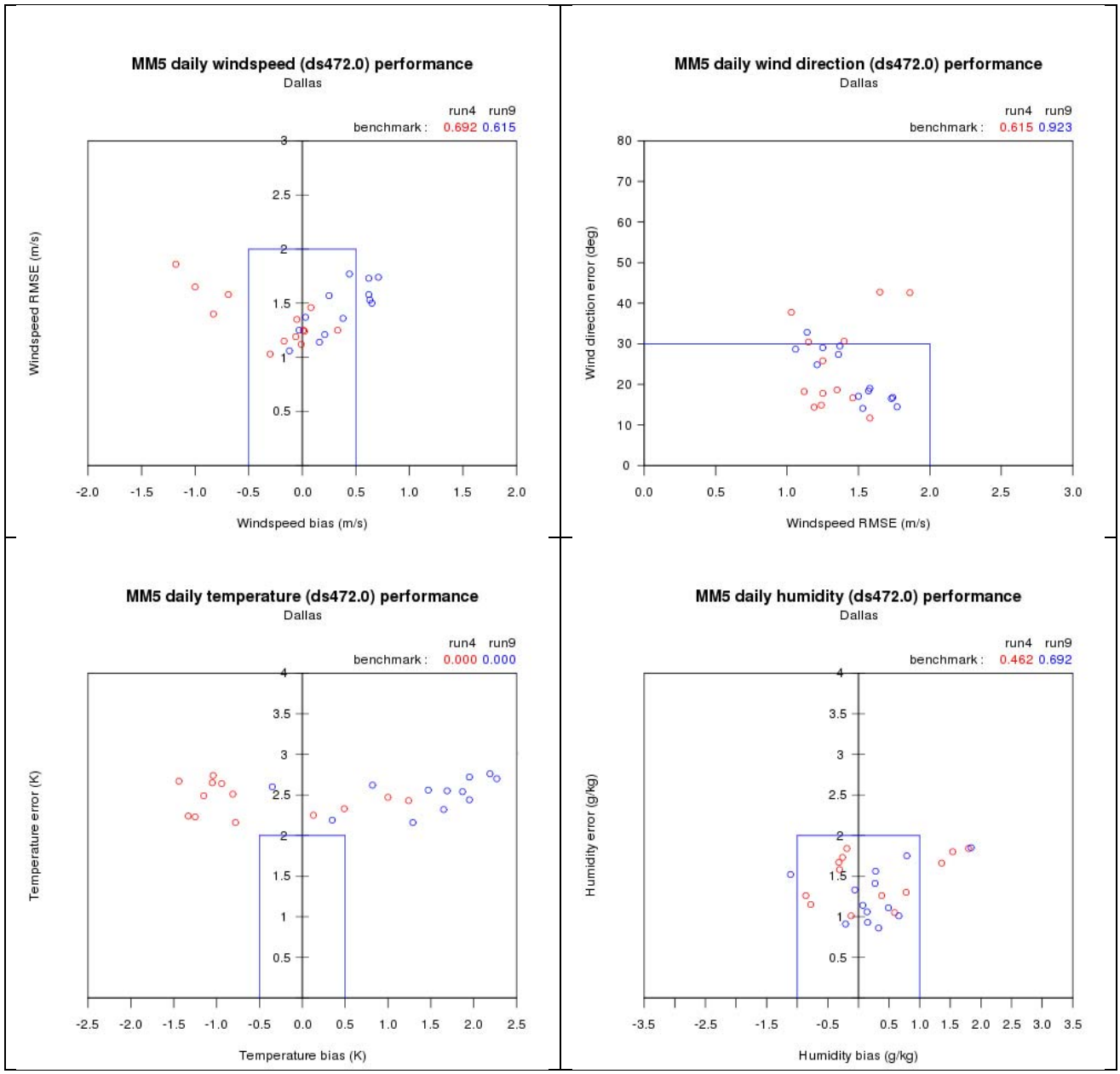

Figure 2-9. Scatter plots of daily statistical performance against DS472 data in Dallas for wind speed (top left), wind direction (top right), temperature (bottom left) and humidity (bottom right). Each plot shows daily performance from AACOG/CAPCOG Run 4 (red dots) and Run 9 (blue dots). The blue boxes represent the bias/error space bounded by the statistical performance benchmarks described in Section 1.

2.4 NORTHEAST TEXAS

Figures 2-10 and 2-11 show scatter plots of hourly MM5 wind speed, wind direction, temperature, and humidity against DS472 observations in the Northeast Texas analysis region for MM5 Runs 4 and 9. Figure 2-12 shows scatter plots of daily statistical performance against DS472 observations for wind speed, wind direction, temperature, and humidity in the Northeast Texas analysis region.

Results for all variables are similar to the effects seen in Dallas. Hourly wind speed shifts from under predictions to over predictions at night, and to a more balanced mix of over and under predictions during the day. These changes result in slightly worse hourly statistical performance, but the results are still very good; in fact, daily speed performance has improved greatly with most days within the statistical benchmarks. Hourly wind direction scatter is much improved in Run 9 as well, especially for daytime hours. However, there is no significant impact on daily average wind direction performance.

Consistent with all other cities, hourly temperature performance in Run 9 shows over predictions of daytime temperature, but much improved nighttime temperatures. Again, this shifts the daily temperature bias to large over predictions with no significant change to daily gross error. As similarly seen in Dallas, hourly humidity scatter diagrams are greatly improved relative to Run 4, and given the proximity of these two areas, performance gains are likely driven by the same effect. The daily statistics show improved humidity bias and error and overall a very good simulation.

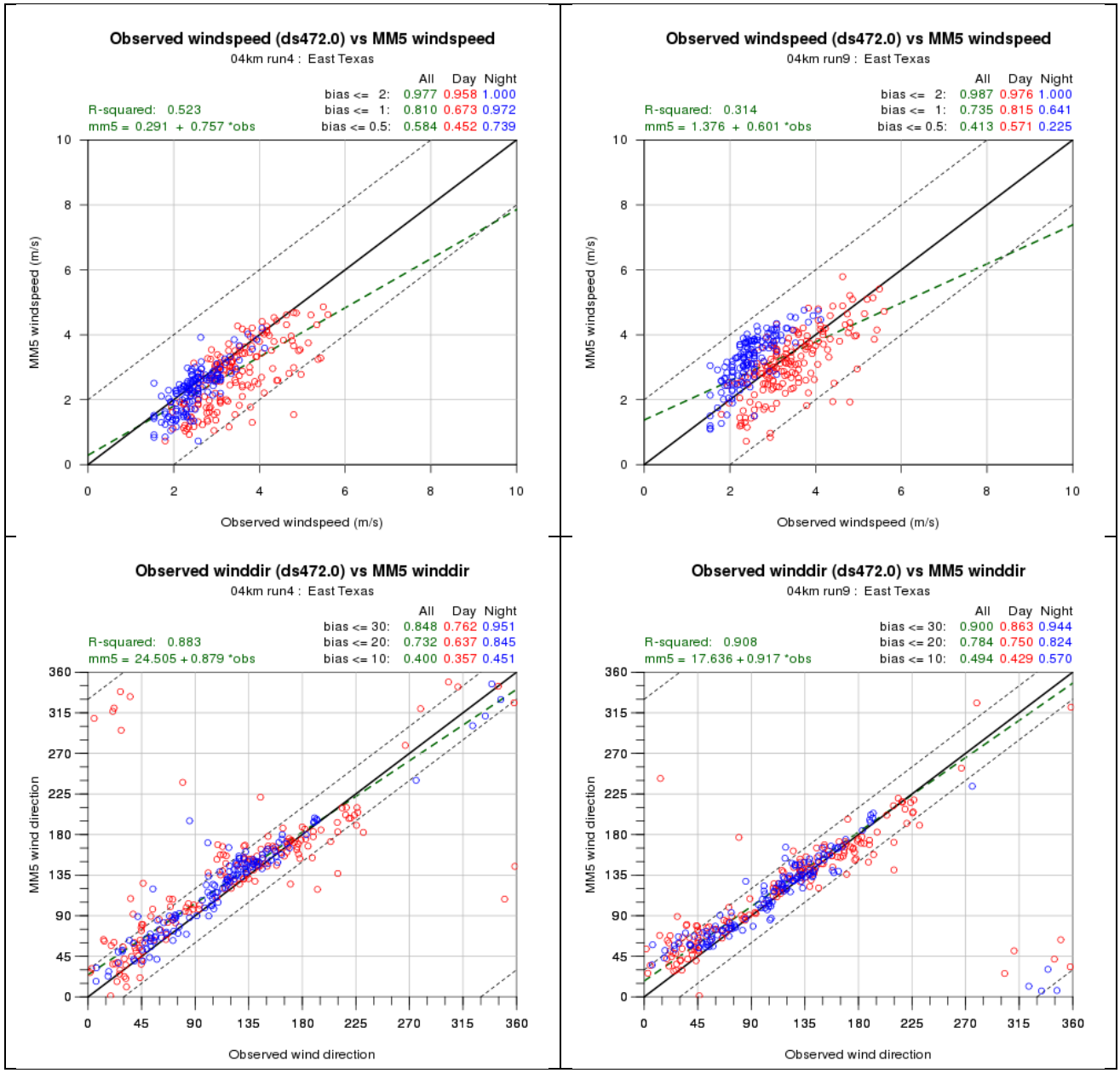

Figure 2-10. Scatter plots of hourly wind speed (m/s; top) and hourly wind direction (degrees, bottom) at DS472 sites in Northeast Texas for AACOG/CAPCOG Run 4 (left) and for Run 9 (right). Blue points are nighttime hours, red point are daytime hours. The green dash line is the best fit line to all data; the black dotted lines are the ±2 m/s error envelope (top) and the ±30 degree error envelope (bottom). Fractions of data points within different bias ranges are shown at the top right of each plot.

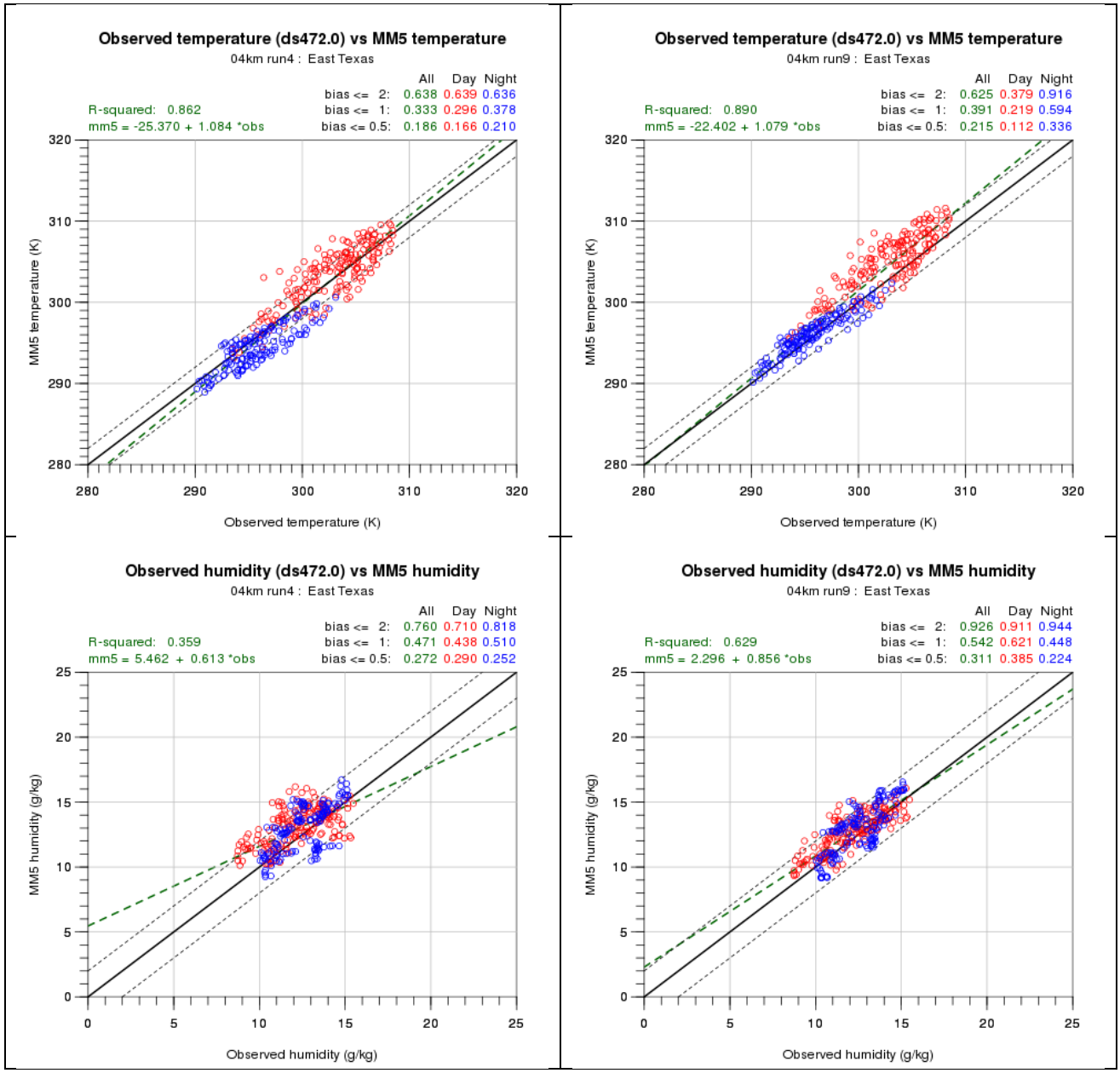

Figure 2-11. Scatter plots of hourly temperature (K; top) and hourly humidity (g/kg, bottom) at DS472 sites in Northeast Texas for AACOG/CAPCOG Run 4 (left) and for Run 9 (right). Blue points are nighttime hours, red point are daytime hours. The green dash line is the best fit line to all data; the black dotted lines are the ±2 K error envelope (top) and the ±2 g/kg error envelope (bottom). Fractions of data points within different bias ranges are shown at the top right of each plot.

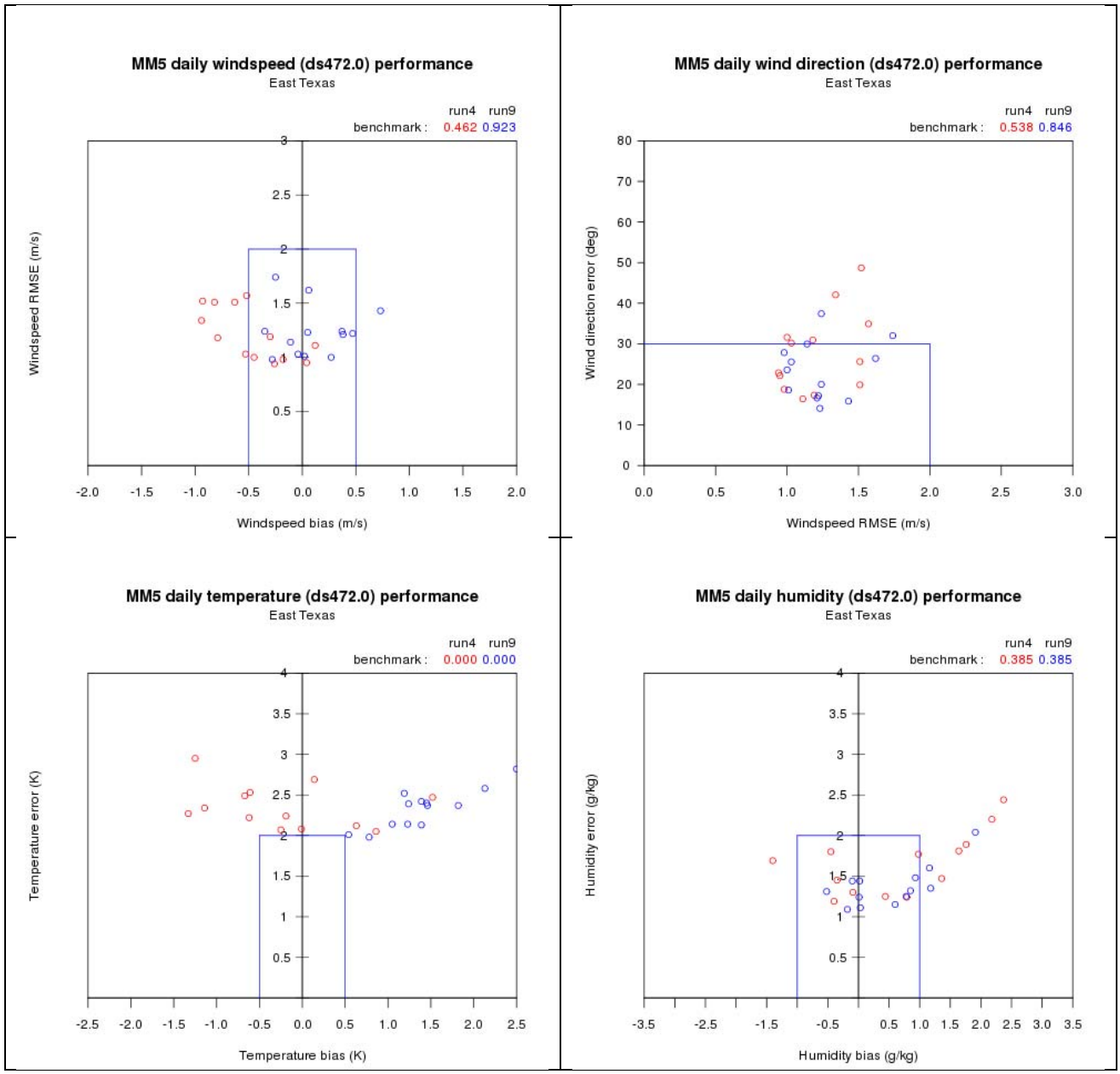

Figure 2-12. Scatter plots of daily statistical performance against DS472 data in Northeast Texas for wind speed (top left), wind direction (top right), temperature (bottom left) and humidity (bottom right). Each plot shows daily performance from AACOG/CAPCOG Run 4 (red dots) and Run 9 (blue dots). The blue boxes represent the bias/error space bounded by the statistical performance benchmarks described in Section 1.

2.5 EVALUATION OF PBL AND PRECIPITATION

We compared simulated PBL depths against diagnosed mixing depths from five profiler sites in eastern Texas (see Section 1), and following the approach described by Emery et al. (2009a), evaluated cloud/precipitation and surface wind patterns on June 13/14 to evaluate the simulation of convection and its impacts on wind patterns.

Figures 2-13 through 2-17 display comparisons of hourly MM5 simulated PBL depths from Runs 8 and 9 against diagnosed PBL depths from profiler data at New Braunfels, Moody, Huntsville, Cleburne, and Lonview from May 30 through June 16. The most notable characteristic of Run 8 is the consistent under prediction of PBL depth, which is a trait often seen with the Eta PBL scheme. Furthermore, MM5 starts the morning rise of mixing too late, and tends to collapse the afternoon PBL too early (except on June 3). Both Run 8 and observed PBL profiles are impacted by cloud buildup in the afternoon, which is evident by the sharp hour-to-hour variations in the mixing depths. However, the effect in Run 8 at New Braunfels is usually much stronger than observed, and this is another common trait of this particular model configuration. As expected, Run 9 with the MRF PBL scheme increases daily PBL depths markedly and improves agreement with the observations for most days and sites. The morning rate of rise also agrees better with the diagnosed PBL depths. Finally, Run 9 tends to exhibit less hour-to-hour variations in PBL depth, which suggests a reduction in midday convective activity at these sites. Note that our comparison implicitly assumes that the "observed" mixing depth is accurate. There are some questionable features in the observed profiles that may be product of the automated diagnostic method.

Figure 2-18 compares daily MM5 Run 8 and 9 precipitation against AHPS observed conditions between 7 AM June 13 to 7 AM June 14. As is typical of MM5, the model over predicts both the coverage and intensity of rainfall. While the observations do show that convection built up on June 13-14, it was confined to southeast Texas, whereas Run 8 generated rainfall throughout eastern Texas as far north as Dallas and as far west as Bexar County. On the other hand, Run 9 shows significantly less rainfall than Run 8 with much improved agreement with observations in southeast Texas. Run 9 continues to generate some light rainfall east of Fort Worth, which was not observed. The deeper mixing generated by the MRF PBL may have successfully vented heat and moisture, reducing the release of this energy in the form of convective precipitation.

Figures 2-19 and 2-20 display snapshots of surface wind fields, cloud cover (expressed as cloud optical depth – an input to CAMx), and precipitation at 4 PM on June 13 for Run 8 and 9, respectively. In Run 8, convective cells are apparent in the Houston area and just to the east of the San Antonio – Austin corridor, and this has generated some cloudiness and wind "bomb-bursts" throughout the area. Run 9 shows reduced convective activity constrained between Austin and Houston with less impacts on the wind fields. However, Run 9 exhibits more widespred (non-precipitating) cloud cover over southeast Texas.

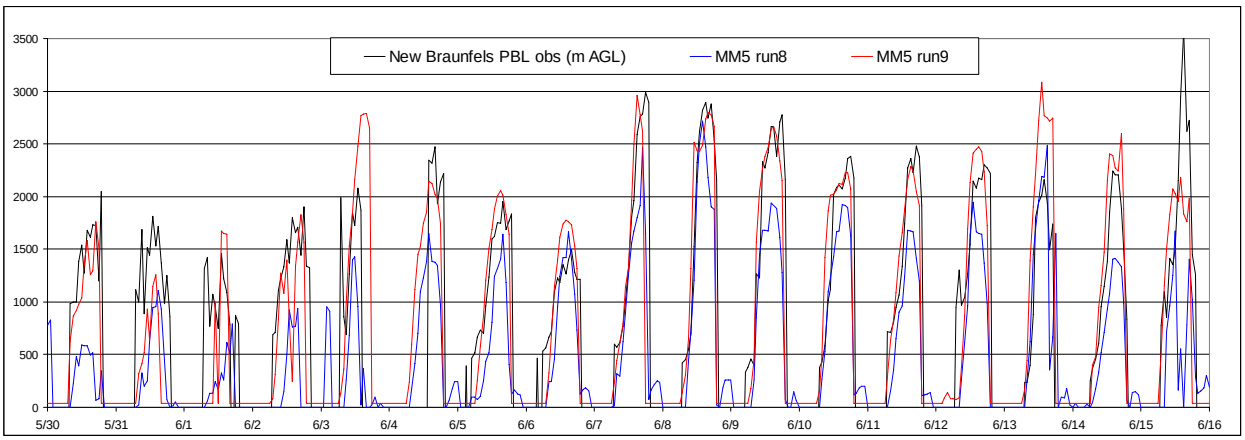

Figure 2-13. Hourly time series of predicted (MM5 Runs 8 and 9) and diagnosed PBL depths from the New Braunfels wind profiler.

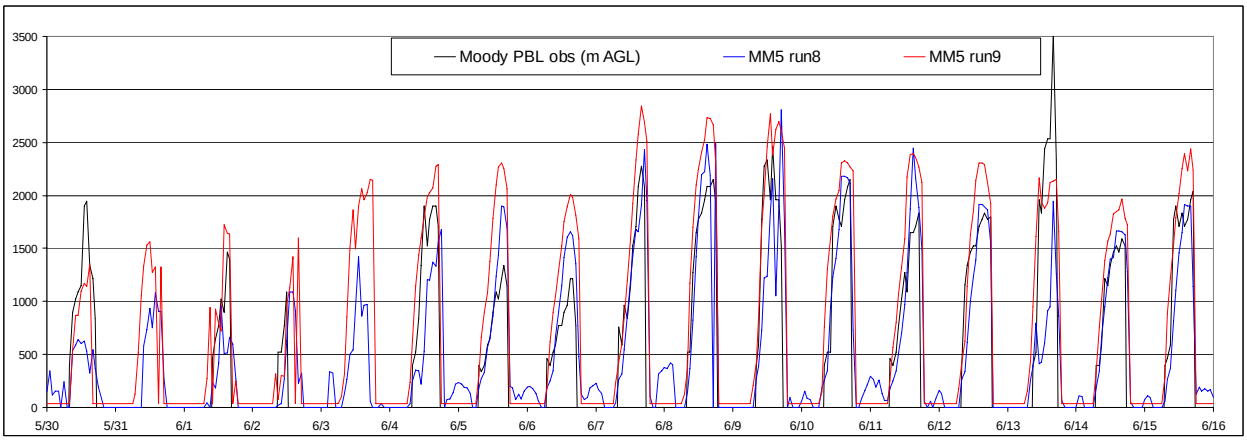

Figure 2-14. Hourly time series of predicted (MM5 Runs 8 and 9) and diagnosed PBL depths from the Moody wind profiler.

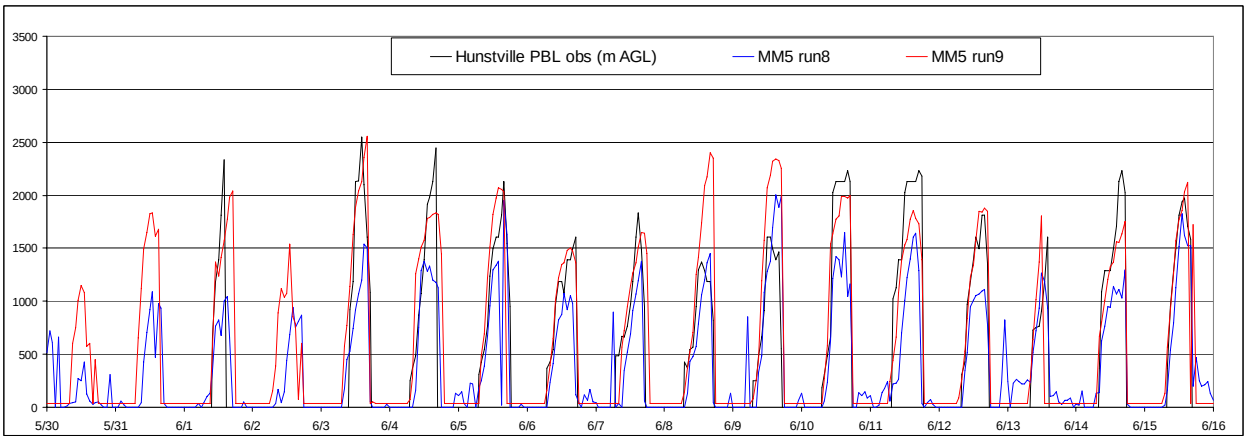

Figure 2-15. Hourly time series of predicted (MM5 Runs 8 and 9) and diagnosed PBL depths from the Hunstville wind profiler.

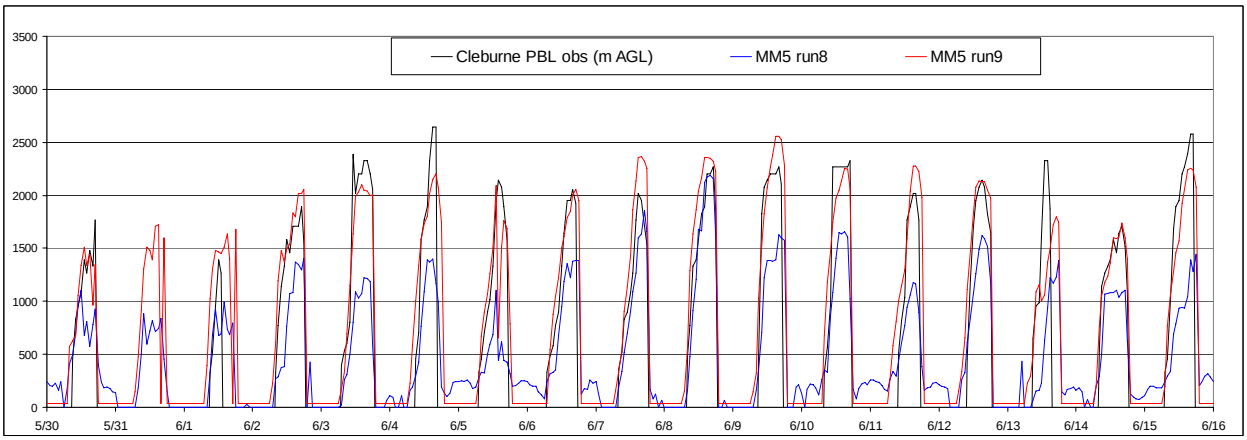

Figure 2-16. Hourly time series of predicted (MM5 Runs 8 and 9) and diagnosed PBL depths from the Cleburne wind profiler.

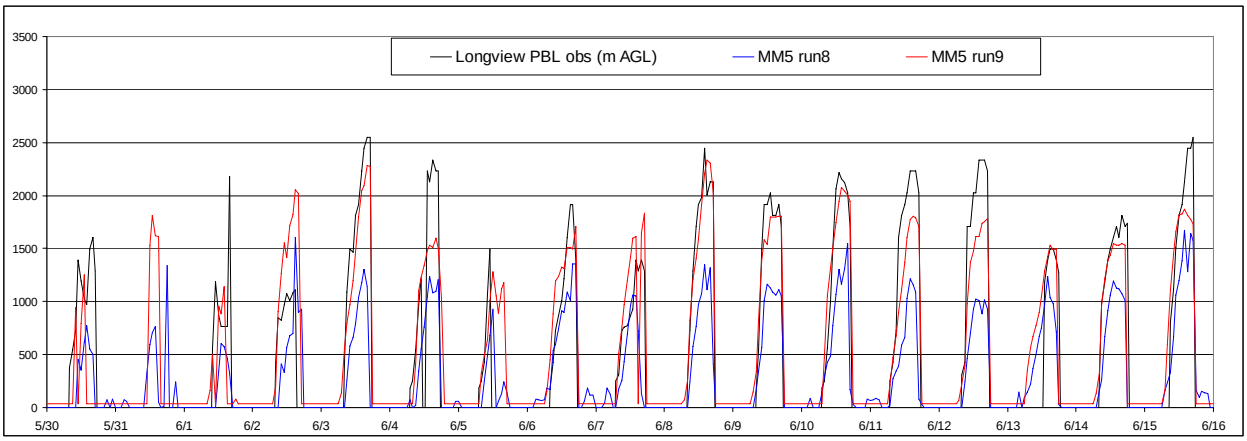

Figure 2-17. Hourly time series of predicted (MM5 Runs 8 and 9) and diagnosed PBL depths from the Longview wind profiler.

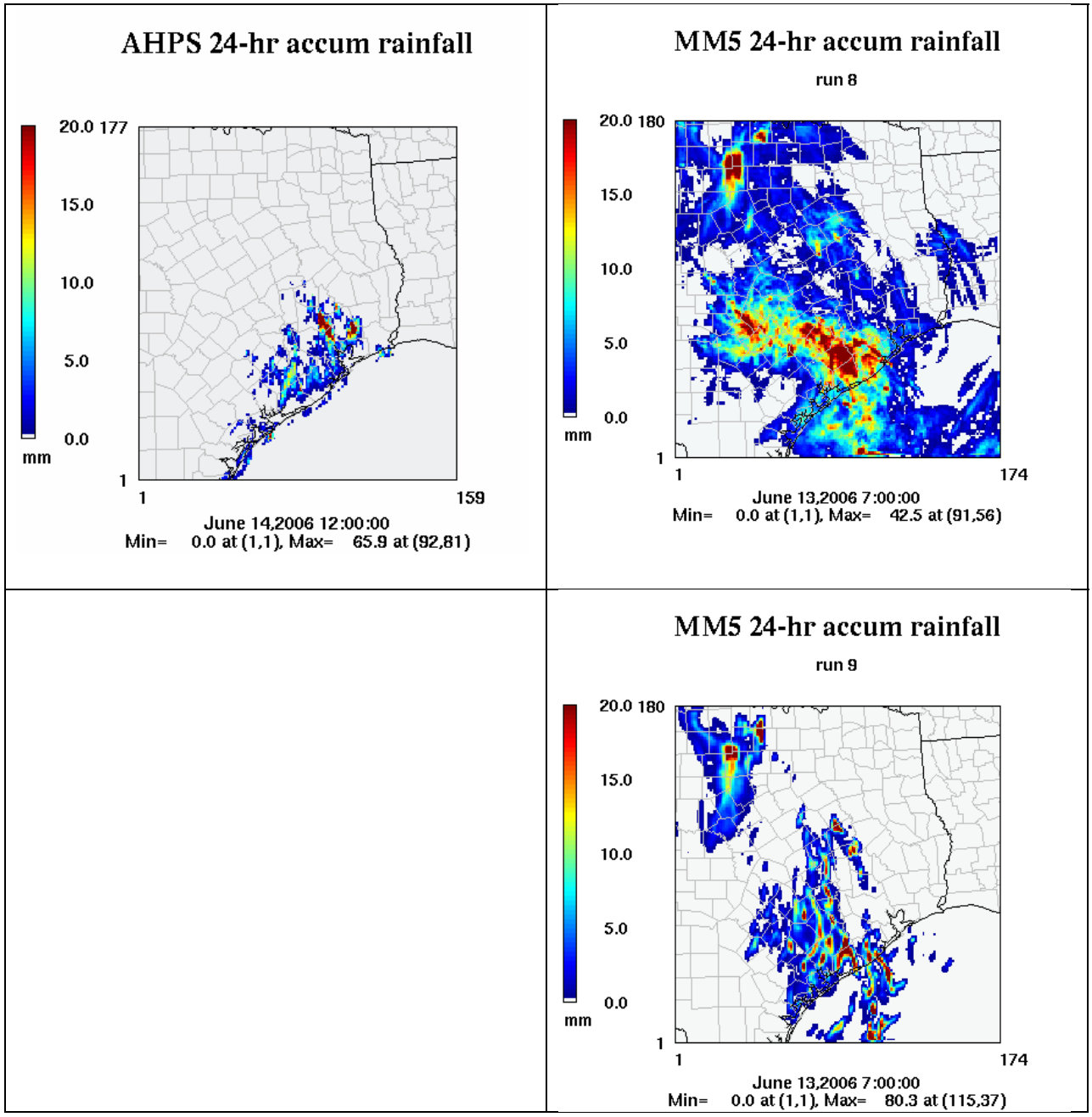

Figure 2-18. Observed (AHPS; top left) and MM5 simulated 24-hour accumulated precipitation (mm) for Runs 8 (top right) and 9 (bottom right), 7 AM June 14 to 7 AM June 15, 2006.

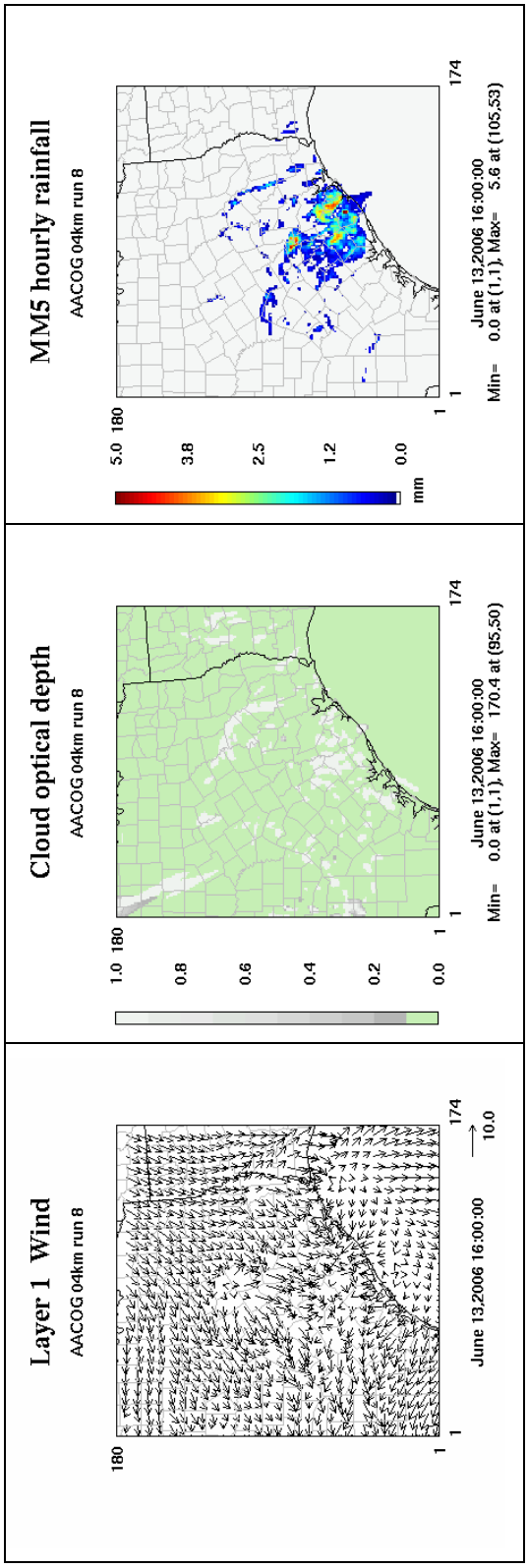

Figure 2-19. Simulated wind fields (left), CAMx cloud cover (middle), and rainfall (right) from MM5 Run 8 at 4 PM, June 13, 2006.

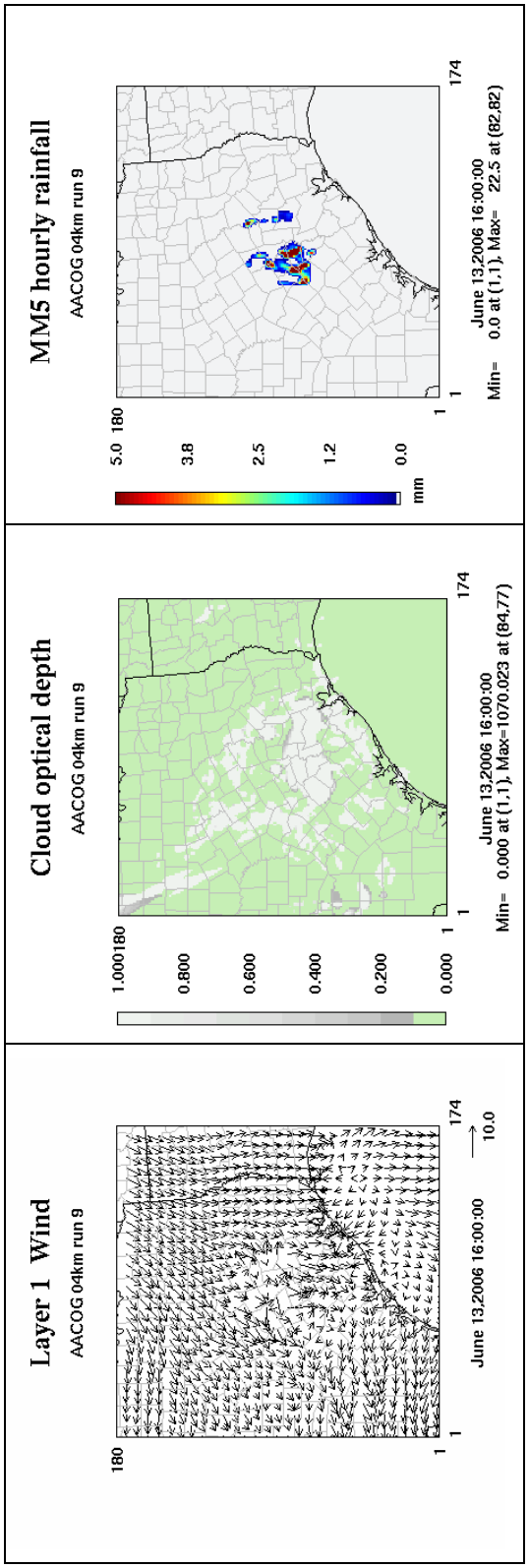

Figure 2-20. Simulated wind fields (left), CAMx cloud cover (middle), and rainfall (right) from MM5 Run 9 at 4 PM, June 13, 2006.

3. ALTERNATIVE SOIL MODEL

The next MM5 simulation (Run 10) was identical to Run 9, but replaced the NOAH LSM with the simpler 5-layer soil model option, which derives soil characteristics according to input landcover fields and internal lookup tables of soil moisture availability and various thermal properties. This test was performed to investigate model sensitivity to the choice of LSM, specifically with regard to surface temperature performance and afternoon convection. The LSM change required that all grids be re-run, and we continued to follow the original TCEQ methodology for multi-grid simulations: the 108/36/12-km grids were run 2-way interactive, while the 4-km grid run separately using 1-way nesting with boundary conditions derived from the 12-km results via the NESTDOWN processor.

Run 10 performance was compared against Run 9 performance in the same manner as described in Section 2.

3.1 SAN ANTONIO

Figures 3-1 and 3-2 show scatter plots of hourly MM5 wind speed, wind direction, temperature, and humidity against DS472 observations in the San Antonio analysis region for MM5 Runs 9 and 10. Figure 3-3 shows scatter plots of daily statistical performance against DS472 observations for wind speed, wind direction, temperature, and humidity in the San Antonio analysis region. Each plot shows daily performance from Run 4 (red points) and Run 10 (blue points) to illustrate performance differences relative to the baseline AACOG/CAPCOG simulation.

Very similar hourly wind speed and direction performance results are achieved with Runs 9 and 10, with a very slight degradation in wind speed statistics. Daily wind statistics for Run 10 are generally improved over Run 4, and are very similar to Run 9. The change in LSM did not have much of an impact on winds, and this was an expected result.

On the other hand, hourly and daily temperature performance is dramatically improved with the use of the simple 5-layer soil model. The hourly scatter plots show that the daytime temperature over prediction bias is reduced substantially, while minimal change occurs for the already good nighttime performance. The net effect on the daily statistics is quite obvious; temperature gross error is reduced by 1.5-2 K, with a small net under prediction bias of 0.5 to 1 K. The cause of this is probably related to different soil moisture content and possibly different thermal properties (conductance and heat capacity). Hourly humidity scatter diagrams are consistent with the theory of higher soil moisture content; both daytime and nighttime humidity is shifted upward. While daytime humidity is better balanced between over and under predictions (better statistics), nighttime humidity is generally over predicted in Run 10 (degraded statistics). The net effect is for slightly worse hourly statistics overall. The Run 10 daily humidity statistics continue to be better than Run 4, but show a marked shift to over predictions compared to Run 9 (see Figure 2-3).

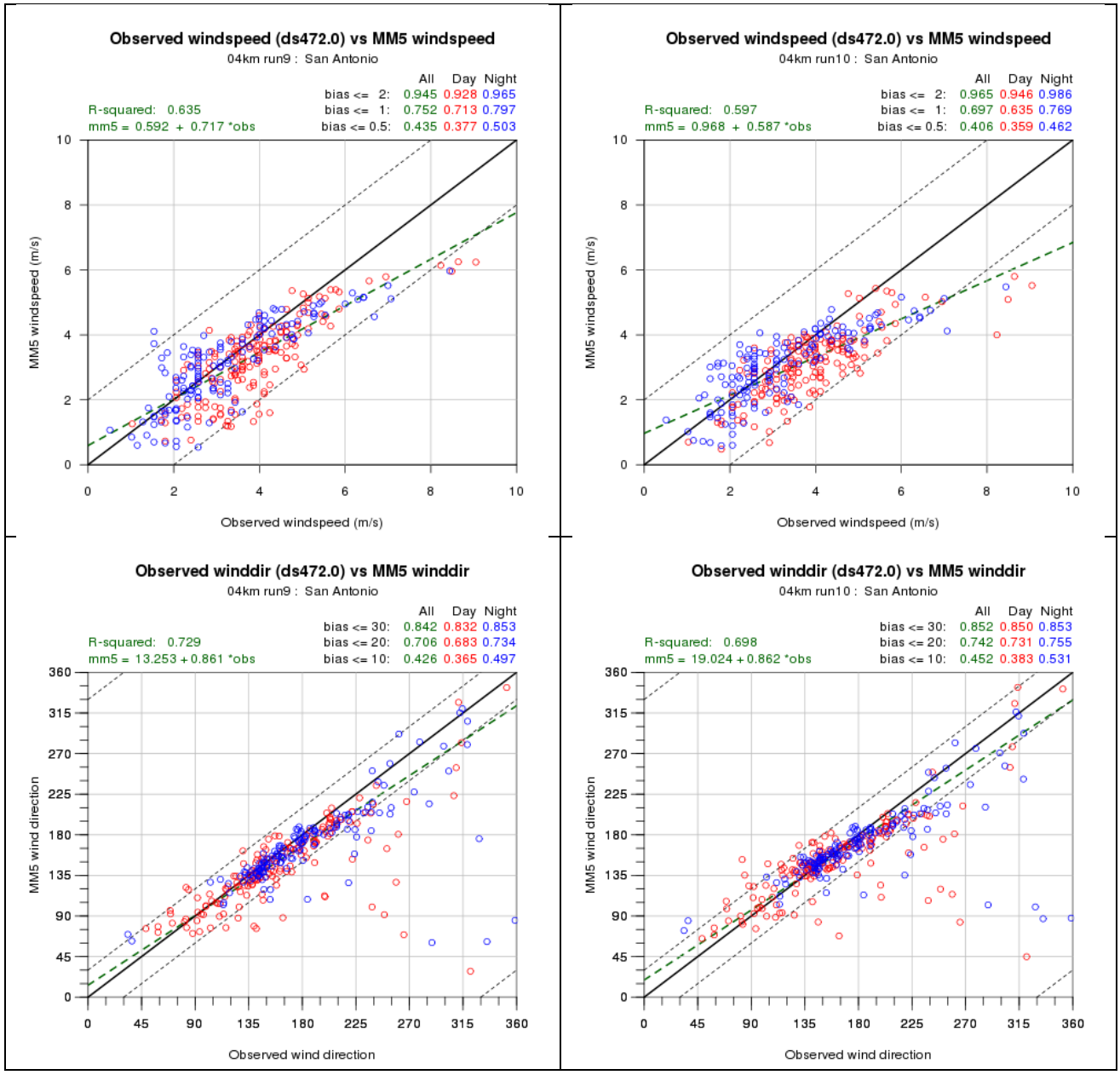

Figure 3-1. Scatter plots of hourly wind speed (m/s; top) and hourly wind direction (degrees, bottom) at DS472 sites in San Antonio for Run 9 (left) and for Run 10 (right). Blue points are nighttime hours, red point are daytime hours. The green dash line is the best fit line to all data; the black dotted lines are the ±2 m/s error envelope (top) and the ±30 degree error envelope (bottom). Fractions of data points within different bias ranges are shown at the top right of each plot.

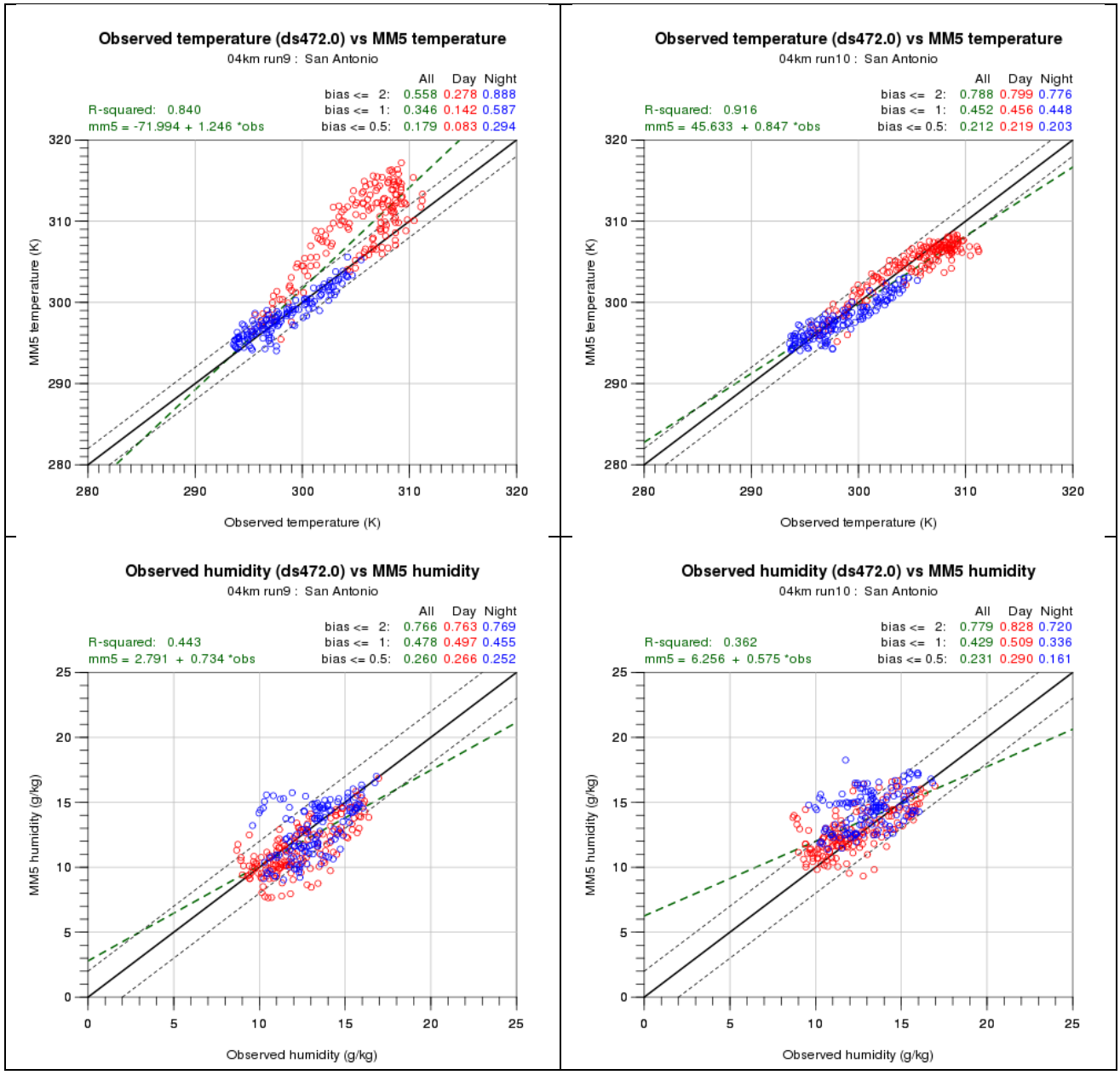

Figure 3-2. Scatter plots of hourly temperature (K; top) and hourly humidity (g/kg, bottom) at DS472 sites in San Antonio for Run 9 (left) and for Run 10 (right). Blue points are nighttime hours, red point are daytime hours. The green dash line is the best fit line to all data; the black dotted lines are the ±2 K error envelope (top) and the ±2 g/kg error envelope (bottom). Fractions of data points within different bias ranges are shown at the top right of each plot.

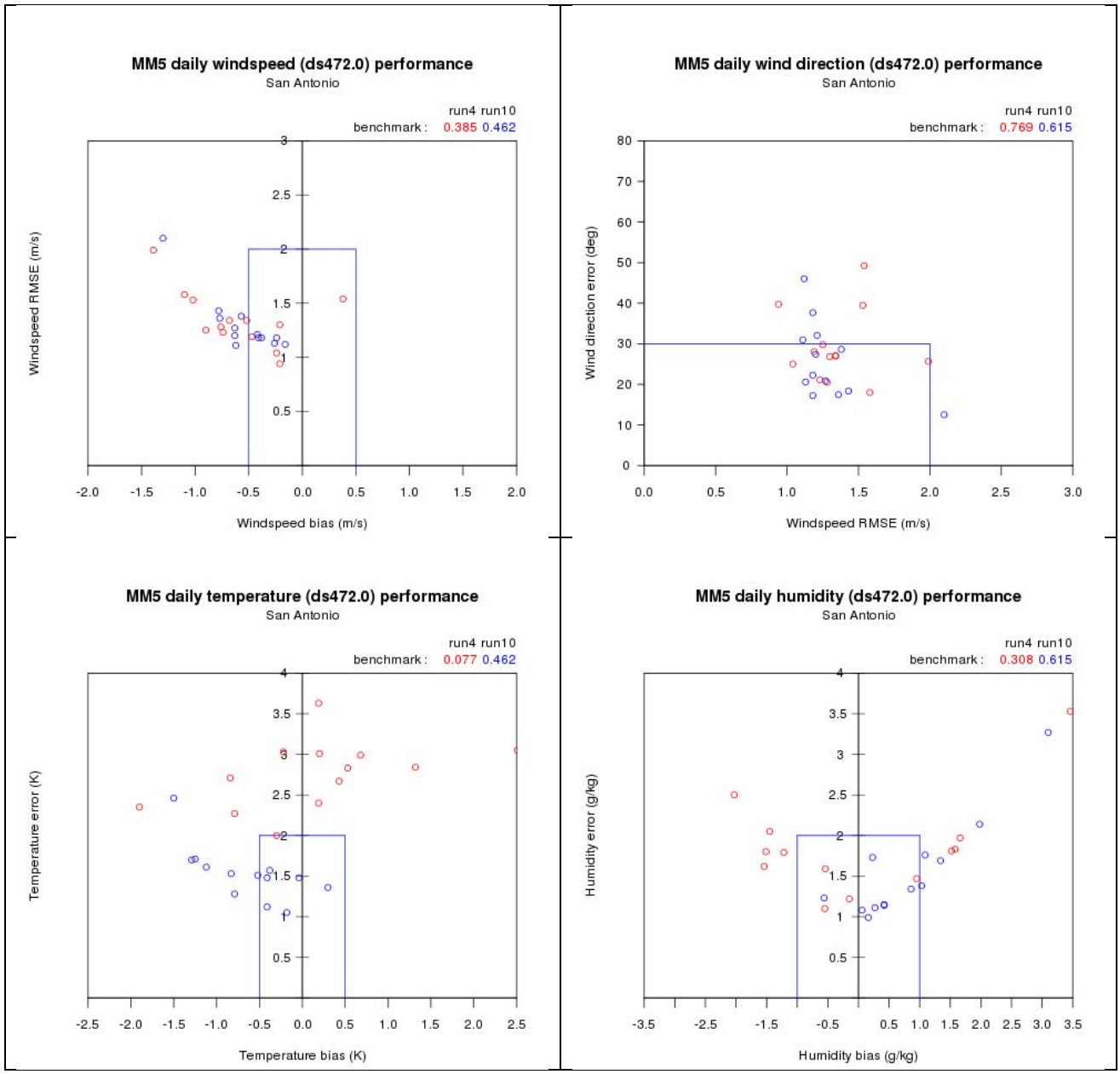

Figure 3-3. Scatter plots of daily statistical performance against DS472 data in San Antonio for wind speed (top left), wind direction (top right), temperature (bottom left) and humidity (bottom right). Each plot shows daily performance from AACOG/CAPCOG Run 4 (red dots) and Run 10 (blue dots). The blue boxes represent the bias/error space bounded by the statistical performance benchmarks described in Section 1.

3.2 AUSTIN

Figures 3-4 and 3-5 show scatter plots of hourly MM5 wind speed, wind direction, temperature, and humidity against DS472 observations in the Austin analysis region for MM5 Runs 9 and 10. Figure 3-6 shows scatter plots of daily statistical performance against DS472 observations for wind speed, wind direction, temperature, and humidity in the Austin analysis region.

Very little difference is seen in hourly and daily wind speed/direction performance between Runs 9 and 10. Overall, wind performance continues to be quite good in Austin.

As similarly seen in San Antonio, hourly temperature performance in Run 10 is improved substantially by the reduction of the daytime over prediction bias. Relative to Run 4, this simulation greatly improves daily temperature performance with most days within the benchmarks. Hourly humidity performance is slightly degraded by the shift toward higher humidity during both daytime and nighttime hours, with a bit more scatter in the data points (gross error). Little change is seen in the daily statistics relative to either Run 4 or Run 9.

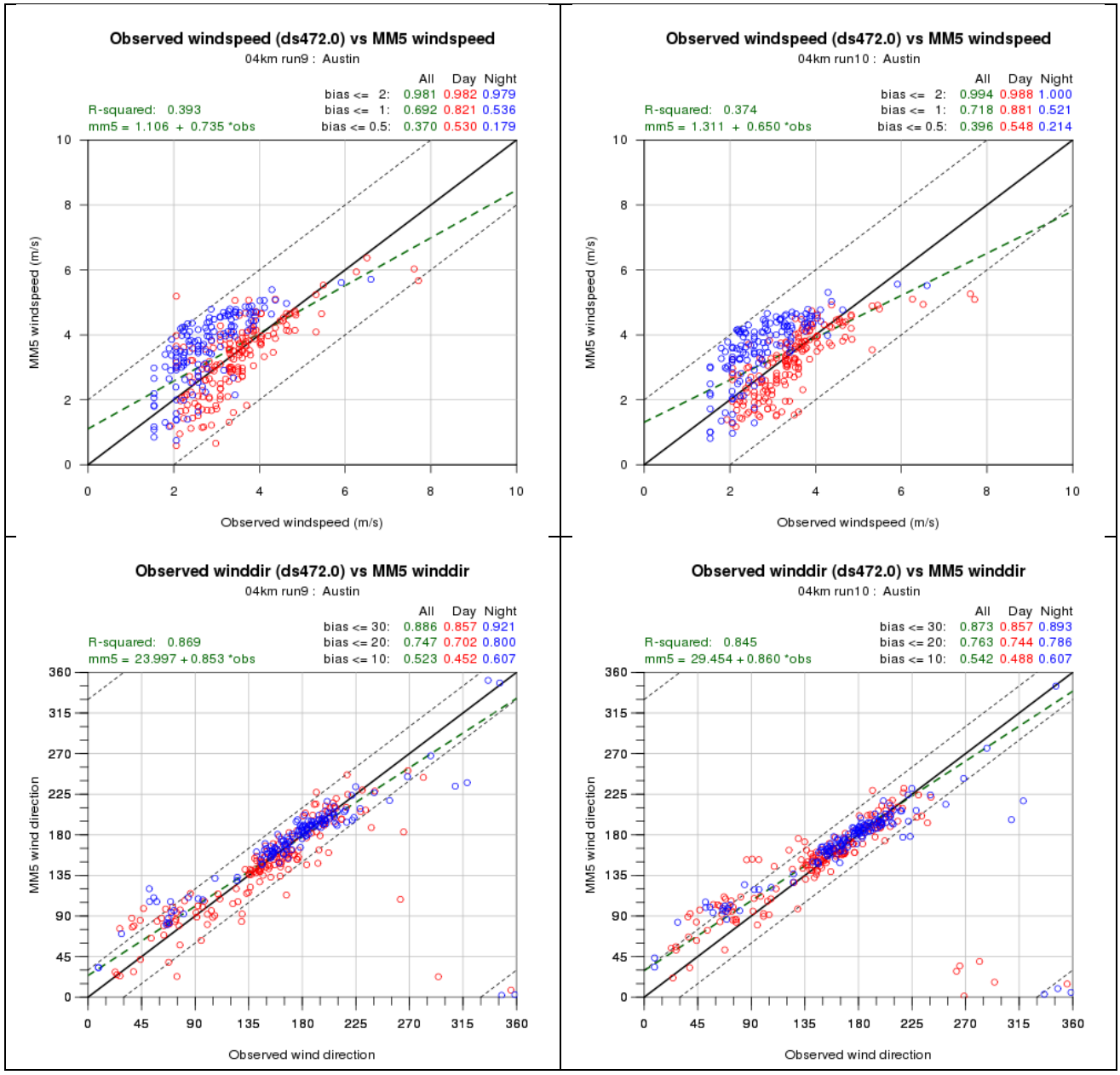

Figure 3-4. Scatter plots of hourly wind speed (m/s; top) and hourly wind direction (degrees, bottom) at DS472 sites in Austin for Run 9 (left) and for Run 10 (right). Blue points are nighttime hours, red point are daytime hours. The green dash line is the best fit line to all data; the black dotted lines are the ±2 m/s error envelope (top) and the ±30 degree error envelope (bottom). Fractions of data points within different bias ranges are shown at the top right of each plot.

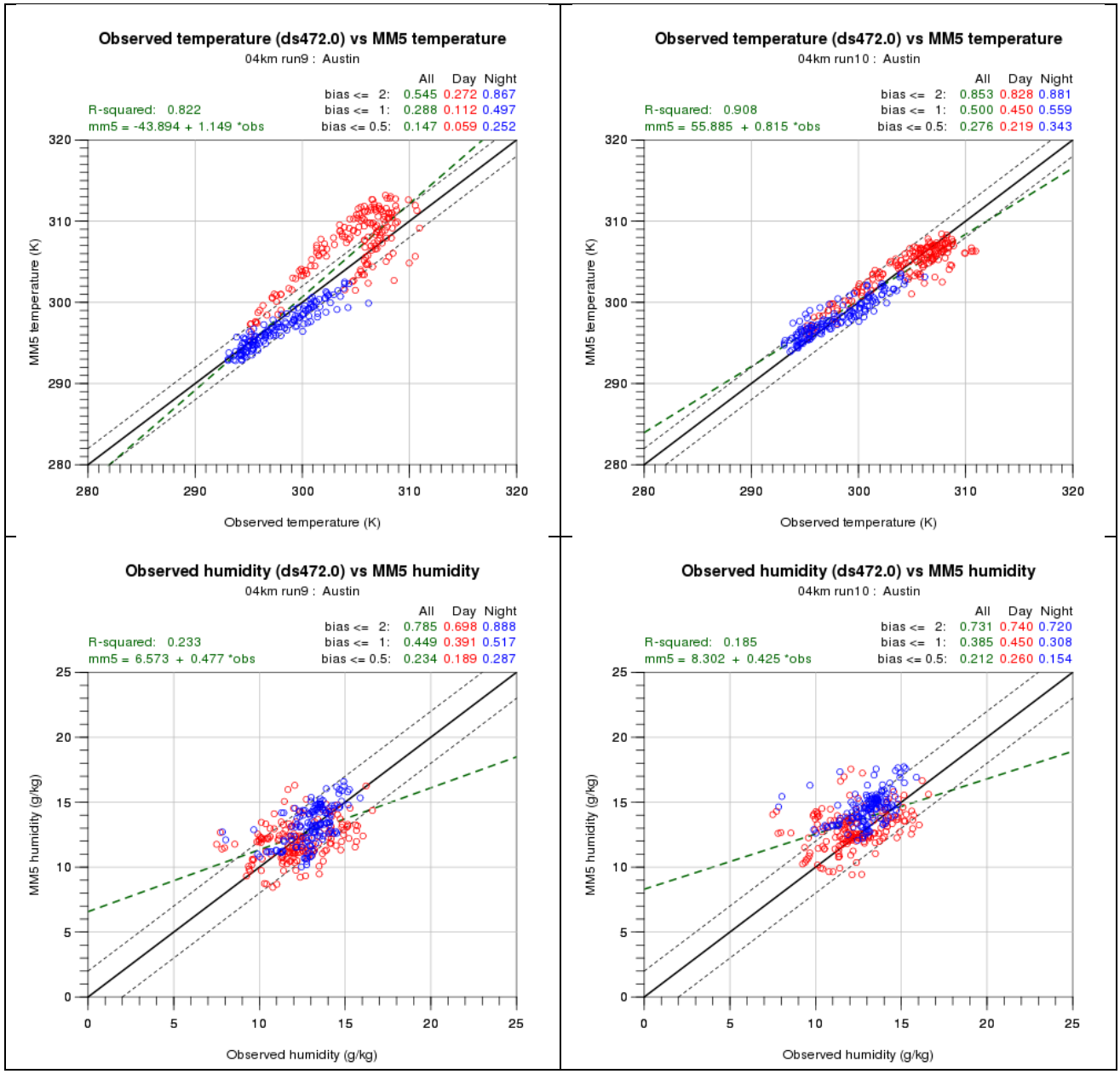

Figure 3-5. Scatter plots of hourly temperature (K; top) and hourly humidity (g/kg, bottom) at DS472 sites in Austin for Run 9 (left) and for Run 10 (right). Blue points are nighttime hours, red point are daytime hours. The green dash line is the best fit line to all data; the black dotted lines are the ±2 K error envelope (top) and the ±2 g/kg error envelope (bottom). Fractions of data points within different bias ranges are shown at the top right of each plot.

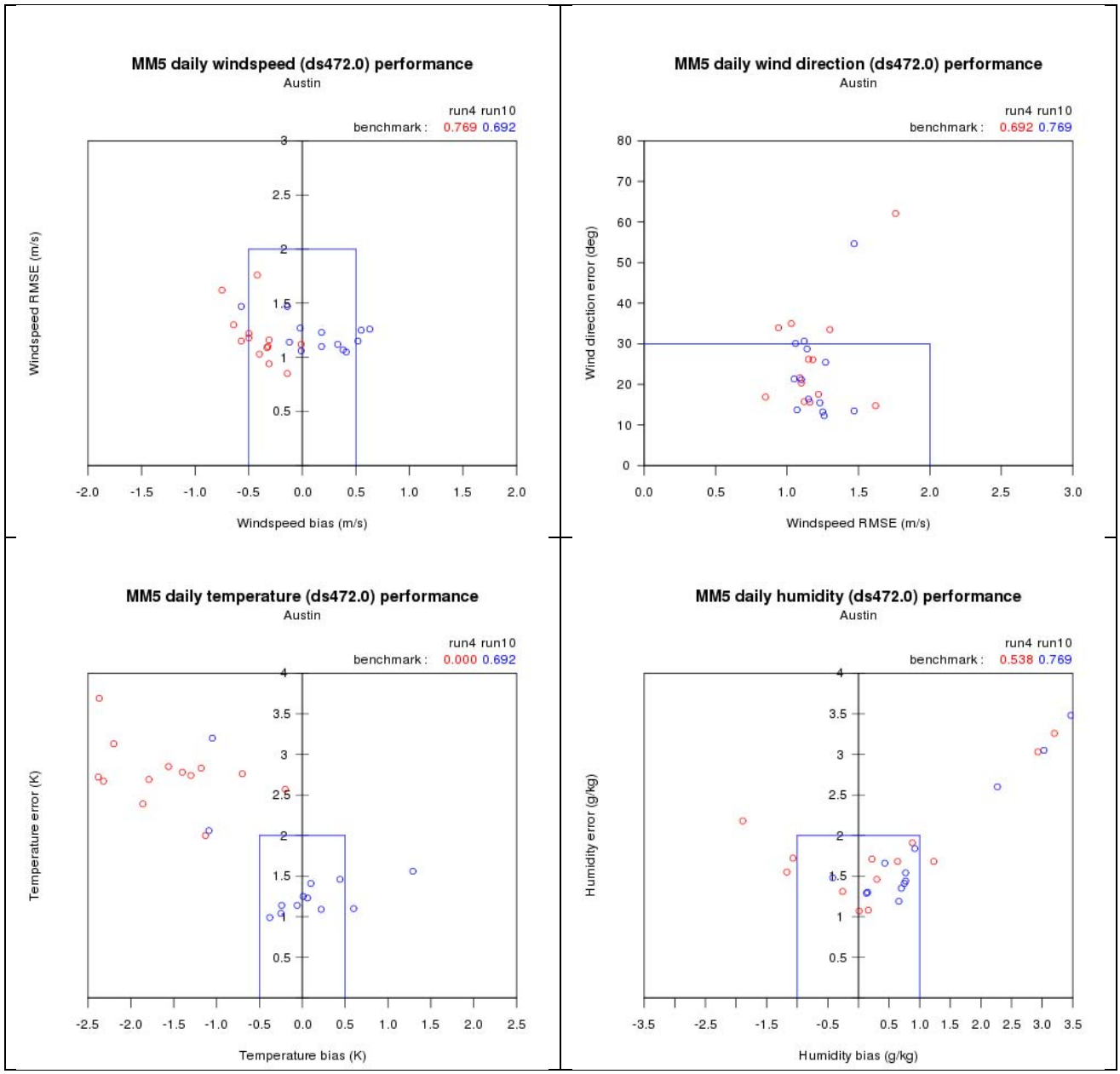

Figure 3-6. Scatter plots of daily statistical performance against DS472 data in Austin for wind speed (top left), wind direction (top right), temperature (bottom left) and humidity (bottom right). Each plot shows daily performance from AACOG/CAPCOG Run 4 (red dots) and Run 10 (blue dots). The blue boxes represent the bias/error space bounded by the statistical performance benchmarks described in Section 1.

3.3 DALLAS

Figures 3-7 and 3-8 show scatter plots of hourly MM5 wind speed, wind direction, temperature, and humidity against DS472 observations in the Dallas analysis region for MM5 Runs 9 and 10. Figure 3-9 shows scatter plots of daily statistical performance against DS472 observations for wind speed, wind direction, temperature, and humidity in the Dallas analysis region.

Very little difference is seen in hourly and daily wind speed/direction performance between Runs 9 and 10. Run 10 exhibits a very slight degradation in daily wind direction performance. Overall, wind performance continues to be quite good in Dallas.

As similarly seen in the southern cities, hourly temperature performance in Run 10 is improved substantially by the reduction of the daytime over prediction bias. Relative to Run 4, this simulation improves daily temperature performance by reducing the overall gross error. Hourly humidity performance is slightly degraded by the shift toward higher humidity during both daytime and nighttime hours, with a bit more scatter in the data points (gross error). Run 10 results in slightly worse daily humidity performance relative to Run 9, and similar performance relative to Run 4.

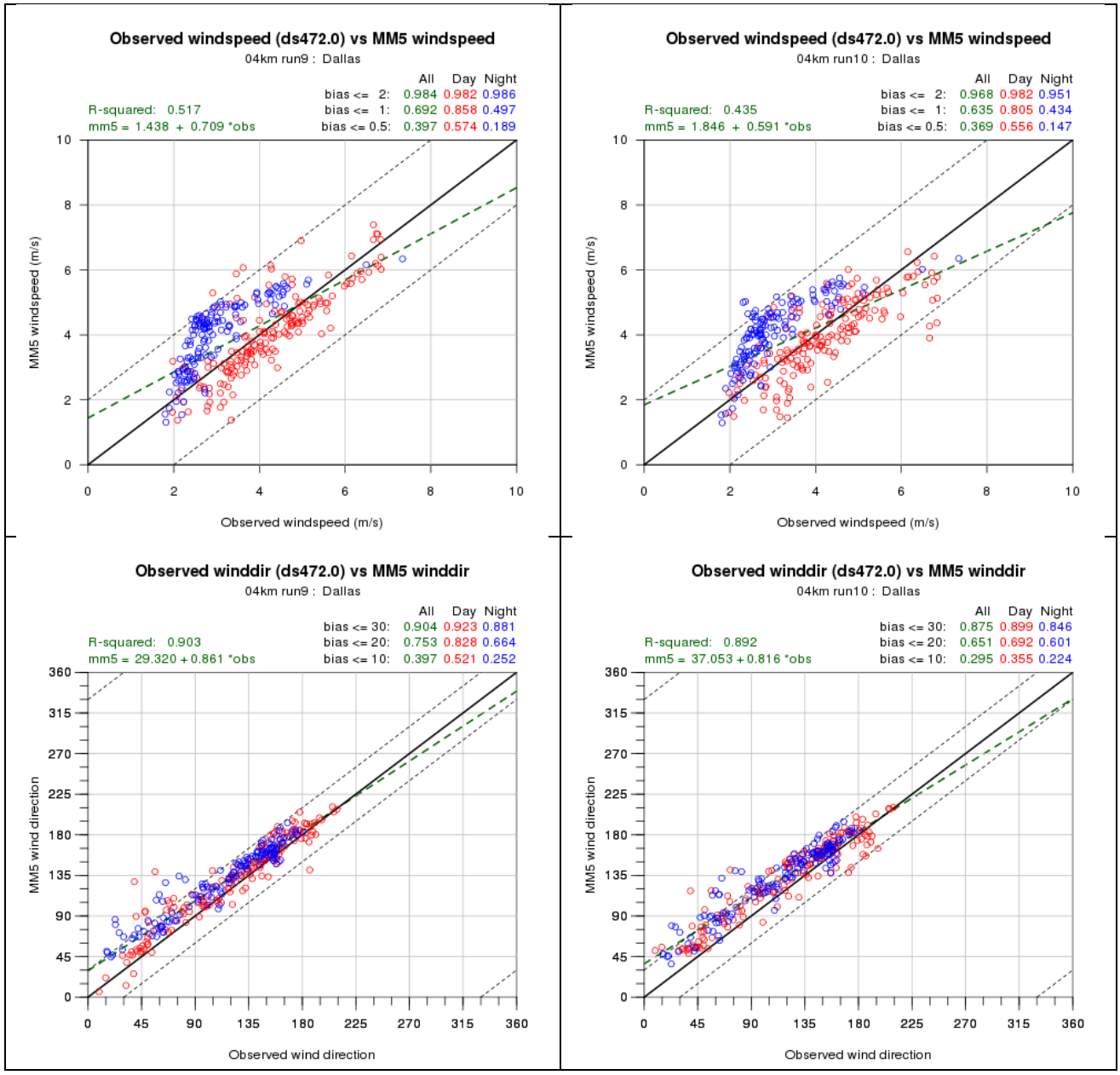

Figure 3-7. Scatter plots of hourly wind speed (m/s; top) and hourly wind direction (degrees, bottom) at DS472 sites in Dallas for Run 9 (left) and for Run 10 (right). Blue points are nighttime hours, red point are daytime hours. The green dash line is the best fit line to all data; the black dotted lines are the ±2 m/s error envelope (top) and the ±30 degree error envelope (bottom). Fractions of data points within different bias ranges are shown at the top right of each plot.

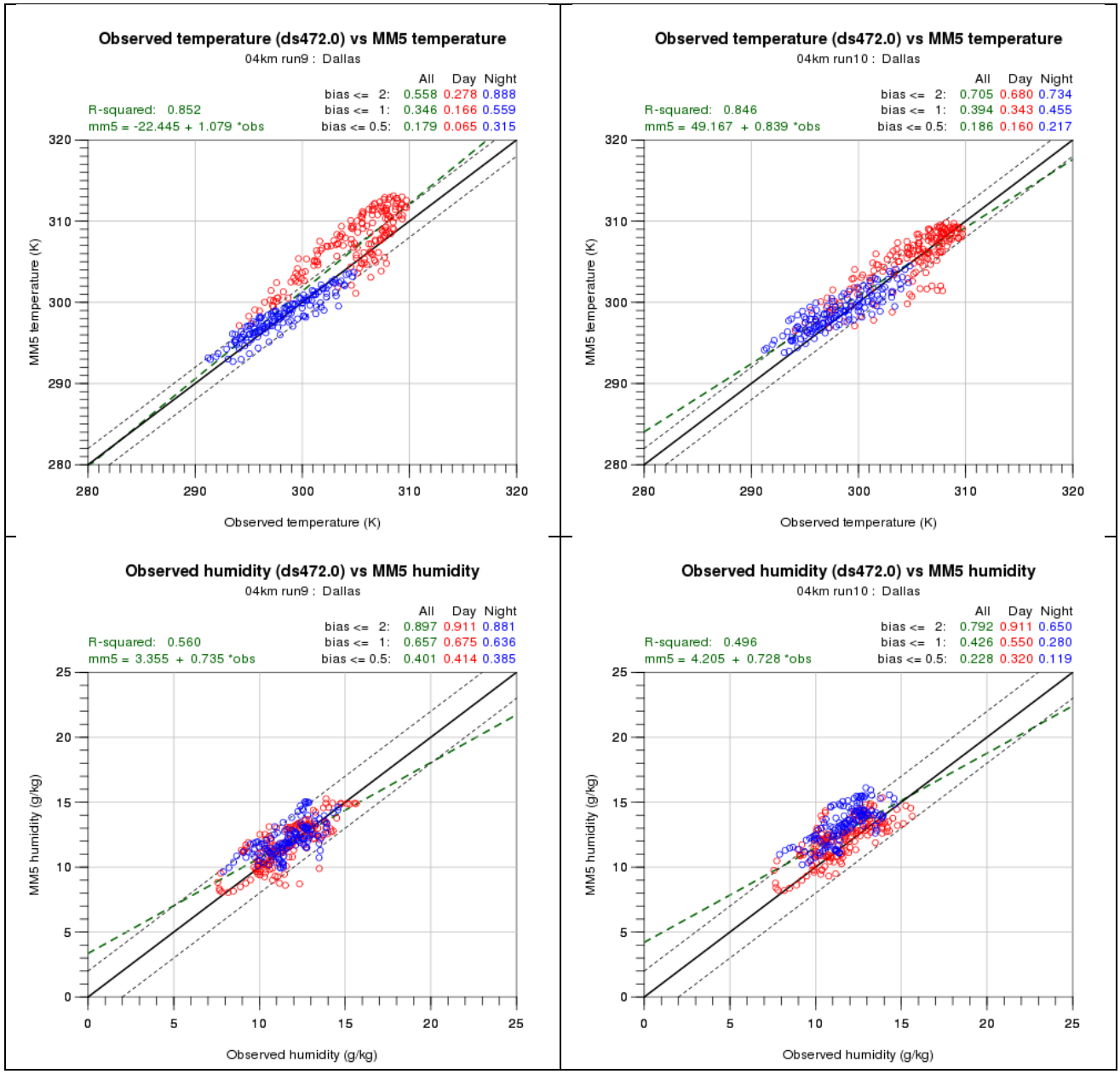

Figure 3-8. Scatter plots of hourly temperature (K; top) and hourly humidity (g/kg, bottom) at DS472 sites in Dallas for Run 9 (left) and for Run 10 (right). Blue points are nighttime hours, red point are daytime hours. The green dash line is the best fit line to all data; the black dotted lines are the ±2 K error envelope (top) and the ±2 g/kg error envelope (bottom). Fractions of data points within different bias ranges are shown at the top right of each plot.

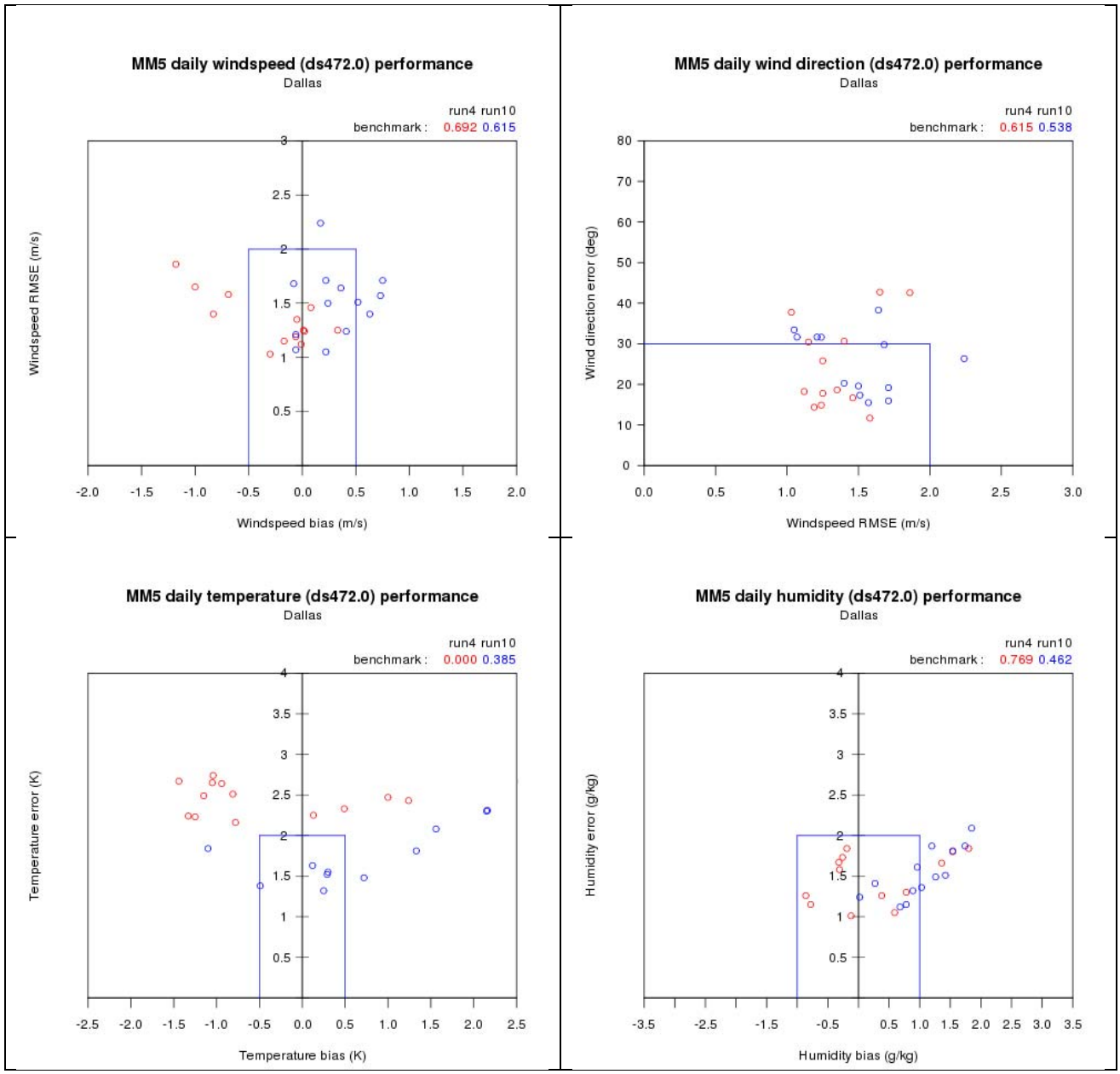

Figure 3-9. Scatter plots of daily statistical performance against DS472 data in Dallas for wind speed (top left), wind direction (top right), temperature (bottom left) and humidity (bottom right). Each plot shows daily performance from AACOG/CAPCOG Run 4 (red dots) and Run 10 (blue dots). The blue boxes represent the bias/error space bounded by the statistical performance benchmarks described in Section 1.

3.4 NORTHEAST TEXAS

Figures 3-10 and 3-11 show scatter plots of hourly MM5 wind speed, wind direction, temperature, and humidity against DS472 observations in the Northeast Texas analysis region for MM5 Runs 9 and 10. Figure 3-12 shows scatter plots of daily statistical performance against DS472 observations for wind speed, wind direction, temperature, and humidity in the Northeast Texas analysis region.

Results for all variables are similar to the effects seen in Dallas. Very little difference is seen in hourly and daily wind speed/direction performance between Runs 9 and 10. Run 10 exhibits a very slight degradation in daily wind direction performance. Overall, wind performance continues to be quite good in Northeast Texas.

Consistent with all other cities, hourly temperature performance in Run 10 is improved by the reduction of the daytime over prediction bias, but in this case Run 10 increases nighttime temperatures slightly to an over prediction bias. The net effect on daily performance is to reduce the gross error relative to Runs 4 and 9, but to maintain a tendency for over predictions by 1 to 2 K. Hourly humidity performance is slightly degraded by the shift toward higher humidity during both daytime and nighttime hours, with a bit more scatter in the data points (gross error). Daily humidity performance is similar among Runs 4, 9, and 10.

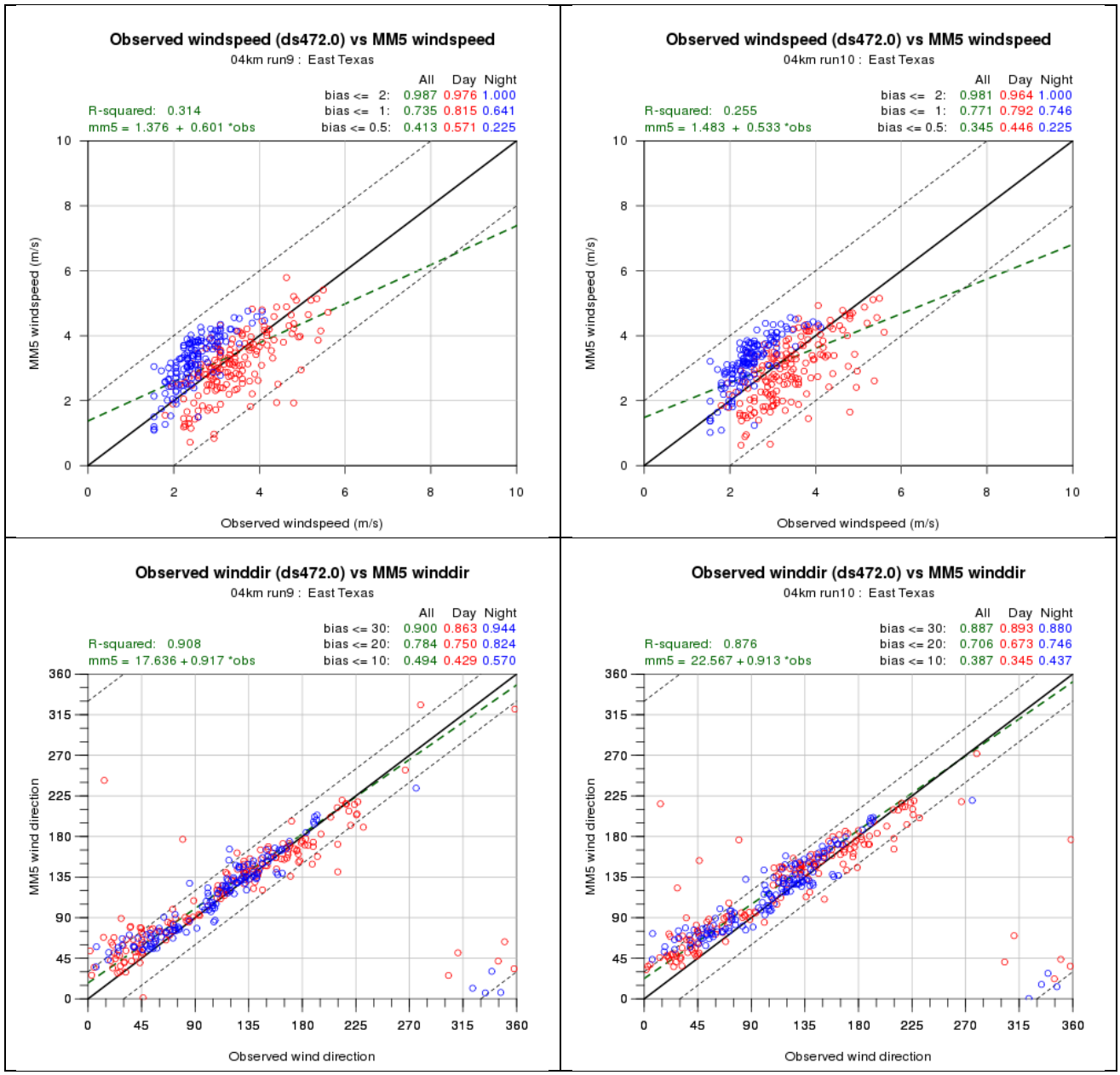

Figure 3-10. Scatter plots of hourly wind speed (m/s; top) and hourly wind direction (degrees, bottom) at DS472 sites in Northeast Texas for Run 9 (left) and for Run 10 (right). Blue points are nighttime hours, red point are daytime hours. The green dash line is the best fit line to all data; the black dotted lines are the ±2 m/s error envelope (top) and the ±30 degree error envelope (bottom). Fractions of data points within different bias ranges are shown at the top right of each plot.

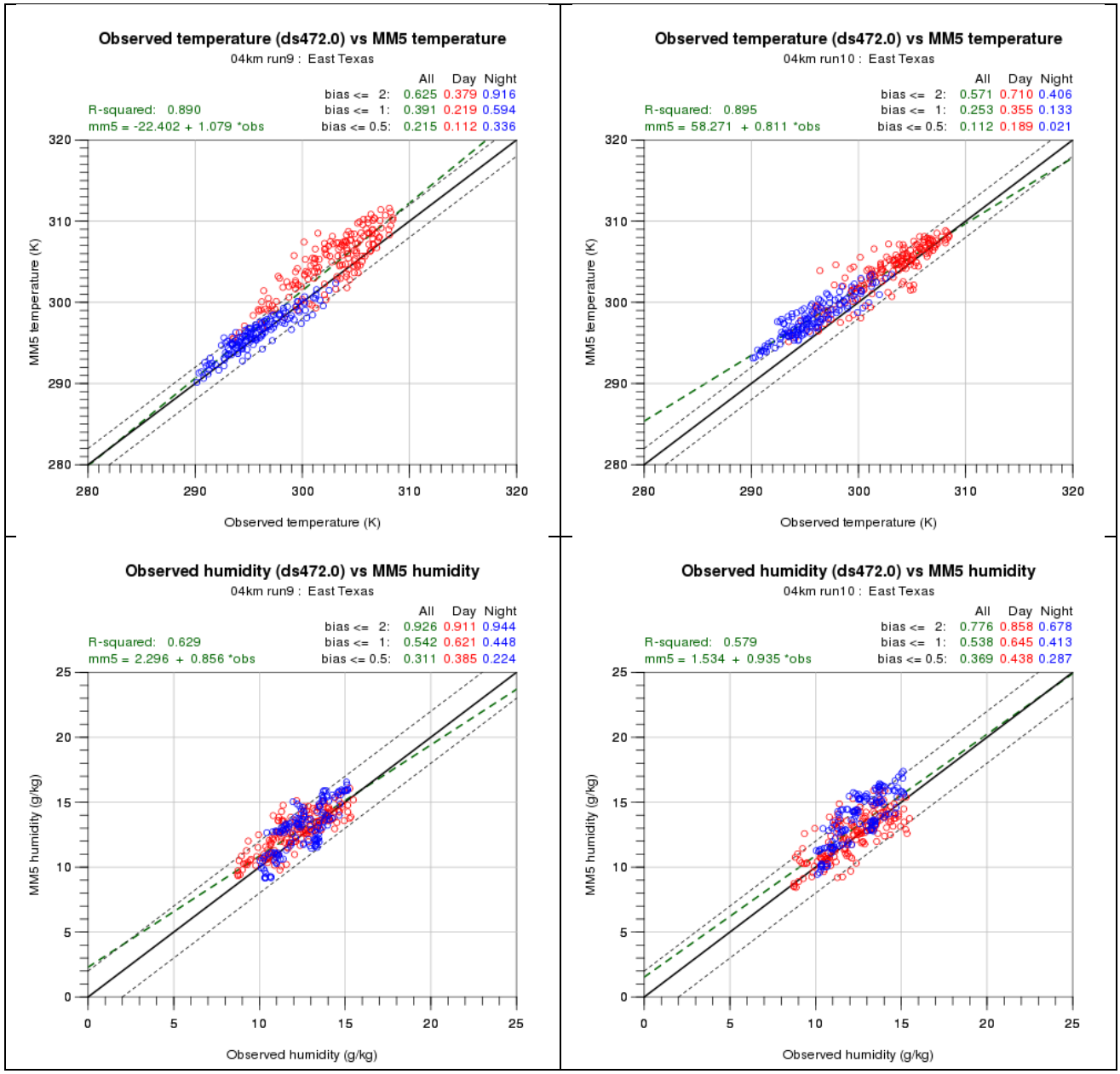

Figure 3-11. Scatter plots of hourly temperature (K; top) and hourly humidity (g/kg, bottom) at DS472 sites in Northeast Texas for Run 9 (left) and for Run 10 (right). Blue points are nighttime hours, red point are daytime hours. The green dash line is the best fit line to all data; the black dotted lines are the ±2 K error envelope (top) and the ±2 g/kg error envelope (bottom). Fractions of data points within different bias ranges are shown at the top right of each plot.

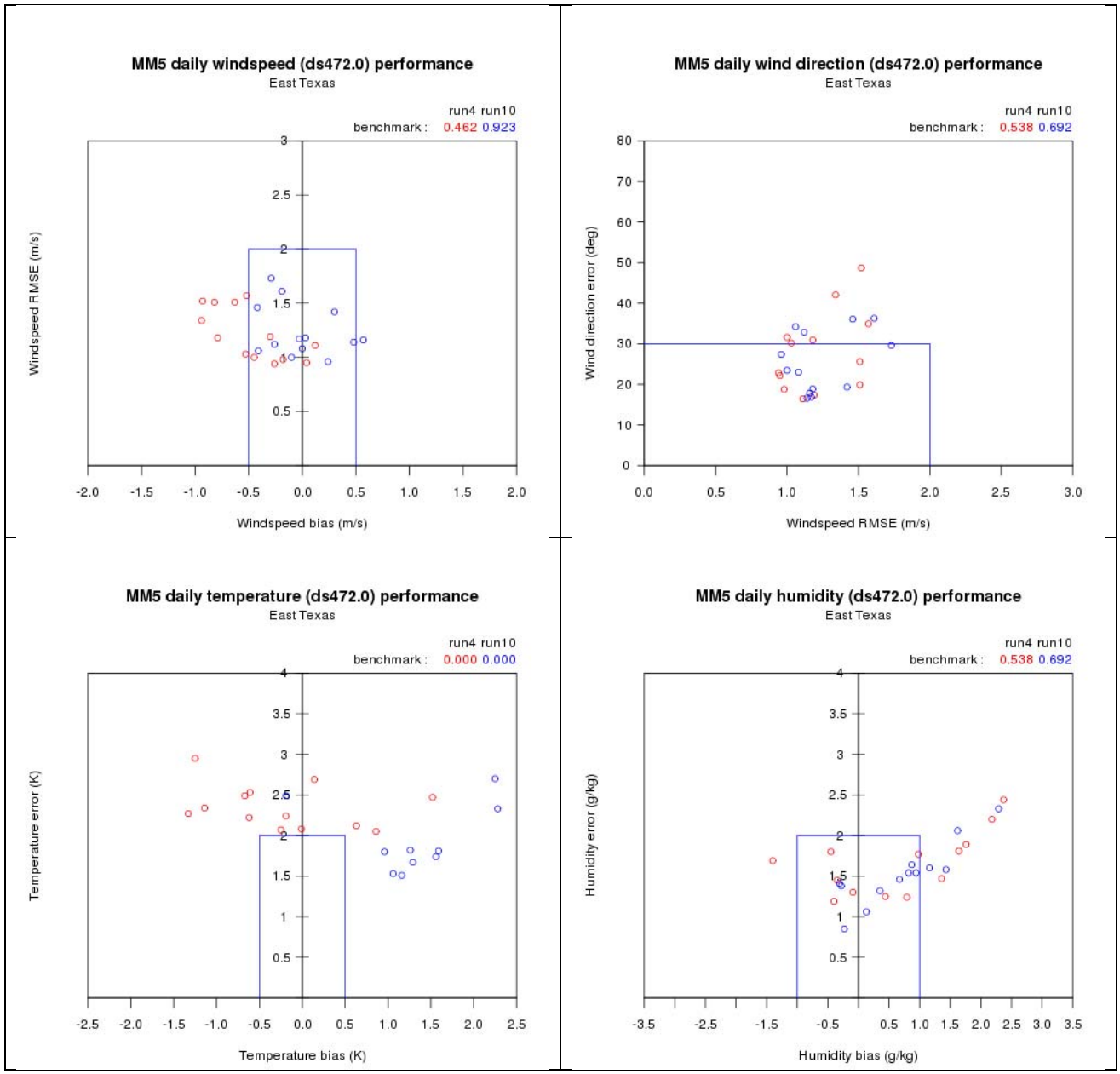

Figure 3-12. Scatter plots of daily statistical performance against DS472 data in Northeast Texas for wind speed (top left), wind direction (top right), temperature (bottom left) and humidity (bottom right). Each plot shows daily performance from AACOG/CAPCOG Run 4 (red dots) and Run 10 (blue dots). The blue boxes represent the bias/error space bounded by the statistical performance benchmarks described in Section 1.

3.5 EVALUATION OF PBL AND PRECIPITATION

Figures 3-13 through 3-17 display comparisons of hourly MM5 simulated PBL depths from Runs 9 and 10 against diagnosed PBL depths from profiler data at New Braunfels, Moody, Huntsville, Cleburne, and Lonview from May 30 through June 16. In general, the PBL depths are similar between Runs 9 and 10, with some days exhibiting some notable differences. Comparisons at New Braunfels and Moody show that Run 10 leads to lower maximum PBL depths than Run 9 on most days, while the opposite is true for Huntsville, Cleburne and Longview. The reasons for this are not particularly obvious and probably vary day-to-day, but we expect that the reduced afternoon surface temperatures lead to lower PBL depths in Run 10 for some sites/days, and this competes with reduced afternoon cloudiness that leads to higher PBL depths in Run 10 for other sites/days.

Figure 3-18 compares daily MM5 Run 9 and 10 precipitation against AHPS observed conditions between 7 AM June 13 to 7 AM June 14. The comparisons shown in this figure are more consistent between Runs 9 and 10 than the comparisons between Run 9 and the AACOG/ CAPCOG simulation. Run 10 rainfall is substantially reduced in the Houston area, while rainfall is more widespread in north-central Texas and along the San Antonio – Austin corridor. Both effects tend in a direction that is opposite of observed patterns, but Run 10 is still considerably better than the results of Run 8 shown in Section 2.

Figures 3-19 and 3-20 display snapshots of surface wind fields, cloud cover (expressed as cloud optical depth – an input to CAMx), and precipitation at 4 PM on June 13 for Run 9 and 10, respectively. Run 10 further reduces afternoon convective activity to near zero in southeastern Texas, and also reduces cloud cover in that area. However, more cloud cover is evident in north-central Texas. With the reduction in afternoon convective activity, wind fields exhibit much more calm conditions in east-central Texas.

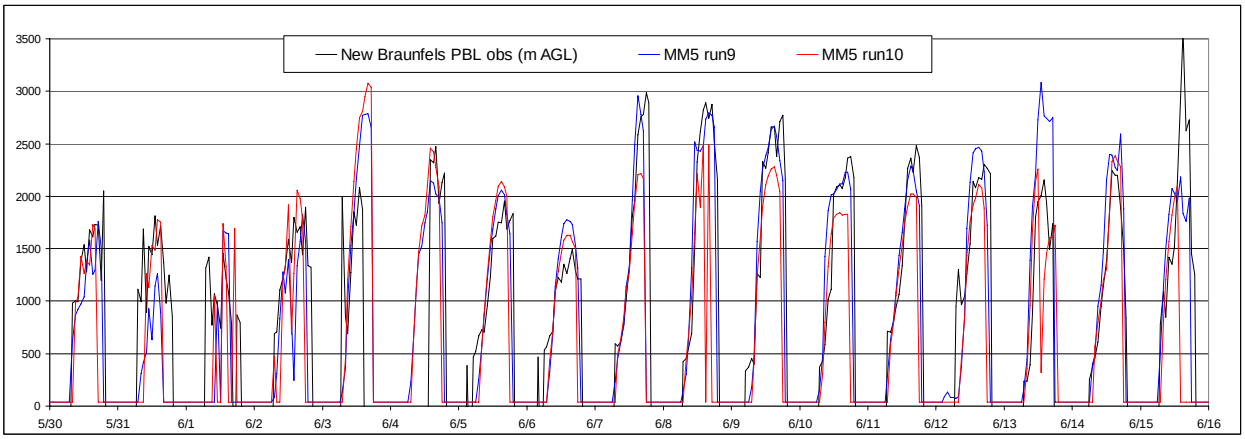

Figure 3-13. Hourly time series of predicted (MM5 Runs 9 and 10) and diagnosed PBL depths from the New Braunfels wind profiler.

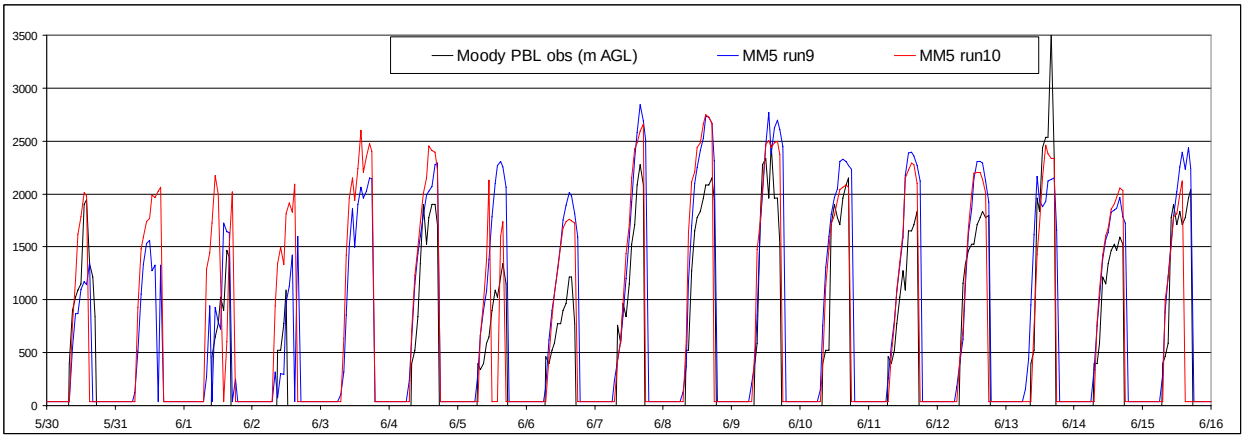

Figure 3-14. Hourly time series of predicted (MM5 Runs 9 and 10) and diagnosed PBL depths from the Moody wind profiler.

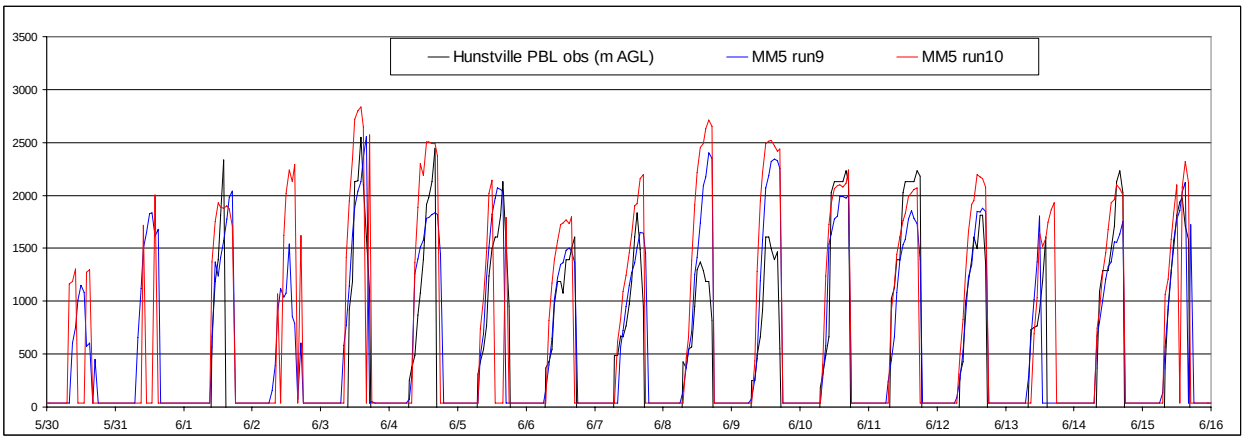

Figure 3-15. Hourly time series of predicted (MM5 Runs 9 and 10) and diagnosed PBL depths from the Hunstville wind profiler.

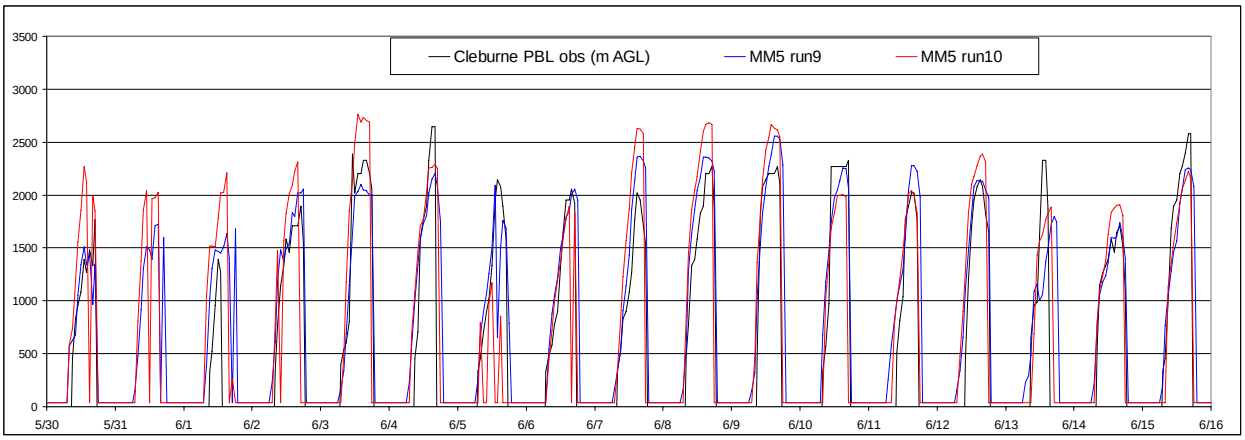

Figure 3-16. Hourly time series of predicted (MM5 Runs 9 and 10) and diagnosed PBL depths from the Cleburne wind profiler.

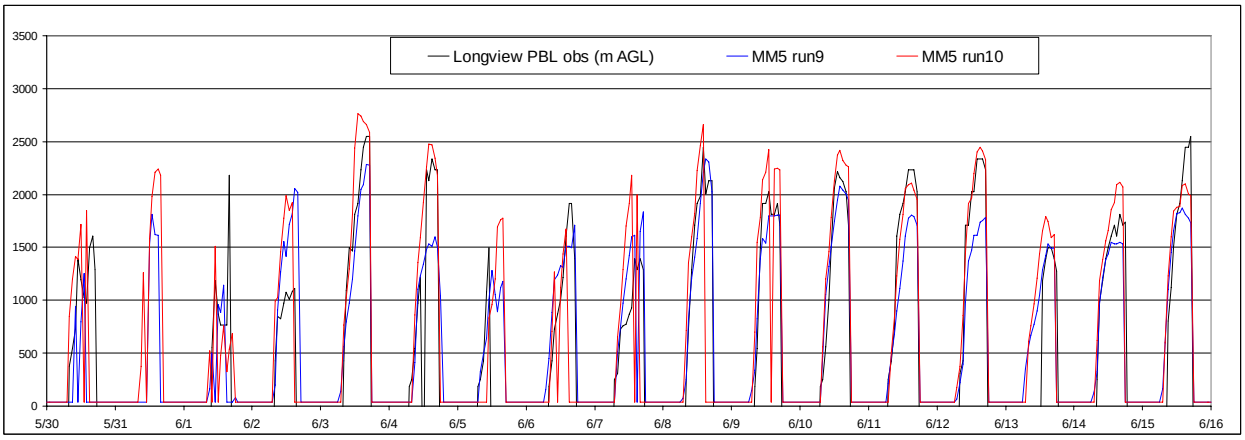

Figure 3-17. Hourly time series of predicted (MM5 Runs 9 and 10) and diagnosed PBL depths from the Longview wind profiler.

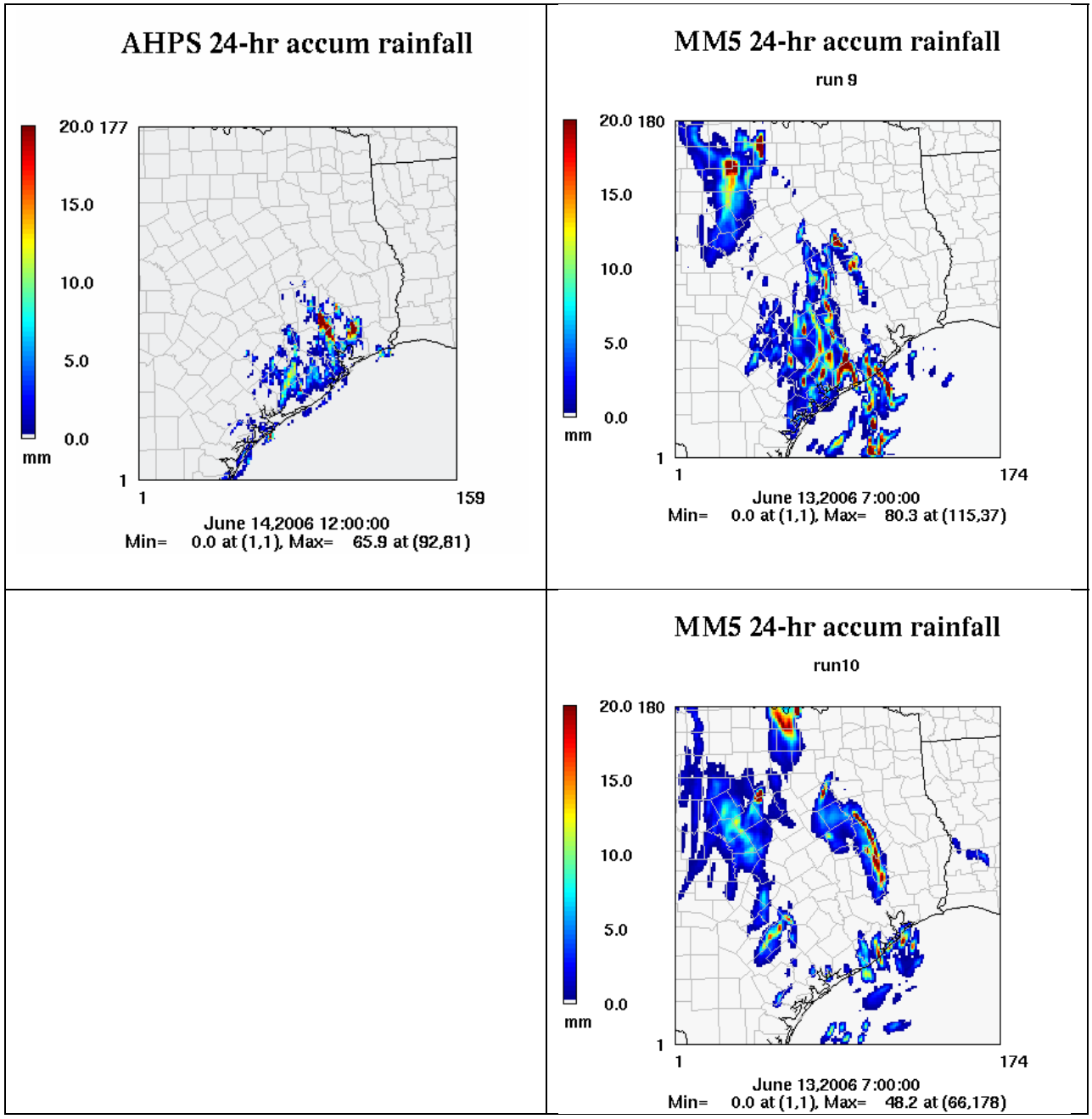

Figure 3-18. Observed (AHPS; top left) and MM5 simulated 24-hour accumulated precipitation (mm) for Runs 9 (top right) and 10 (bottom right), 7 AM June 14 to 7 AM June 15, 2006.

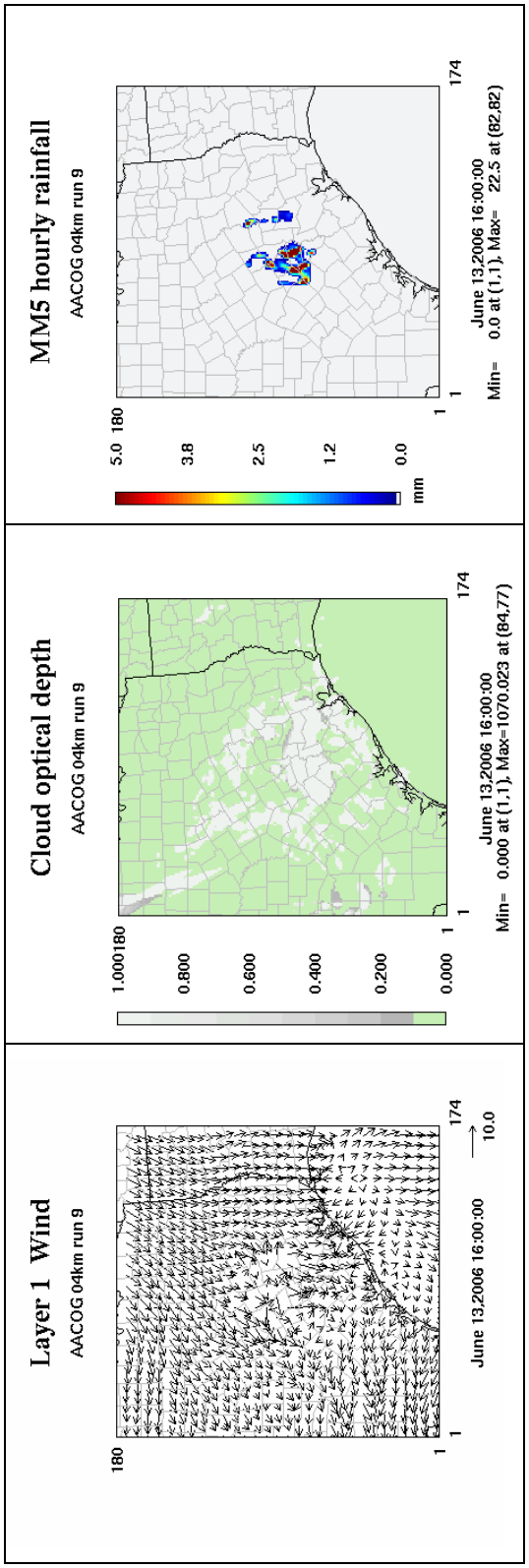

Figure 3-19. Simulated wind fields (left), CAMx cloud cover (middle), and rainfall (right) from MM5 Run 9 at 4 PM, June 13, 2006.

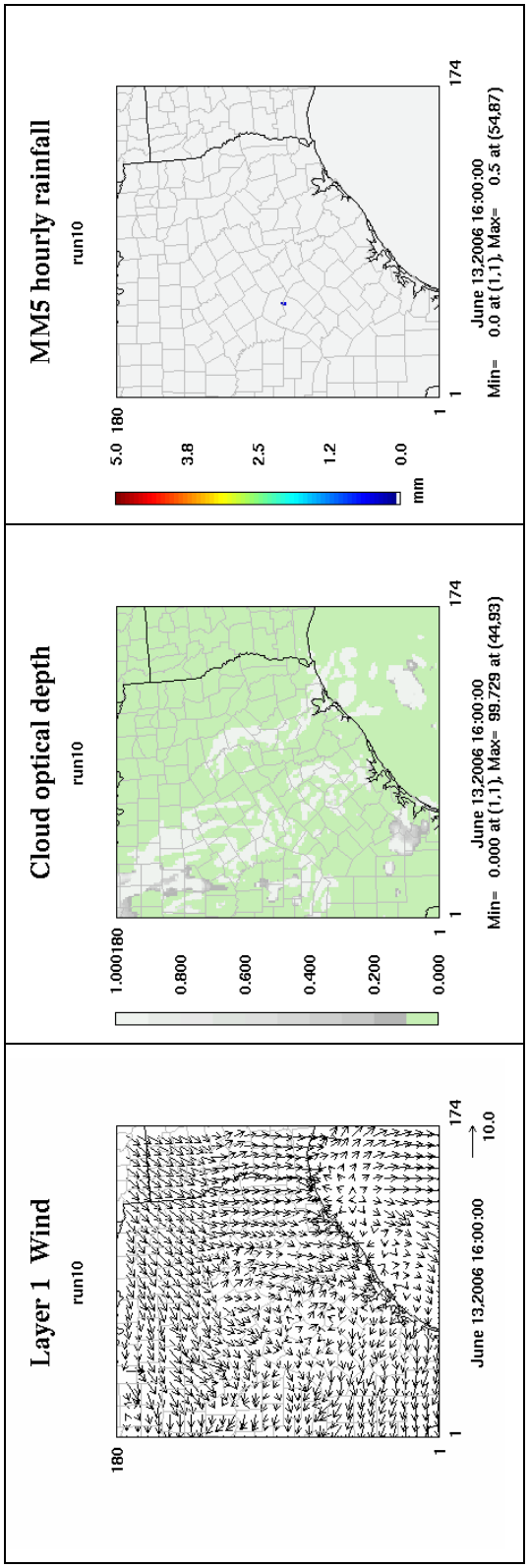

Figure 3-20. Simulated wind fields (left), CAMx cloud cover (middle), and rainfall (right) from MM5 Run 10 at 4 PM, June 13, 2006.

4. SURFACE ANALYSIS NUDGING

The final MM5 simulation (Run 11) was identical to Run 10, but replaced the hourly surface wind *observational* nudging with hourly surface wind *analysis* nudging. There were no changes to the nudging strength. The analysis nudging files were developed using the "little_r" preprocessor to blend 1-hour ADP observations into 3-hour EDAS analyses. A similar technique was used in MM5 modeling to support the Baton Rouge 8-hour SIP with outstanding results. The difference between surface observational and analysis nudging is that in the former case only portions of the grid are nudged toward point observations (with a Gaussian-shaped nudging factor radiating from each point) whereas in the latter case the entire grid is nudged continuously. This test was performed to determine if the alternative approach for surface wind nudging could further improve wind statistical performance. Run 11 was performed on the expanded 4-km grid only using boundary conditions derived from the 12-km Run 10 simulation.

4.1 SAN ANTONIO

Figures 4-1 and 4-2 show scatter plots of hourly MM5 wind speed, wind direction, temperature, and humidity against DS472 observations in the San Antonio analysis region for MM5 Runs 10 and 11. Figure 4-3 shows scatter plots of daily statistical performance against DS472 observations for wind speed, wind direction, temperature, and humidity in the San Antonio analysis region. Each plot shows daily performance from Run 4 (red points) and Run 10 (blue points) to illustrate performance differences relative to the baseline AACOG/CAPCOG simulation.

Similar hourly wind speed and direction performance results are achieved with Runs 10 and 11. Daytime wind speeds are slightly improved in Run 11, while both daytime and nighttime wind directions show statistical improvement. Daily statistics for Run 11 wind speed are nearly identical to Run 10 (compare to Figure 3-3), but the daily wind direction bias is reduced 10 to 20 degrees, which is significant. These results are consistent with our experience: altering the type and/or strength of surface wind nudging usually results in improved directions and minimal change in speeds.

As expected, hourly and daily temperature and humidity statistics are insignificantly impacted by the change in surface wind nudging. Some slight improvements to daily temperature and humidity are notable in Figure 4-3, with a few more days closer to and within the benchmarks.

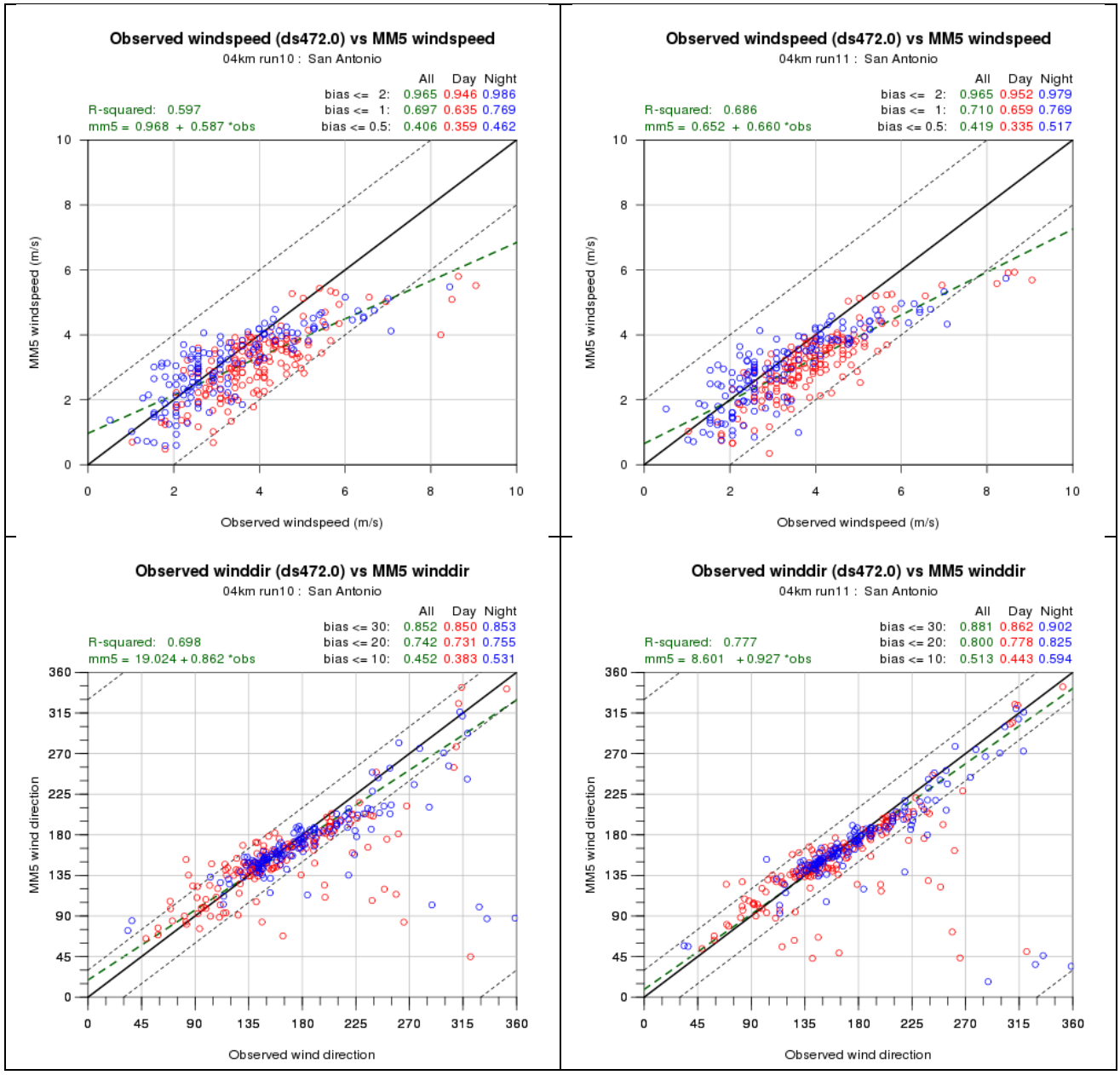

Figure 4-1. Scatter plots of hourly wind speed (m/s; top) and hourly wind direction (degrees, bottom) at DS472 sites in San Antonio for Run 10 (left) and for Run 11 (right). Blue points are nighttime hours, red point are daytime hours. The green dash line is the best fit line to all data; the black dotted lines are the ±2 m/s error envelope (top) and the ±30 degree error envelope (bottom). Fractions of data points within different bias ranges are shown at the top right of each plot.

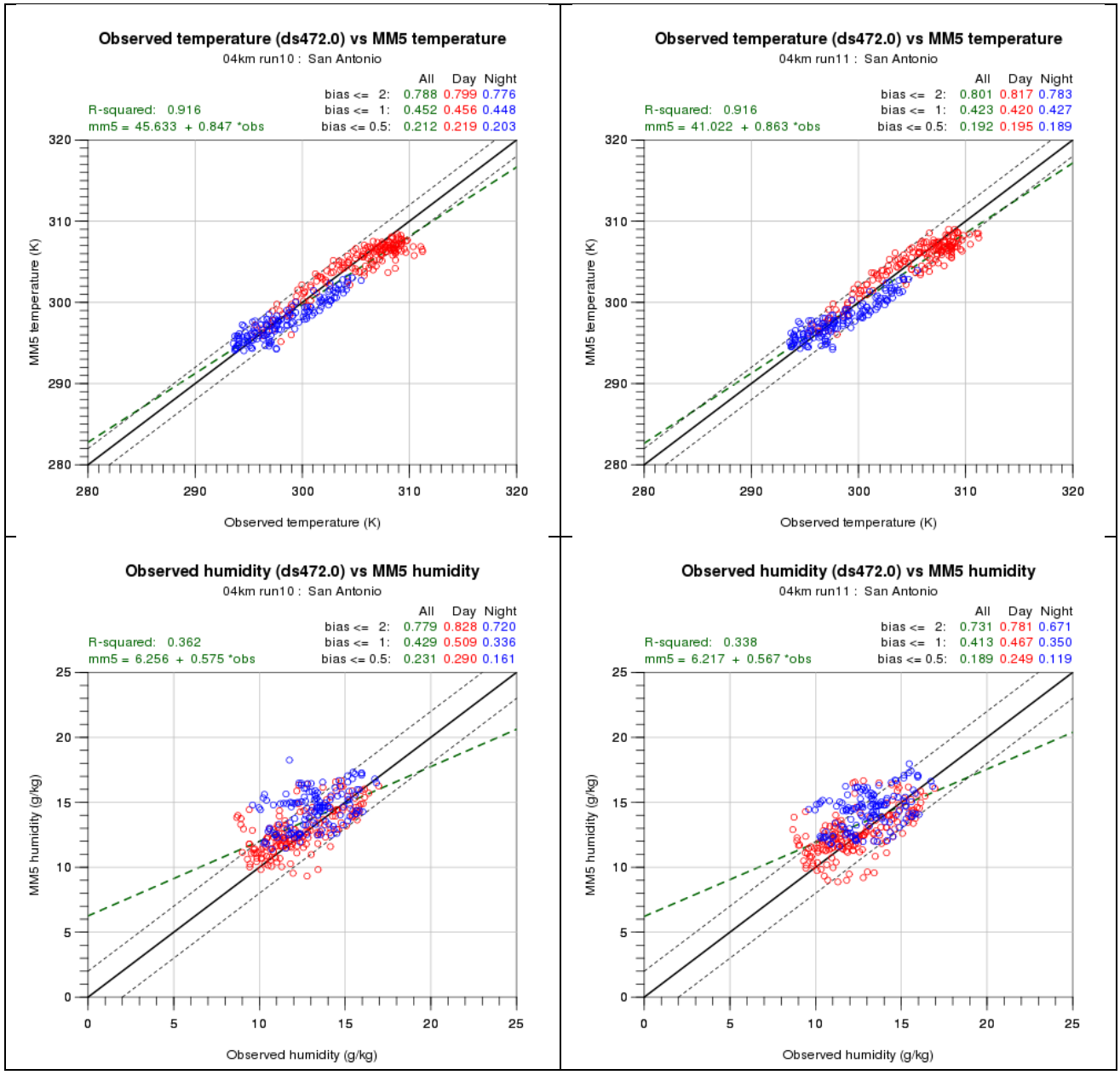

Figure 4-2. Scatter plots of hourly temperature (K; top) and hourly humidity (g/kg, bottom) at DS472 sites in San Antonio for Run 10 (left) and for Run 11 (right). Blue points are nighttime hours, red point are daytime hours. The green dash line is the best fit line to all data; the black dotted lines are the ±2 K error envelope (top) and the ±2 g/kg error envelope (bottom). Fractions of data points within different bias ranges are shown at the top right of each plot.

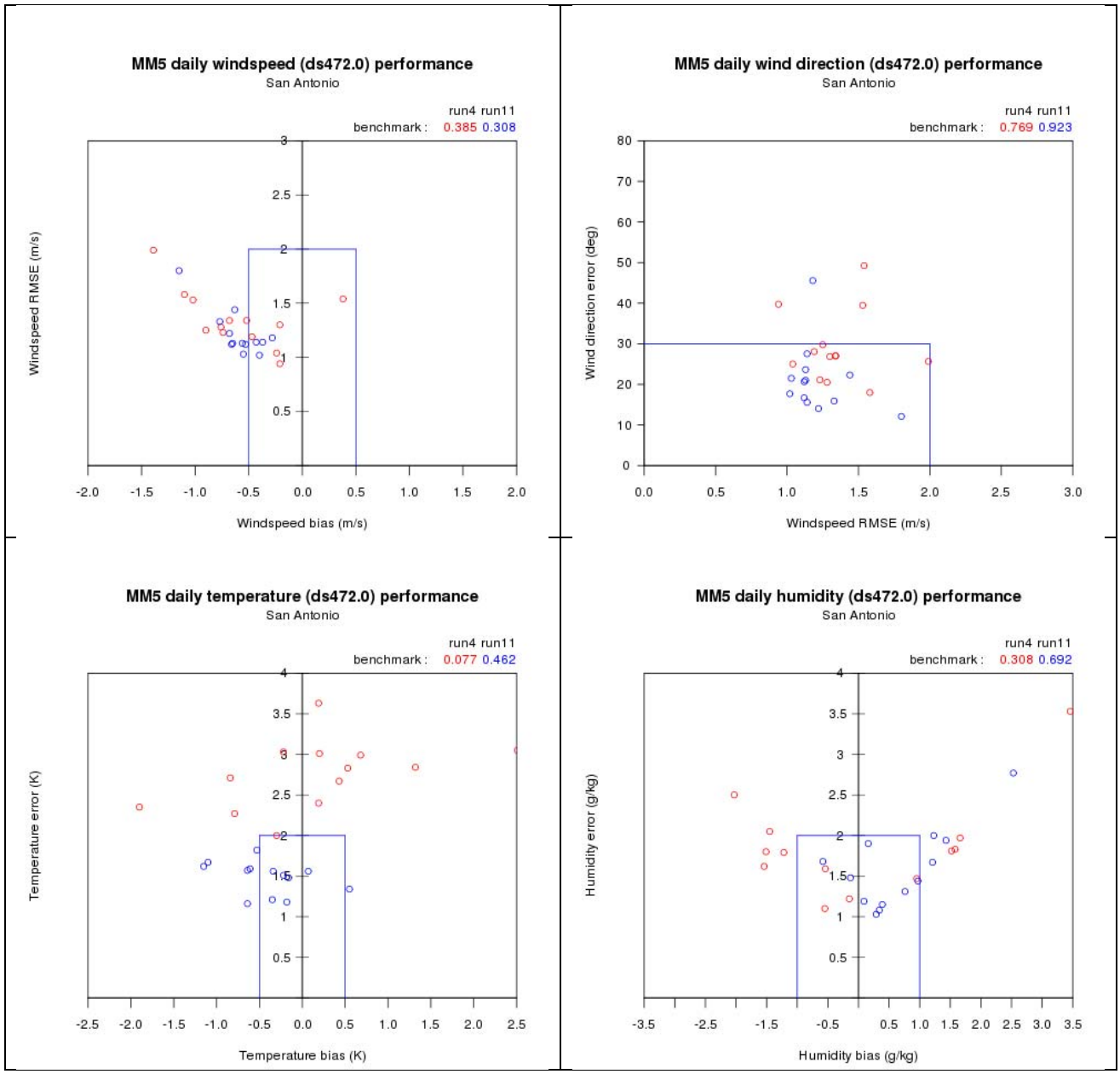

Figure 4-3. Scatter plots of daily statistical performance against DS472 data in San Antonio for wind speed (top left), wind direction (top right), temperature (bottom left) and humidity (bottom right). Each plot shows daily performance from AACOG/CAPCOG Run 4 (red dots) and Run 11 (blue dots). The blue boxes represent the bias/error space bounded by the statistical performance benchmarks described in Section 1.

4.2 AUSTIN

Figures 4-4 and 4-5 show scatter plots of hourly MM5 wind speed, wind direction, temperature, and humidity against DS472 observations in the Austin analysis region for MM5 Runs 10 and 11. Figure 4-6 shows scatter plots of daily statistical performance against DS472 observations for wind speed, wind direction, temperature, and humidity in the Austin analysis region.

As similarly seen in San Antonio, hourly wind speeds from Run 11 exhibit a slight performance improvement for daytime hours (with little impact at night), but the hourly wind directions are uniformly improved both day and night. Daily wind speed performance is better than in Run 10, and while daily direction performance is also better, it is not as substantial as seen in San Antonio. This is probably because Austin wind performance in Run 9 was generally better than San Antonio performance.

Very little difference is seen in hourly and daily temperature and humidity performance between Runs 10 and 11.

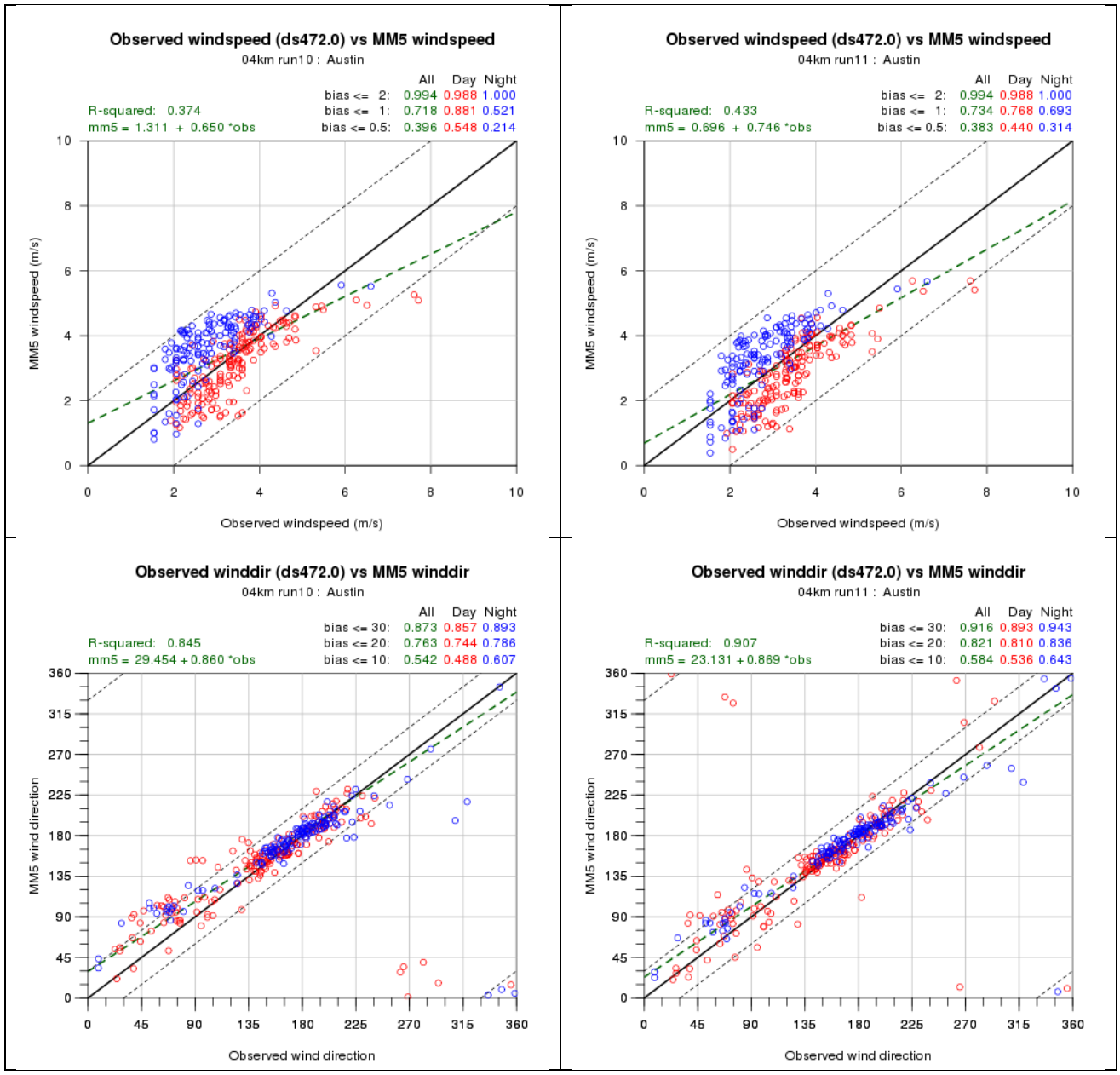

Figure 4-4. Scatter plots of hourly wind speed (m/s; top) and hourly wind direction (degrees, bottom) at DS472 sites in Austin for Run 10 (left) and for Run 11 (right). Blue points are nighttime hours, red point are daytime hours. The green dash line is the best fit line to all data; the black dotted lines are the ±2 m/s error envelope (top) and the ±30 degree error envelope (bottom). Fractions of data points within different bias ranges are shown at the top right of each plot.

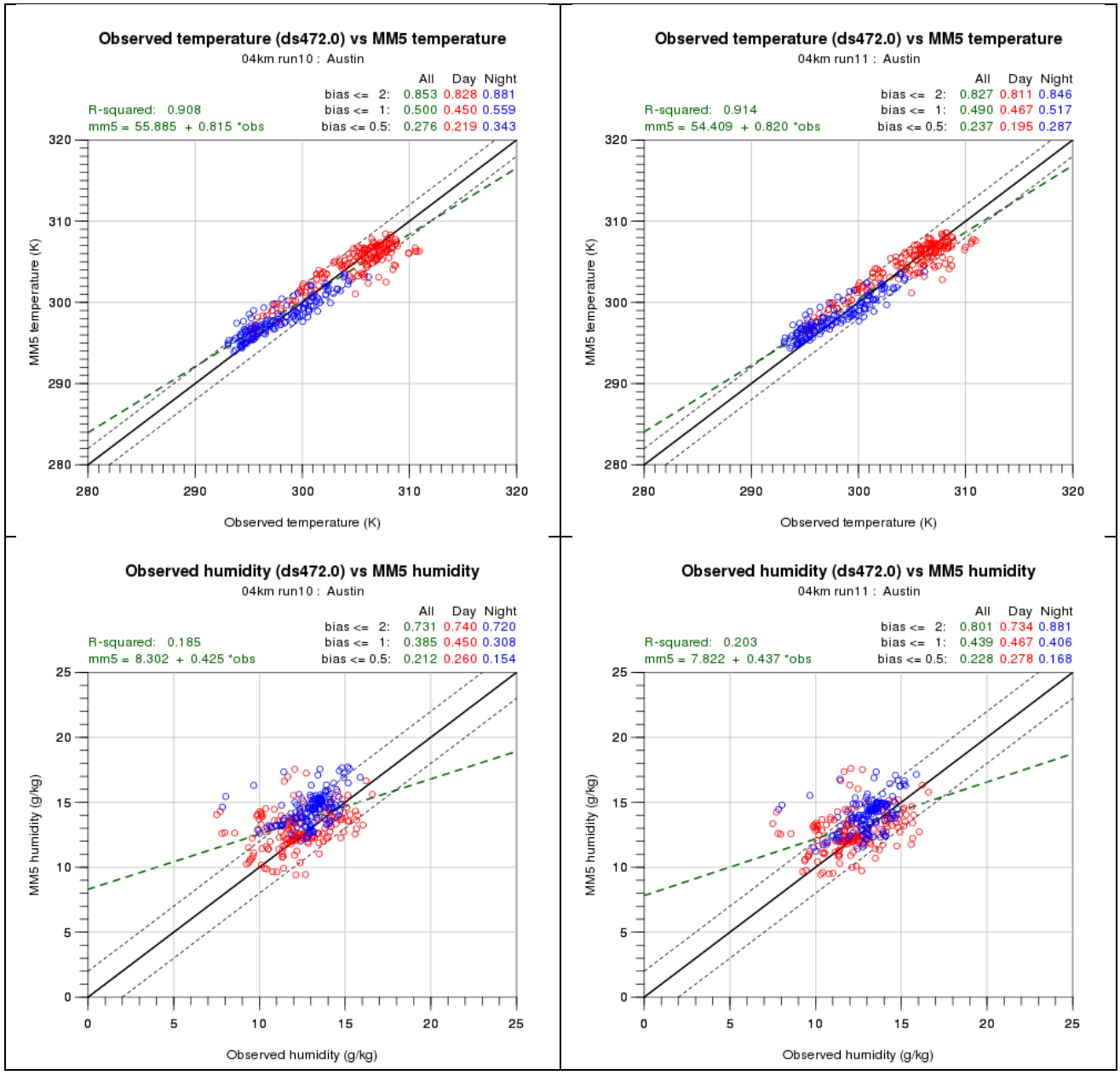

Figure 4-5. Scatter plots of hourly temperature (K; top) and hourly humidity (g/kg, bottom) at DS472 sites in Austin for Run 10 (left) and for Run 11 (right). Blue points are nighttime hours, red point are daytime hours. The green dash line is the best fit line to all data; the black dotted lines are the ±2 K error envelope (top) and the ±2 g/kg error envelope (bottom). Fractions of data points within different bias ranges are shown at the top right of each plot.

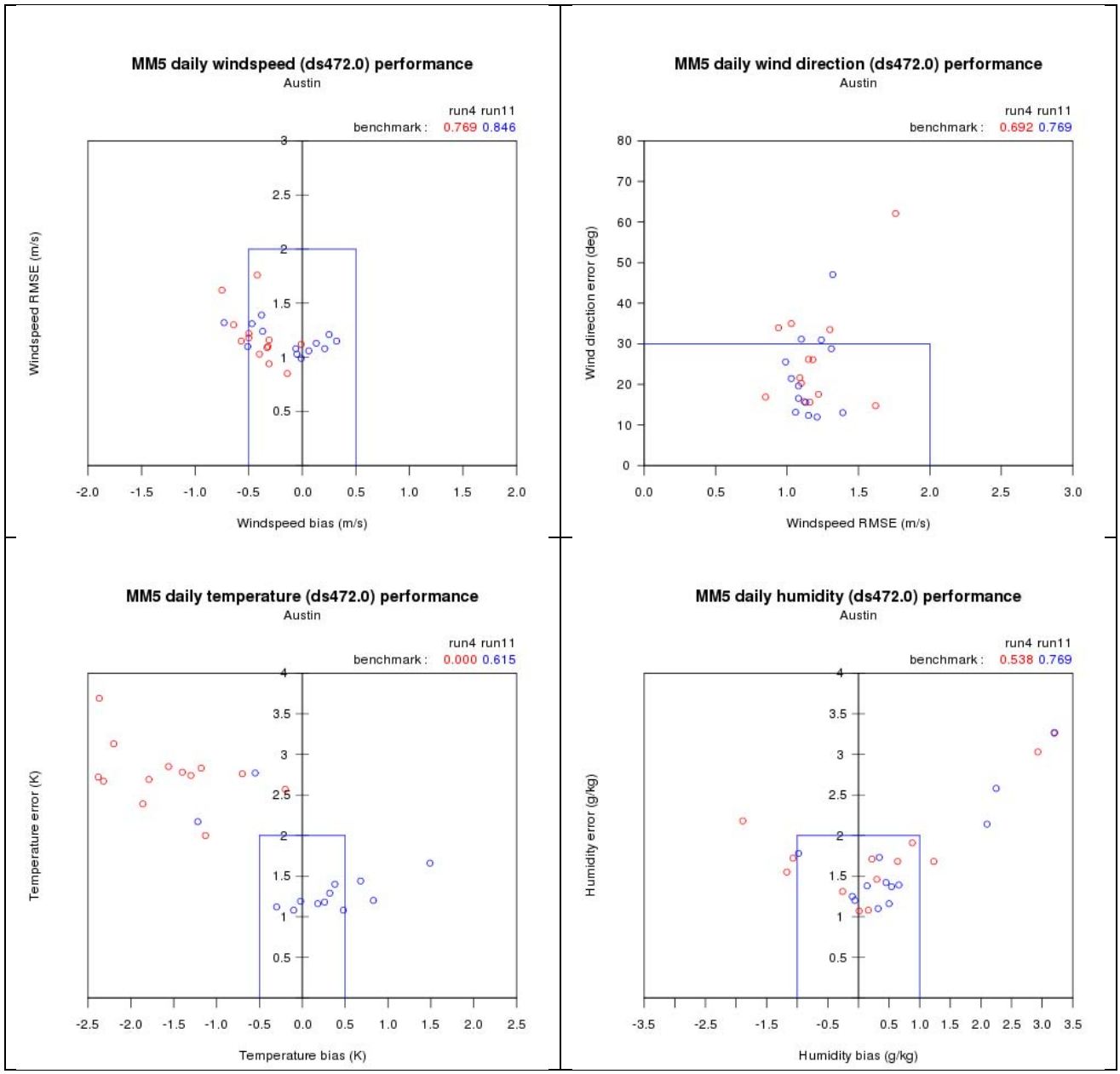

Figure 4-6. Scatter plots of daily statistical performance against DS472 data in Austin for wind speed (top left), wind direction (top right), temperature (bottom left) and humidity (bottom right). Each plot shows daily performance from AACOG/CAPCOG Run 4 (red dots) and Run 11 (blue dots). The blue boxes represent the bias/error space bounded by the statistical performance benchmarks described in Section 1.

4.3 DALLAS

Figures 4-7 and 4-8 show scatter plots of hourly MM5 wind speed, wind direction, temperature, and humidity against DS472 observations in the Dallas analysis region for MM5 Runs 10 and 11. Figure 4-9 shows scatter plots of daily statistical performance against DS472 observations for wind speed, wind direction, temperature, and humidity in the Dallas analysis region.

Less impact to wind speed performance is evident in Run 11 than in the southern cities. In this case, Run 11 resulted in very similar daytime results, but slightly improved nighttime statistics. Again, the biggest impact from the change in surface wind nudging is seen in the wind directions, with improvements both day and night. Nearly all days are brought into benchmark ranges for both wind speed and direction.

Very little difference is seen in hourly and daily temperature and humidity performance between Runs 10 and 11.

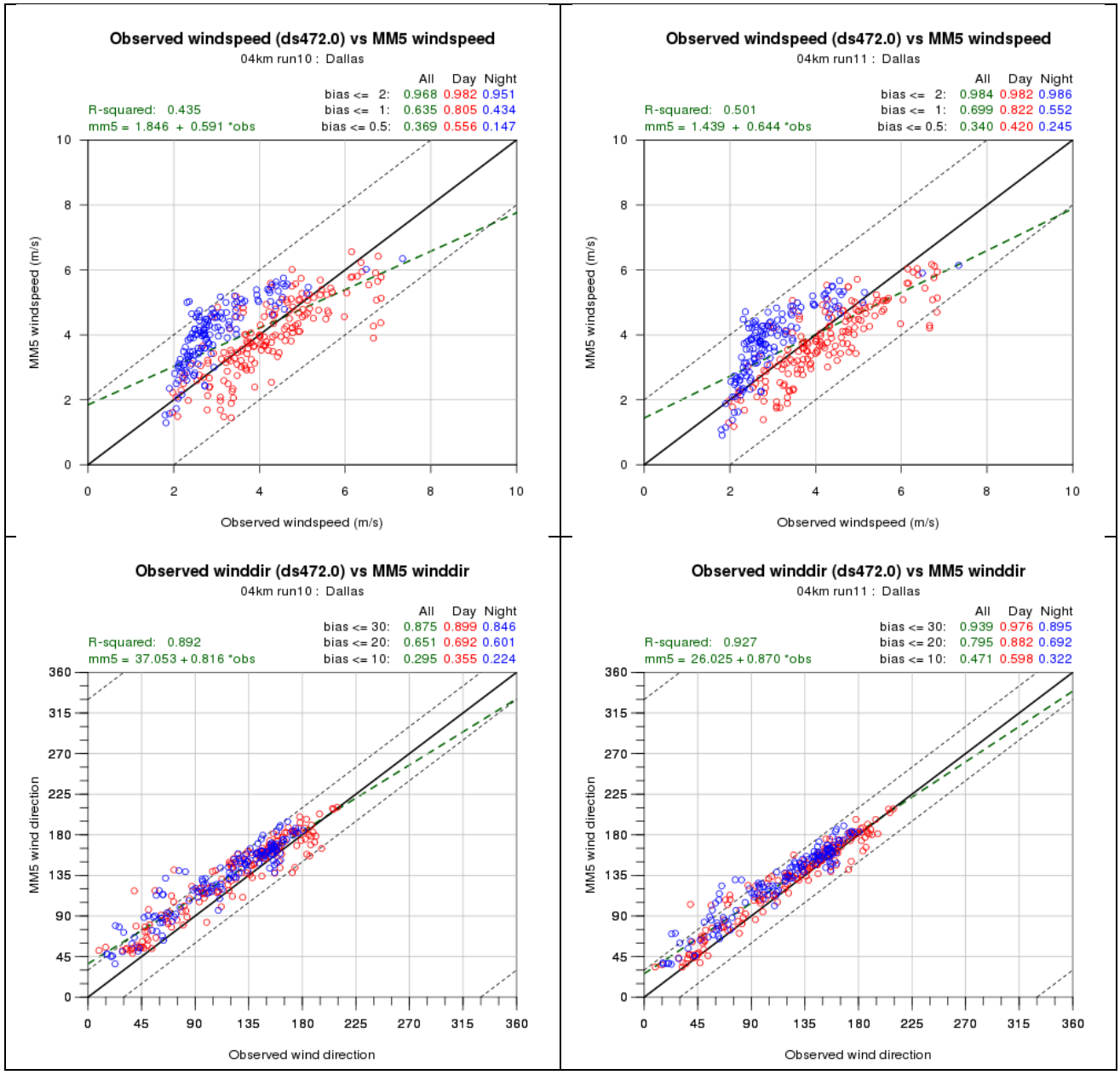

Figure 4-7. Scatter plots of hourly wind speed (m/s; top) and hourly wind direction (degrees, bottom) at DS472 sites in Dallas for Run 10 (left) and for Run 11 (right). Blue points are nighttime hours, red point are daytime hours. The green dash line is the best fit line to all data; the black dotted lines are the ±2 m/s error envelope (top) and the ±30 degree error envelope (bottom). Fractions of data points within different bias ranges are shown at the top right of each plot.

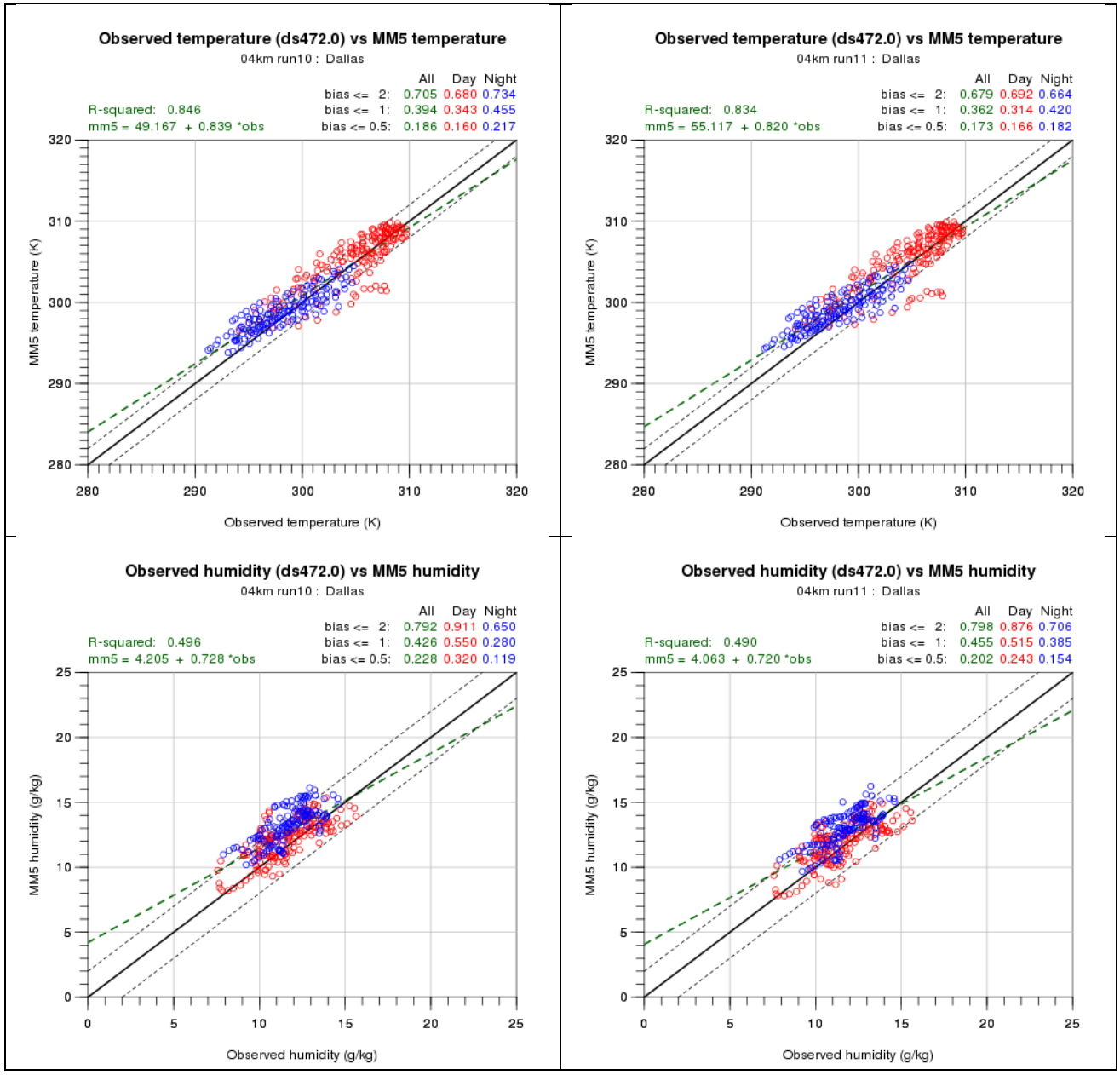

Figure 4-8. Scatter plots of hourly temperature (K; top) and hourly humidity (g/kg, bottom) at DS472 sites in Dallas for Run 10 (left) and for Run 11 (right). Blue points are nighttime hours, red point are daytime hours. The green dash line is the best fit line to all data; the black dotted lines are the ±2 K error envelope (top) and the ±2 g/kg error envelope (bottom). Fractions of data points within different bias ranges are shown at the top right of each plot.

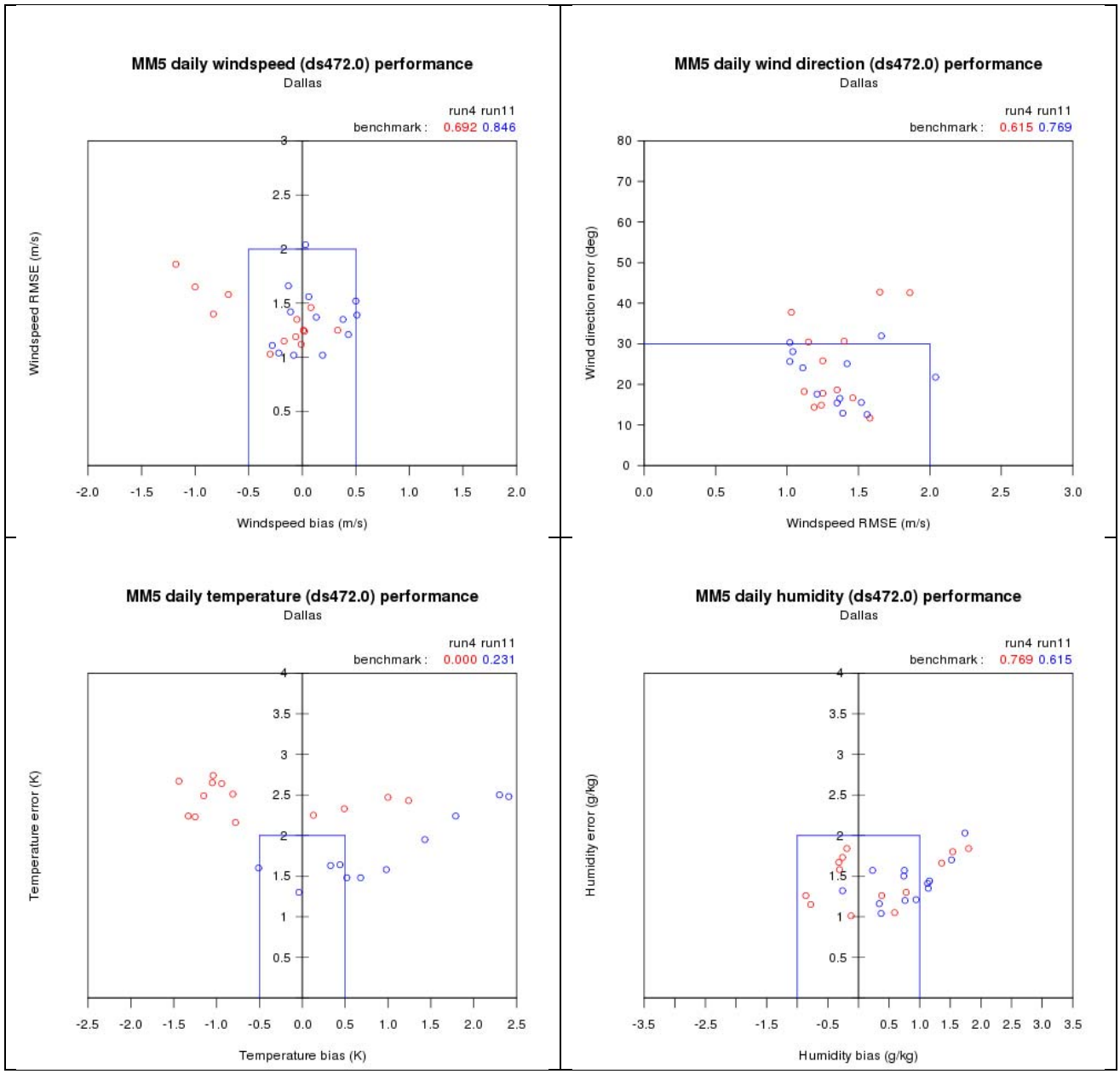

Figure 4-9. Scatter plots of daily statistical performance against DS472 data in Dallas for wind speed (top left), wind direction (top right), temperature (bottom left) and humidity (bottom right). Each plot shows daily performance from AACOG/CAPCOG Run 4 (red dots) and Run 11 (blue dots). The blue boxes represent the bias/error space bounded by the statistical performance benchmarks described in Section 1.

4.4 NORTHEAST TEXAS

Figures 4-10 and 4-11 show scatter plots of hourly MM5 wind speed, wind direction, temperature, and humidity against DS472 observations in the Northeast Texas analysis region for MM5 Runs 10 and 11. Figure 4-12 shows scatter plots of daily statistical performance against DS472 observations for wind speed, wind direction, temperature, and humidity in the Northeast Texas analysis region.

Results for all variables are similar to the effects seen in Dallas. Very little difference is seen in hourly and daily wind speed (there is some nominal nighttime performance improvement). Wind direction performance is slightly improved in Run 11 both day and night, but since performance in Run 10 was already quite good, the improvements are not as large as seen in other cities.

Hourly and daily temperature and humidity performance between Runs 10 and 11 are similar, but there is evidence that daily temperature and humidity statistics improved slightly in Run 11. This final run reduced the over predicted daily temperature and humidity on several days.

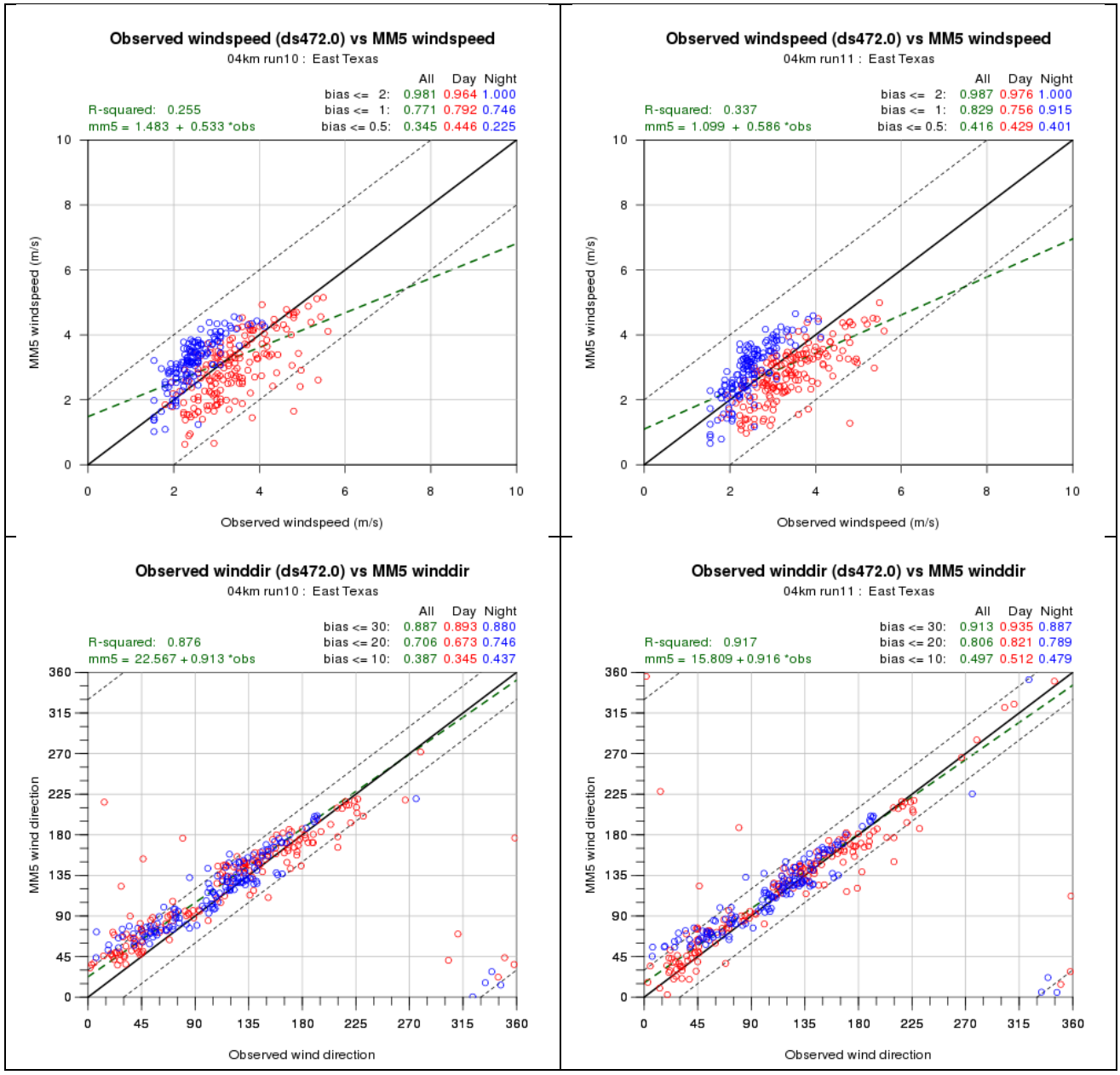

Figure 4-10. Scatter plots of hourly wind speed (m/s; top) and hourly wind direction (degrees, bottom) at DS472 sites in Northeast Texas for Run 10 (left) and for Run 11 (right). Blue points are nighttime hours, red point are daytime hours. The green dash line is the best fit line to all data; the black dotted lines are the ±2 m/s error envelope (top) and the ±30 degree error envelope (bottom). Fractions of data points within different bias ranges are shown at the top right of each plot.

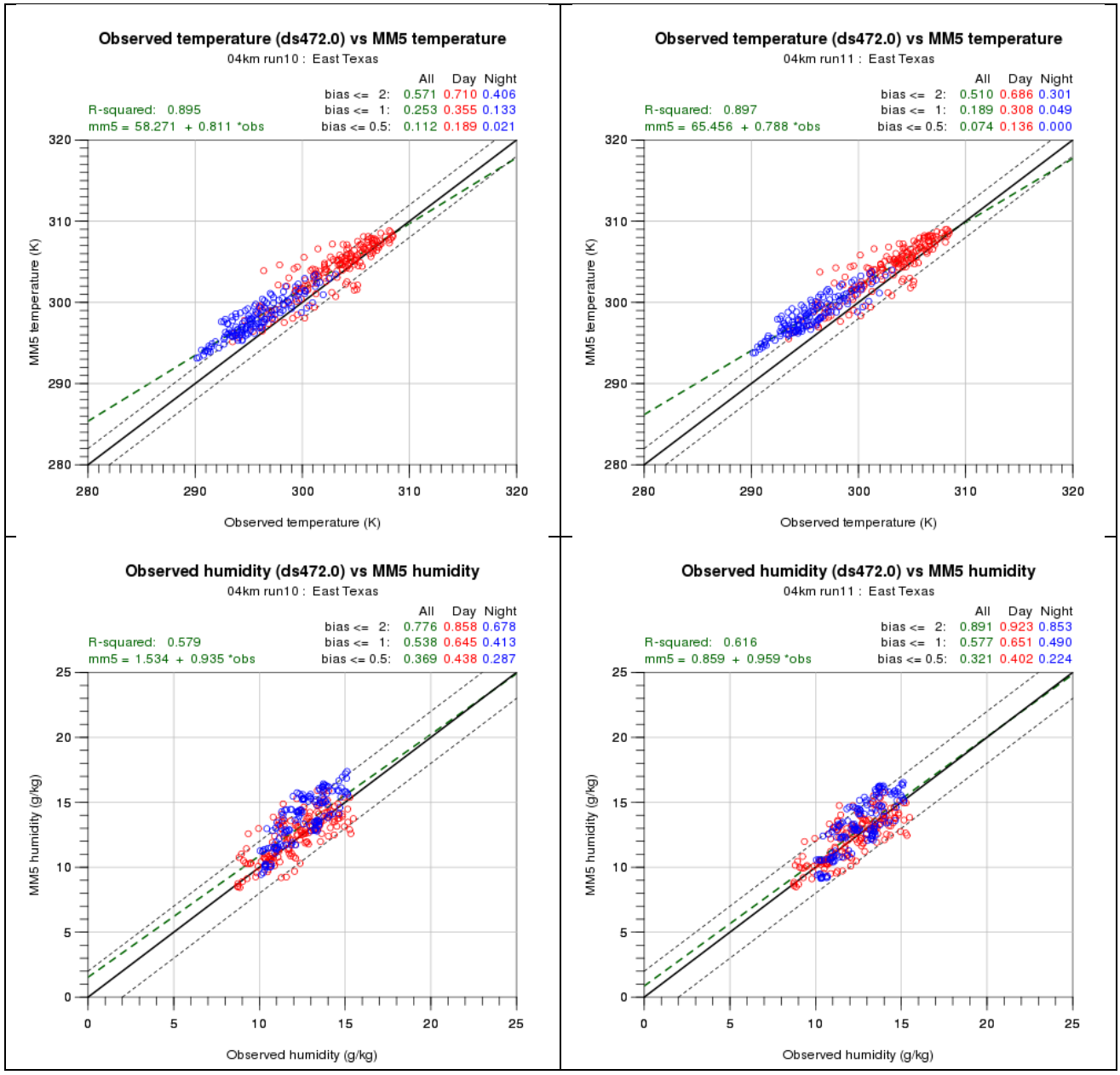

Figure 4-11. Scatter plots of hourly temperature (K; top) and hourly humidity (g/kg, bottom) at DS472 sites in Northeast Texas for Run 10 (left) and for Run 11 (right). Blue points are nighttime hours, red point are daytime hours. The green dash line is the best fit line to all data; the black dotted lines are the ±2 K error envelope (top) and the ±2 g/kg error envelope (bottom). Fractions of data points within different bias ranges are shown at the top right of each plot.

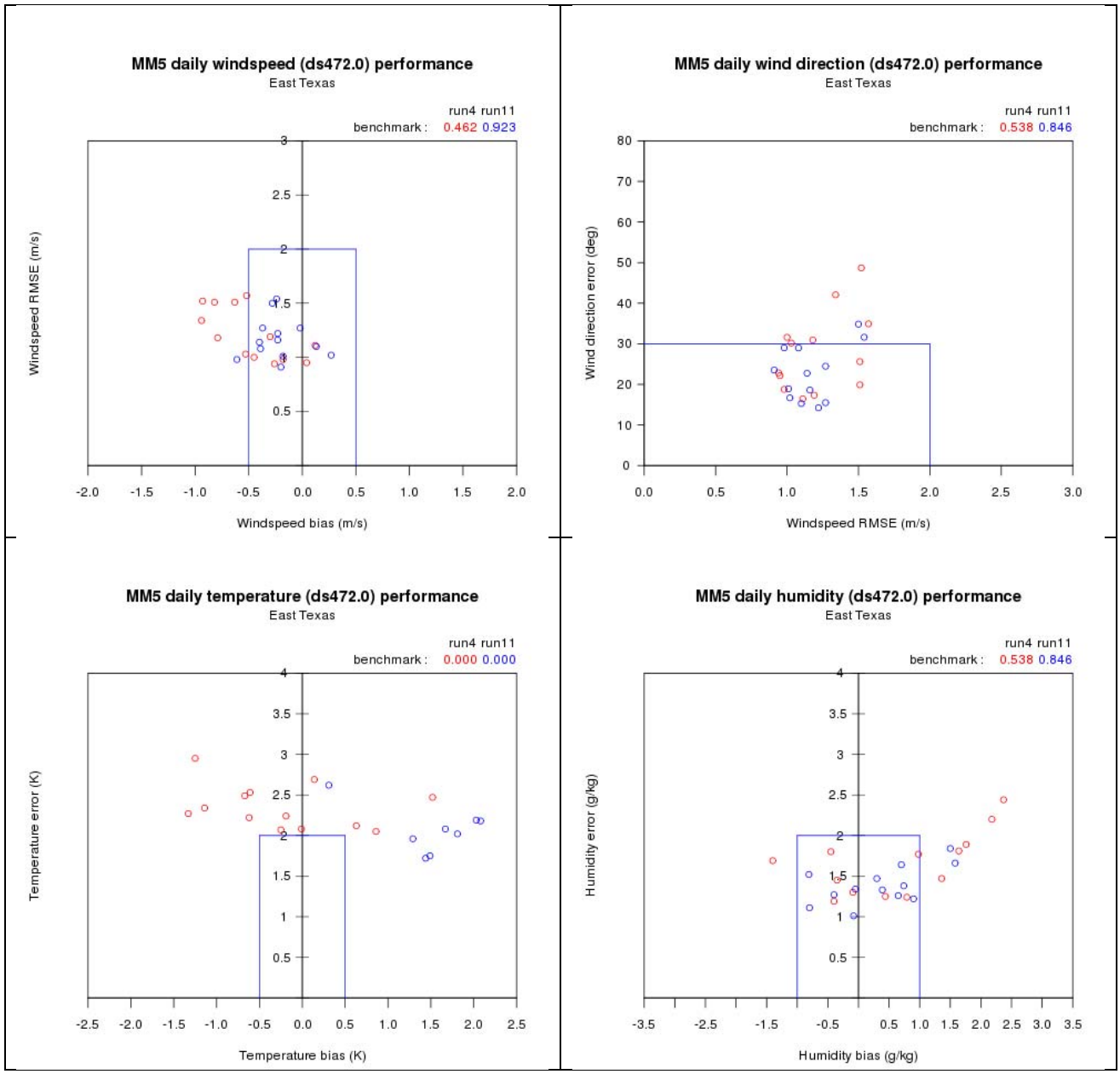

Figure 4-12. Scatter plots of daily statistical performance against DS472 data in Northeast Texas for wind speed (top left), wind direction (top right), temperature (bottom left) and humidity (bottom right). Each plot shows daily performance from AACOG/CAPCOG Run 4 (red dots) and Run 11 (blue dots). The blue boxes represent the bias/error space bounded by the statistical performance benchmarks described in Section 1.

4.5 EVALUATION OF PBL AND PRECIPITATION

Figures 4-13 through 4-17 display comparisons of hourly MM5 simulated PBL depths from Runs 10 and 11 against diagnosed PBL depths from profiler data at New Braunfels, Moody, Huntsville, Cleburne, and Lonview from May 30 through June 16. In general, the PBL depths are very similar between Runs 10 and 11, with a few days exhibiting some differences associated with changes in cloud cover and/or rain (evidenced by introduction or removal of hourly midday increases/decreases in PBL depth). The introduction of surface wind analysis nudging made no appreciable difference in PBL structures on most days at any of these five sites.

Figure 4-18 compares daily MM5 Run 9 and 10 precipitation against AHPS observed conditions between 7 AM June 13 to 7 AM June 14. Run 11 rainfall replaces the convective rainfall in the Houston area that was removed in Run 10. It also slightly reduces the extent and magnitude of rainfall in central and northern Texas. The impact of surface wind nudging in this regard was larger than expected. Overall the Run 11 precipitation simulation on this day is quite good.

Figures 4-19 and 4-20 display snapshots of surface wind fields, cloud cover (expressed as cloud optical depth – an input to CAMx), and precipitation at 4 PM on June 13 for Run 9 and 10, respectively. Run 11 maintains minimal afternoon convective activity in southeastern Texas and results in similar cloud cover patterns as Run 10. The afternoon wind fields similarly exhibit calm conditions in east-central Texas.

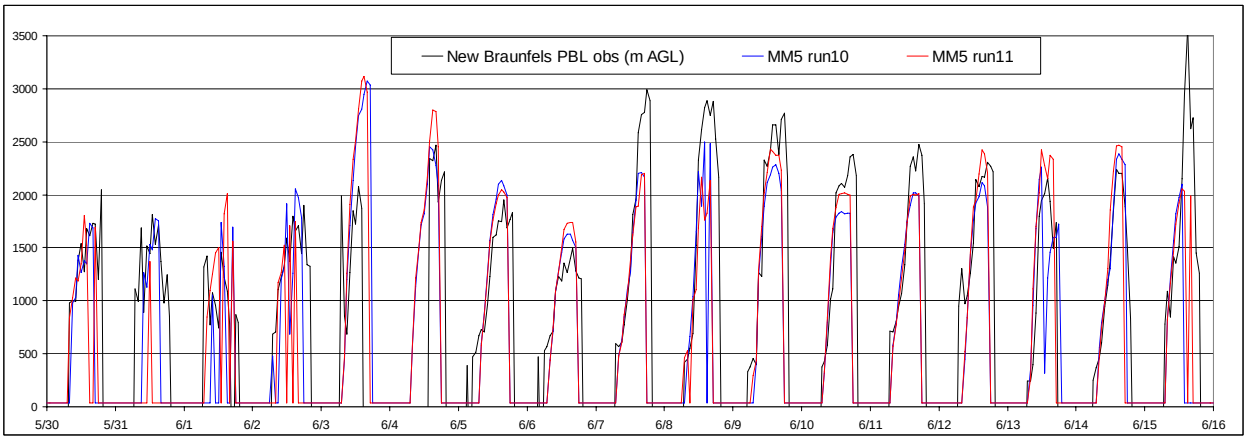

Figure 4-13. Hourly time series of predicted (MM5 Runs 10 and 11) and diagnosed PBL depths from the New Braunfels wind profiler.

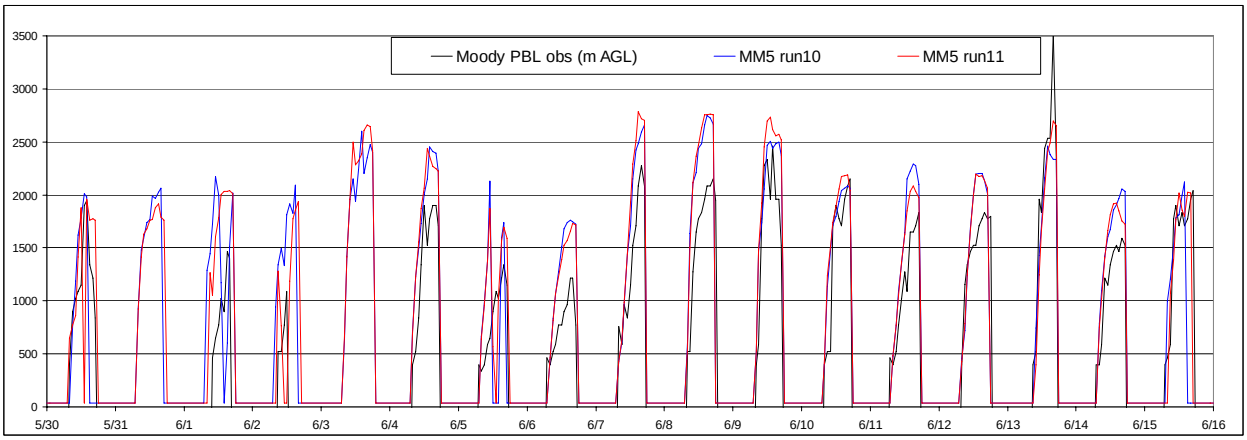

Figure 4-14. Hourly time series of predicted (MM5 Runs 10 and 11) and diagnosed PBL depths from the Moody wind profiler.

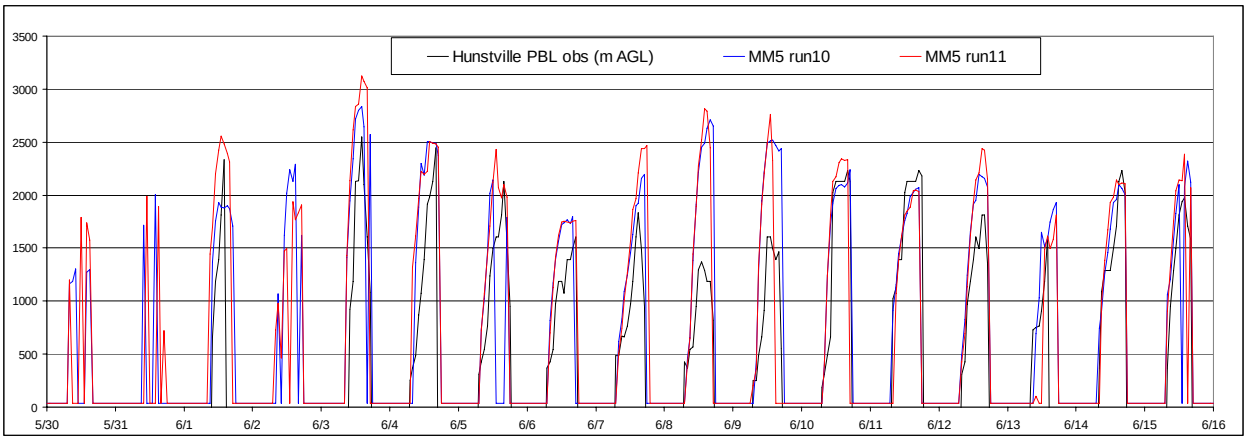

Figure 4-15. Hourly time series of predicted (MM5 Runs 10 and 11) and diagnosed PBL depths from the Hunstville wind profiler.

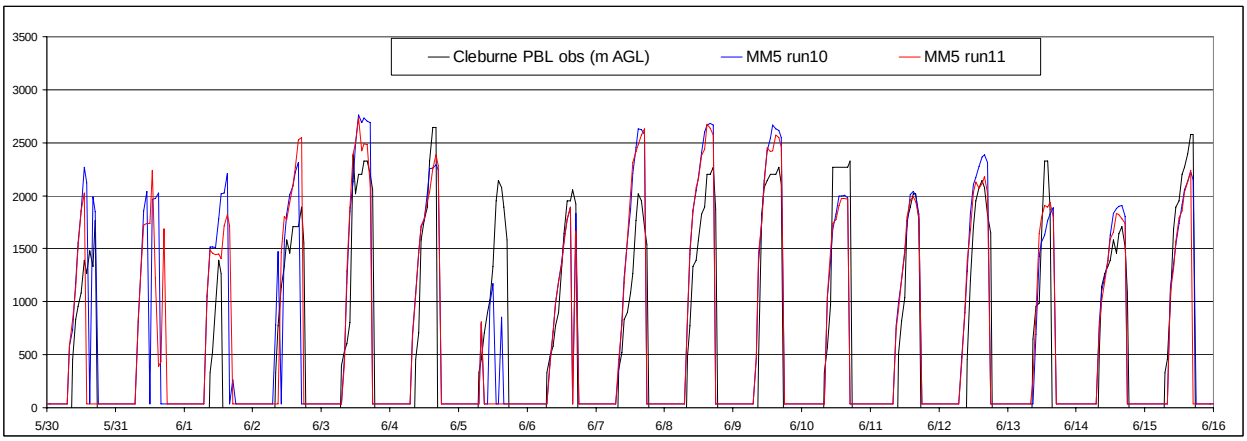

Figure 4-16. Hourly time series of predicted (MM5 Runs 10 and 11) and diagnosed PBL depths from the Cleburne wind profiler.

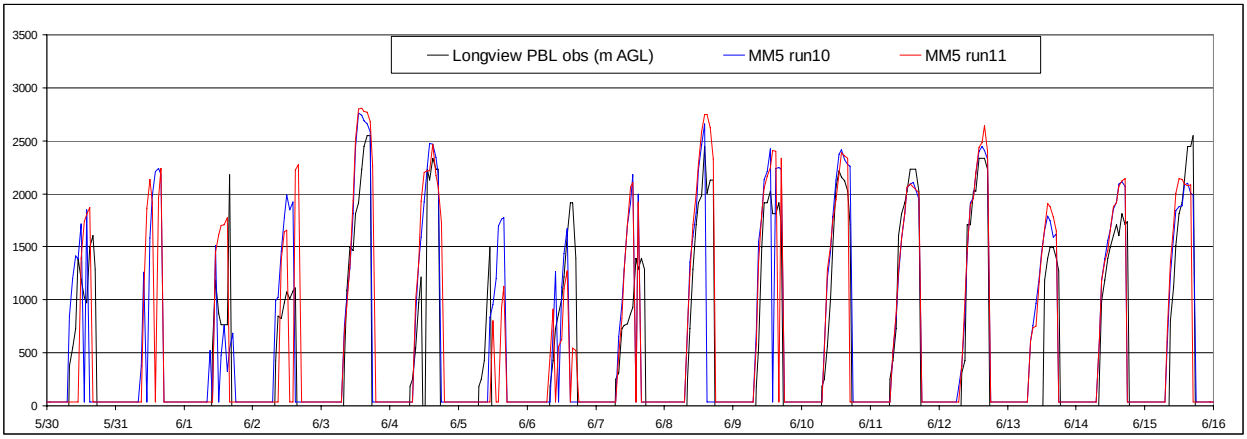

Figure 4-17. Hourly time series of predicted (MM5 Runs 10 and 11) and diagnosed PBL depths from the Longview wind profiler.

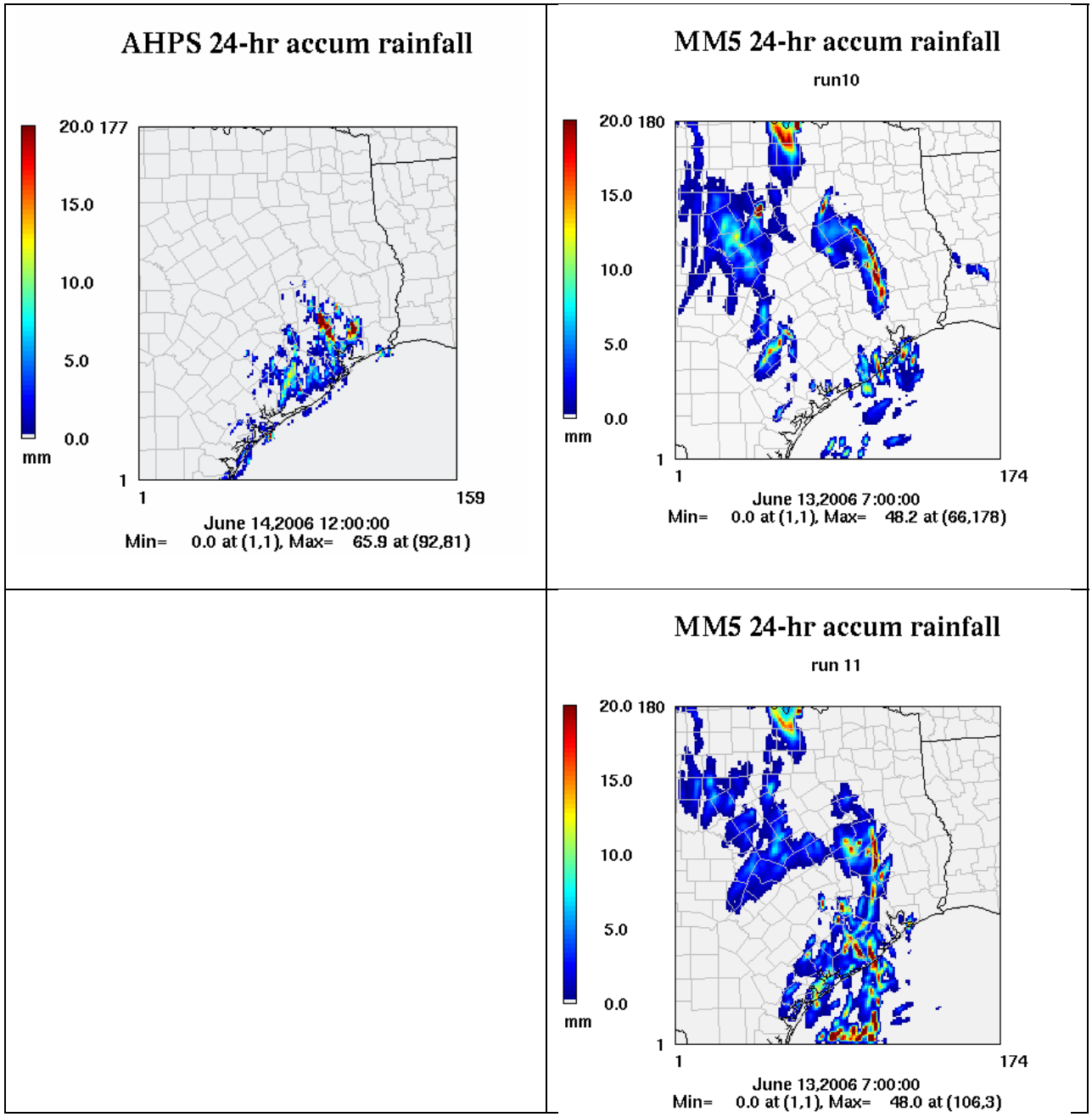

Figure 4-18. Observed (AHPS; top left) and MM5 simulated 24-hour accumulated precipitation (mm) for Runs 10 (top right) and 11 (bottom right), 7 AM June 14 to 7 AM June 15, 2006.

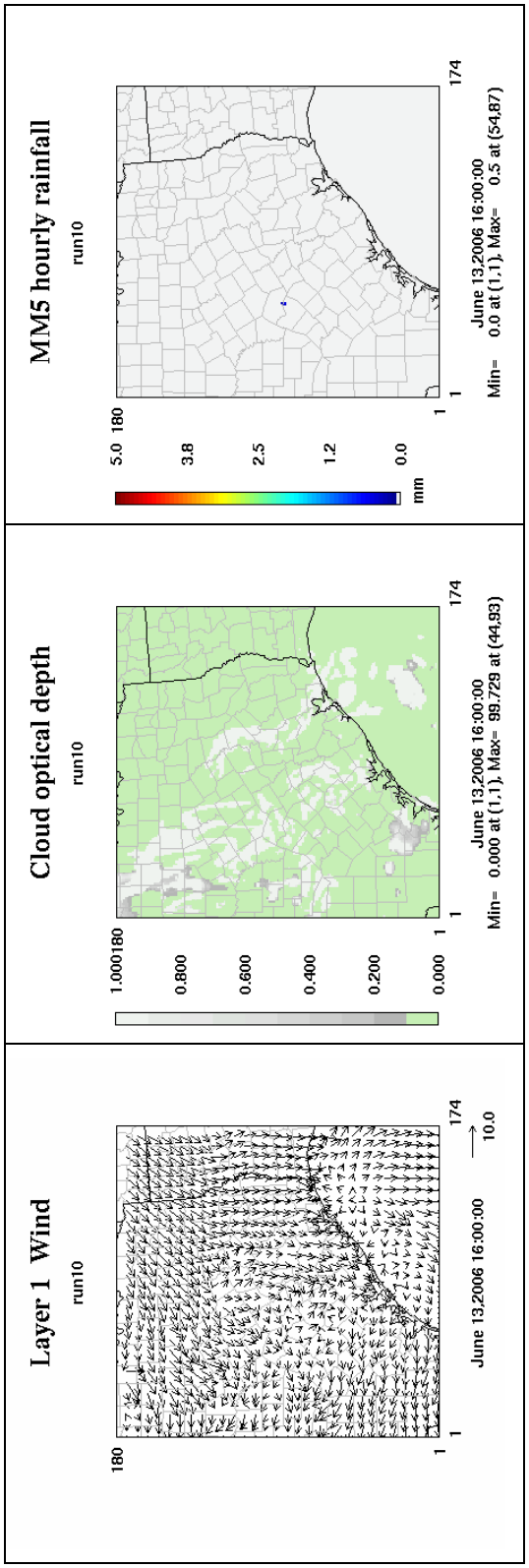

Figure 4-19. Simulated wind fields (left), CAMx cloud cover (middle), and rainfall (right) from MM5 Run 10 at 4 PM, June 13, 2006.

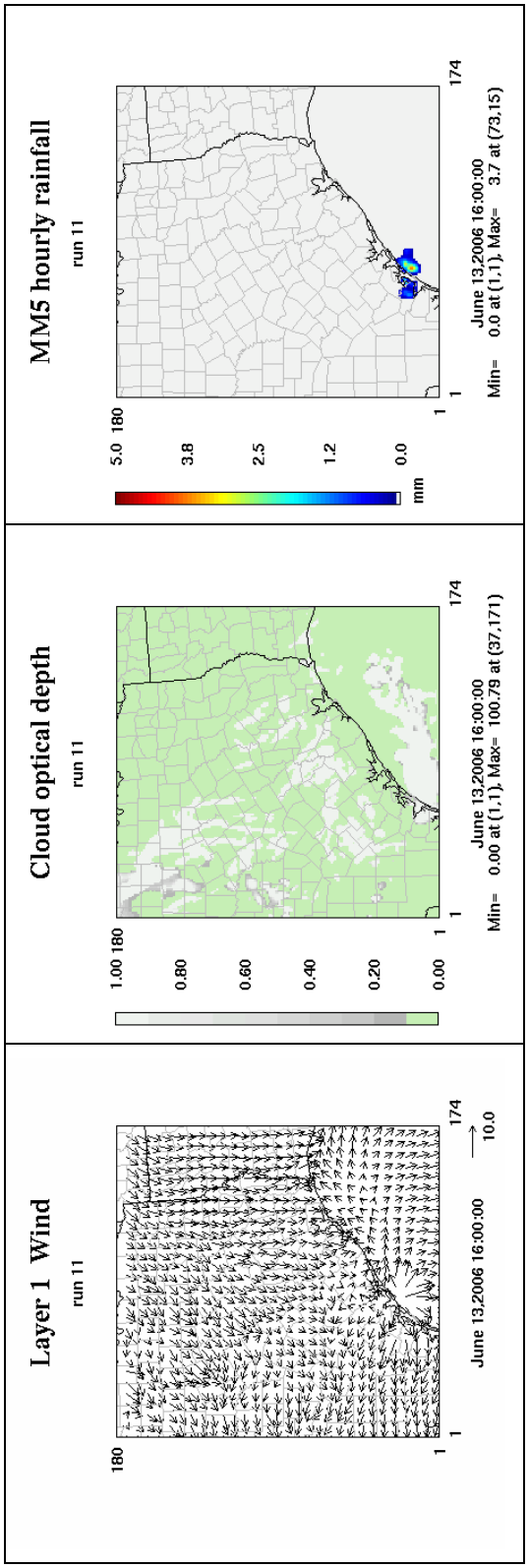

Figure 4-20. Simulated wind fields (left), CAMx cloud cover (middle), and rainfall (right) from MM5 Run 11 at 4 PM, June 13, 2006.

5. CONCLUSION

This report documents the continuation of a meteorological modeling project for the State of Texas to support photochemical modeling of ozone episodes that occurred in the central and eastern Texas during June 2006. In 2007, the TCEQ and ENVIRON International Corporation conducted preliminary meteorological modeling of central/eastern Texas for the June 2006 period. In late 2008, the AACOG and the CAPCOG jointly sponsored a project to improve upon the preliminary modeling with a focus on maximizing model performance in the San Antonio and Austin areas to support immediate photochemical modeling. The purpose of the current project was to continue to improve upon the AACOG/CAPCOG meteorological modeling and to expand the performance evaluation to Dallas and Northeast Texas.

ENVIRON ran three MM5 simulations in a stepwise manner to investigate impacts on performance in replicating local meteorological observation data in San Antonio, Austin, Dallas, and Northeast Texas. The approach followed the recommendations of Emery et al. (2009a) and TCEQ staff. The analysis of MM5 performance for each run was carried out in a manner similar to the previous study. Three new MM5 simulations of the May 29 – June 16, 2006 period were conducted in an attempt to improve upon some of the performance issues identified in the previous study, namely: (1) reducing spurious convection and removing associated ground-level outflow patterns that degraded wind performance; (2) increasing boundary layer depths to levels observed in radar profiler data; and (3) improving the diurnal patterns of surface temperatures and reducing daytime temperature bias. The best of these MM5 simulations are to be used this summer in AACOG's photochemical modeling.

The domain definition and much of the model configuration was based on the TCEQ Houston modeling and the subsequent ENVIRON work reported previously. Note that the definition of the 4-km modeling grid used in this study was consistent with the enlarged domain develop under the AACOG/CAPCOG work so that it would cover the San Antonio/Austin photochemical modeling domain. To ensure consistency with ENVIRON's previous MM5 simulations, and to correctly diagnose the impact of observation nudging and various physics changes on the MM5 results, we carried the previous MM5 domain, physics, and nudging configuration from AACOG/CAPCOG "Run 8" forward into this project.

The configuration and results of each of the three specific runs conducted in this study are briefly described below. In general, impacts from each of the MM5 configuration changes were similar in all four evaluation areas.

Run 9

Configuration: As in Run 8, run for the 4-km grid only, removing the shallow cumulus parameterization and replacing the ETA PBL scheme with the Medium Range Forecast (MRF) PBL scheme to investigate impacts on PBL evolution and cumulus convection.

Results: Wind speed/direction performance was moderately improved, the nighttime temperature under prediction bias was mostly eliminated (large daytime over prediction bias was not impacted), and humidity performance was improved. PBL depths were much better simulated (deeper, with more rapid morning growth rates). Spurious convective rainfall was reduced substantially, reducing impacts on surface wind patterns.

Run 10

Configuration: As in Run 9, replacing the NOAH LSM with the 5-layer soil model (soil parameters defined by internal look-up table) to investigate impacts on surface temperature, PBL evolution, and cumulus convection. The LSM change required that all grids be re-run (108/36/12-km grids run 2-way interactive, 4-km grid run separately using 1-way nesting).

Results: Wind speed/direction performance was not significantly impacted (as expected), but the large daytime over prediction bias was mostly eliminated (good nighttime temperature performance was maintained), and humidity performance was slightly degraded associated with a slight humidity increase with the alternative LSM. The PBL depths were not significantly impacted by this change, but there was some evidence of increased cloud cover. Rainfall was altered substantially, with less convective activity but a shift in patterns that did not agree with observed conditions. The reduction in convective rainfall further reduced impacts on surface wind patterns.

Run 11

Configuration: As in Run 10, but only for the 4-km grid replacing surface wind observation nudging with 1-hour surface wind analysis nudging using a 1-hour ADP observation dataset in conjunction with 3-hour EDAS analyses.

Results: Wind speed/direction performance was improved in each of the four analysis areas (especially wind direction), while temperature and humidity performance remained similar to Run 10. PBL depths were also consistent with Run 10 with only minor differences day-to-day. Rainfall patterns agreed better with observations, but maintained low levels of convective activity with similar cloud cover and little impact on surface wind patterns.

Each of the three simulations described above exhibited incremental improvements in winds, temperature, humidity, PBL, and rainfall performance. Ultimately, Run 11 has resulted in a very good meteorological simulation of May 30 – June 16, 2006 for each of the four areas of Texas evaluated in this study. Statistical performance for Run 11 is superior in all respects to the last AACOG/CAPCOG simulation (Run 8), and based on our experience, Run 11 is in many ways consistent with or better than many other meteorological simulations recently developed in south-central U.S. (e.g., previous episodes for Dallas, Houston, and Baton Rouge).

Early in this project, we realized that the results from Run 9 were significantly better than Run 8, and so ENVIRON immediately used the Run 9 MM5 output fields in CAMx simulations conducted for AACOG to evaluate impacts to photochemical model performance in San Antonio and Austin. With the additional significant improvements achieved in Runs 10 and 11, ENVIRON has sent these outputs to AACOG as well for follow-up CAMx sensitivity runs to be conducted by AACOG. ENVIRON recommends and endorses the use of MM5 Run 11 for future photochemical modeling of eastern Texas for early June 2006 ozone episodes. ENVIRON further recommends that Run 11 be extended through the remainder of June 2006 to support photochemical modeling of episodes that occurred in late June.

REFERENCES

Anthes, R.A. and T.T. Warner. 1978. "The Development of Mesoscale Models Suitable for Air Pollution and Other Mesometeorological Studies." *Mon. Wea. Rev.*, 106, 1045-1078.

Dudhia, J. 1993. "A Non-hydrostatic Version of the Penn State/NCAR Mesoscale Model: Validation Tests and Simulation of an Atlantic Cyclone and Cold Front." *Mon. Wea. Rev.*, 121, 1493-1513.

Emery, C., E. Tai, and G. Yarwood. 2001. "Enhanced Meteorological Modeling and Performance Evaluation for Two Texas Episodes." Prepared for the Texas Natural Resources Conservation Commission, by ENVIRON, International Corp, Novato, CA.

Emery, C., J. Johnson, P. Piyachaturawat. 2009a. "Application of MM5 for the Austin/San Antonio Joint Meteorological Model Refinement Project." Prepared for the Alamo Area Council of Governments, San Antonio, TX and the Capitol Area Association of Governments, Austin, TX. Prepared by ENVIRON International Corporation, Novato, CA (30 April 2009).

Emery, C., J. Johnson, P. Piyachaturawat. 2009b. "Application of CAMx for the Austin/San Antonio Joint Meteorological Model Refinement Project." Prepared for the Alamo Area Council of Governments, San Antonio, TX and the Capitol Area Association of Governments, Austin, TX. Prepared by ENVIRON International Corporation, Novato, CA (30 June 2009).

Grell, G. A., J. Dudhia, and D. R. Stauffer. 1994. "A Description of the Fifth Generation Penn State/NCAR Mesoscale Model (MM5)." NCAR Technical Note (NCAR TN-398-STR).

Kemball-Cook, S., Y. Jia, E. Tai, G. Yarwood. 2007. "Performance Evaluation of an MM5 Simulation of May 29-July 3, 2006." Prepared for the Texas Commission on Environmental Quality, Austin, TX. Prepared by ENVIRON International Corporation, Novato, CA (August 31, 2007).

Kemball-Cook, S., Y. Jia, C. Emery, R. Morris, Z. Wang and G. Tonnesen. 2004. "Draft Protocol: 2002 Annual MM5 Simulations to Support WRAP CMAQ Visibility Modeling for the Section 308 SIP/TIP." Prepared for the Western Regional Air Partnership, by the Regional Modeling Center (December 10, 2004).

Seaman, N.L. 2000. "Meteorological Modeling for Air Quality Assessments." *Atmos. Environ.*, 34, 12-14, 2231-2260.

Teche, T.W., D.E. McNally, C.A. Emery, E. Tai. 2001. "Evaluation of the MM5 Model Over the Midwestern U.S. for Three Oxidant Episodes." Prepared for the Kansas City Ozone Technical Workgroup, by Alpine Geophysics, LLC, Ft. Wright, KY, and ENVIRON International Corp, Novato, CA.

STI. 2007. "TexAQS II Radar Wind Profiler, Radio Acoustic Sounding System, SODAR, and LIDAR Data Quality Control and Mixing Height Derivation." Prepared for Texas A&M University, College Station, TX. Prepared by Sonoma Technology, Inc., Petaluma, CA (STI-907100-3215-FR, 31 August 2007).

Xiu, A. and J.E. Pleim. 2000. "Development of a land surface model. Part I: application in a mesoscale meteorology model." *J. App. Met.*, 40, 192-209.